CHAPTER THIRTY-TWO

ACTINIDES IN THE GEOSPHERE

Wolfgang Runde and Mary P. Neu

32.1 INTRODUCTION

Since the 1950s actinides have been used to benefit industry, science, health, and national security. The largest industrial application, electricity generation from uranium and thorium fuels, is growing worldwide. Thus, more actinides are being mined, produced, used and processed than ever before. The future of nuclear energy hinges on how these increasing amounts of actinides are contained in each stage of the fuel cycle, including disposition. In addition, uranium and plutonium were built up during the Cold War between the United States and the Former Soviet Union for defense purposes and nuclear energy. These stockpiles have been significantly reduced in the last decade. Considerable amounts of actinide isotopes have been employed in various applications in medicine, science and industry. To take only a few examples, uranium, in the form of oxide, was used in the past as coloring pigment to produce glazes and fluorescent glasses, and is employed today as metal in conventional munitions. Plutonium-238 is used in heat sources that enable space exploration. Californium-252 is critical for reactor start-up and for quality control in fuel rod manufacturing. Americium-241 is widely used in smoke detectors. And both [241]Am and [252]Cf are critical for well-logging in oil exploration. New applications are emerging, such as cancer treatments by applying the daughter of [233]U, [225]Ac. Understanding their use, storage, and disposition can assess both the benefits and negative impacts of actinides to mankind and to the environment.

Man-made actinides were injected into the environment relatively soon after the discovery of nuclear fission. During the first decades of nuclear reactors and weapons design and development, enormous volumes of radioactive effluents and large amounts of solid and gaseous bomb debris were released to the environment. As all industries changed their environmental stewardship beginning in the 1970s and 1980s, and nuclear testing was conducted underground in the early 1990s, the amount of actinides added to the geosphere sharply declined. Stored, isolated nuclear material is increasing globally. In contrast, distributed contamination from weapons testing fallout is roughly constant; and the number of highly contaminated sites is decreasing.

In this chapter we describe the sources of actinides, how actinides have been dispersed, and the prominent mechanisms that can impede or enhance their migration in the geosphere (Fig. 32.1). We focus on the actinides that are most important in nuclear weapons, nuclear energy, and legacy environmental contamination – thorium, uranium, neptunium, plutonium, americium and curium – and allude relatively little to actinium, protactinium and the actinides heavier than curium. Key mechanisms and illustrative examples are described, and references are given for more comprehensive or more detailed information. This chapter is not an inclusive review of methods and studies, nor is it a critical evaluation of quantitative data.

Entire series of books, monographs, conferences, and journal series are devoted to subtopics that are described more briefly here. For example, in 1987 the series of the biennial **MIGRATION** Conferences began and continues for researchers and regulators to discuss issues related to the migration of fission products and actinides in the environment. The Materials Research Society has devoted symposia and proceedings (such as the *Scientific Basis for Nuclear Waste Management* series) to applied studies and materials aspects of nuclear waste management. The Organization for Economic Co-operation and Development (OECD) has published a series of critically reviewed databases of thermodynamic constants that are essential for scientifically-based prediction of the long-term behavior of actinides in the environment. In addition to these sources, numerous symposia on fuel cycles, weapons stockpile reductions, reactor waste forms, actinide behavior in solution and solid state, interfacial phenomena and environmental restoration have provided platforms for extended discussion among researchers and diverse stakeholders. There is also enormous literature available with thousands of publications and reference texts. Overviews of the major aspects regarding the environmental behavior of actinides are quite numerous. Although not exhaustive, a very wide basis of information in the field can be found in books and book chapters (Lutze and Ewing, 1988; Burkart, 1991; Langmuir, 1997; Sterne *et al.*, 1998; Burns and Finch, 1999; Bailey *et al.*, 2002; Choppin *et al.*, 2002; Newton, 2002; Silva and Nitsche, 2002; Livingston, 2004; NATO, 2005) and overview articles (Rai *et al.*, 1980; Choppin, 1983;1988; Moulin *et al.*, 1988; Dozol and Hagemann, 1993;
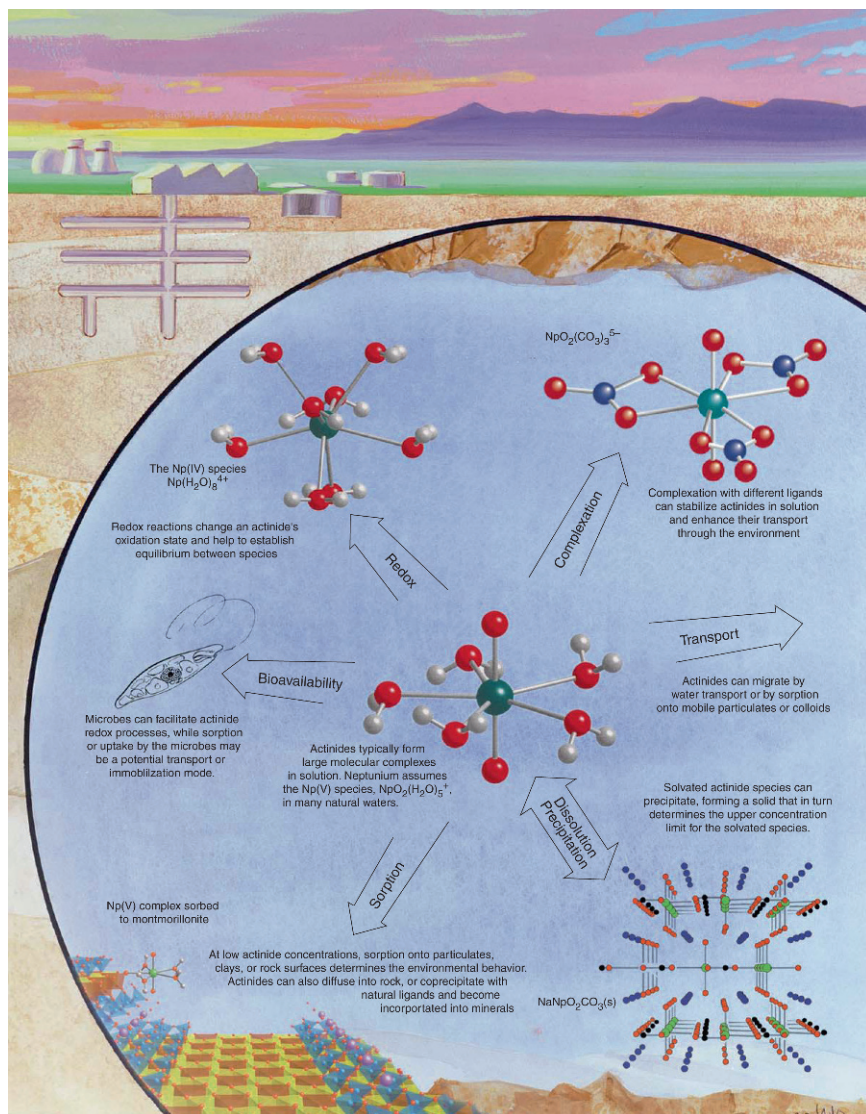
Fig. 32.1 *Schematic illustrating the complex processes that actinides can undergo in natural environments* (*Runde*, 2000).

Kim, 1993; Livens *et al.*, 1996; Runde, 2000; Moulin and Moulin, 2001; Geckeis and Rabung, 2008). We also refer to previous chapters in this work that are relevant to aspects of environmental behavior of the actinides: Chapters 19, 23, 27, and 30.

32.2   SOURCES OF ACTINIDES

Actinides are present in the environment from the origin of the universe, and also from human activities, predominantly related to nuclear weapons and nuclear energy. They can be categorized as follows: (1) the most abundant, thorium and uranium, with millions of tons in ores, minerals, and stores worldwide; (2) the major man-made actinide, plutonium, with up to thousands of metric tons accumulated globally; (3) the light minor actinides, neptunium, americium and curium with up to hundreds of kilograms produced in irradiated uranium-based fuel; (4) californium, which is produced in multigram quantities within spent reactor fuels and specialized reactor campaigns for specific use; and (5) the small quantities of the light actinides, actinium and protactinium, from the decay of uranium and thorium isotopes and of the short-lived, rare heavy actinides, berkelium, and einsteinium to lawrencium.

   Large amounts of actinides were formed during the Big Bang that created the solar system. With the passage of billions of years all but the longest-lived actinide isotopes have decayed away. Today, few transuranium elements (those elements heavier than U) on earth are from extraterrestrial sources, cosmic dust, and remnants of the earth's formation. The development of nuclear weapons and nuclear-generated electricity has produced tons of actinides with inter-mediate half-lives – those just stable enough to be used as fuel in reactors and devices that have relatively low critical mass for neutron-promoted fission. The byproducts of those industries include actinide isotopes that do not have current uses.

32.2.1   Primordial actinides

Our solar system formed from a cloud of dust and gas, apparently from the explosion of a nearby supernova. Only such a supernova can manufacture elements heavier than iron, including the most abundant actinides, thorium and uranium. With a half-life of ca. 700 million years, ^{235}U initially made up nearly half of all uranium when the solar system began some 4.6 billion years ago. Approximately 2 billion years ago more than 1 metric ton of natural ^{239}Pu accumulated in the Oklo uranium mine in Gabon, Africa (see Section 32.2.1 (c)). Most short-lived radioisotopes that existed in the beginning, like ^{26}Al or transuranium elements, have become extinct (Kuroda, 1982). However, we know of the former existence of actinide isotopes by the presence of their decay products in ancient meteorites. Neptunium isotopes have been discovered in the spectrum in some stars. The discovery of fission xenon from the decay of ^{244}Pu in meteorites and in samples collected from the moon has verified that the transuranium elements can be synthesized in exploding stars (Kuroda, 1996). The carbonaceous chondrite Orgueil, which is considered to be among the least altered samples of the solar system, appears to have started to retain ^{136}Xe more

than 5,000 million years ago, when the atom ratio of ^{244}Pu/^{238}U in the solar system was as high as (0.5 ± 0.1). The carbonaceous chondrites Murchison and Murray started to retain their xenon about 4,940 million years ago, when the ^{244}Pu/^{238}U atom ratio was about 0.17 (Kuroda and Myers, 1994; Kuroda, 1996). These abundances of early meteoritic ^{244}Pu prove that ^{244}Pu is a bona fide extinct radionuclide of galactic origin, and that r-process nucleosynthesis was ongoing in the galaxy at the time of the birth of the sun. In 1956, it was hypothesized that ^{254}Cf may be synthesized in a supernova and may be responsible for the form of the decay of light-curves of supernova Type I (Baade *et al.*, 1956; Burbridge *et al.*, 1956). In light of the observed findings of nuclear fission reactions in supernovas, significant quantities of isotopes of the transuranium elements were present in the early history of the solar system. Today, few of the longest-lived isotopes of thorium and uranium remain in significant quantities.

(a) Natural actinide abundance

Remaining from the earth's formation, long-lived actinides have abundances sufficient to contribute to natural background radioactivity. Besides the very long-lived isotopes of the lighter element, such as ^{40}K or ^{87}Rb, most naturally occurring radionuclides stem from the three distinct decay chains of ^{238}U, ^{235}U and ^{232}Th. Both uranium and thorium remain available in large amounts (tens of millions of tons). In fact, thorium comprises about 10–15 ppm of the upper earth's crust (Burkart, 1991; Bailey *et al.*, 2002), similar to lead, tin, and nickel. Uranium has a lower relative abundance of 2–4 ppm (Burkart, 1991; Bailey *et al.*, 2002), similar to tungsten and thallium, but more abundant than cadmium and selenium.

Traces of primordial ^{244}Pu were extracted from bastnaesite, a Precambrian rare earth fluorocarbonate ore from the Mountain Pass deposit in California (Hoffman *et al.*, 1971). Trace amounts of very few actinide isotopes are generated continuously by the decay of naturally-occurring actinide isotopes or by the neutron capture of uranium isotopes. Two successive neutron captures of ^{235}U and ^{238}U produces ^{237}Np and ^{239}Pu, respectively, which are found in minute quantities in uranium-rich minerals and ores (Cowan, 1976). A number of uranium ore samples have shown a near secular equilibrium between ^{238}U and ^{239}Pu with a weighted averaged U/Pu atomic ratio of 3.1×10^{12}. This is very close to the theoretical ratio at secular equilibrium, 3.0×10^{12} (Curtis *et al.*, 1992). The current total amount of naturally produced ^{239}Pu in the upper earth crust is estimated to be several kilograms.

Clearly, the amounts of naturally occurring primordial transuranium elements are relatively small compared to the man-made dispersions of actinides into the environment since 1945. Today, most plutonium and americium in the environment originated from nuclear weapons testing, releases from reactor operations, and the transport and disposal of radioactive materials from weapons and energy processes.

(b) Natural decay series

Three main decay chains are observed in nature, commonly called the thorium series, the uranium–radium series, and the uranium–actinium series, all ending in three different, stable isotopes of lead (Fig. 32.2). The mass number of every isotope in these chains can be represented as $A = 4n$, $A = (4n + 2)$ and $A = (4n + 3)$, respectively. The corresponding long-lived starting isotopes ^{232}Th, ^{238}U and ^{235}U have existed since the formation of the earth in amounts according to their decay properties. In nature, the radionuclides in these three series are
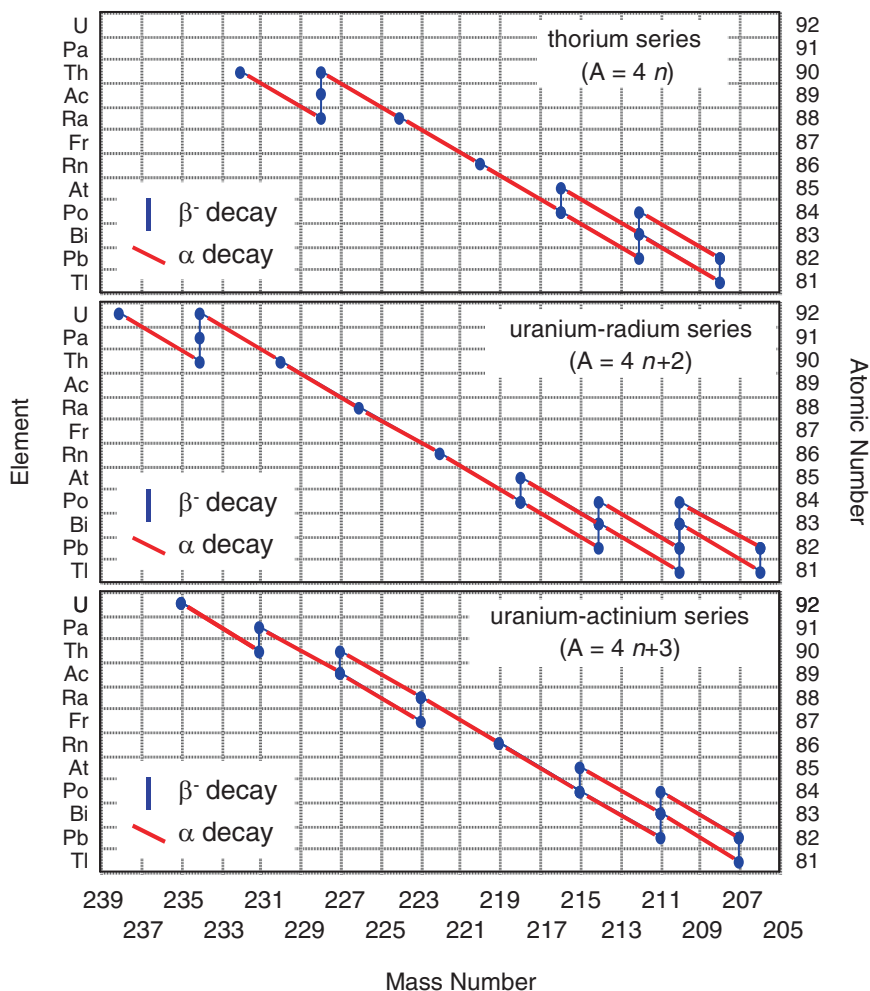

Fig. 32.2 *The three naturally occurring decay series. The neptunium series is not shown since it is already extinct.*

approximately in a state of secular equilibrium, in which the activities of all radionuclides within each series are nearly equal. A fourth chain, the neptunium series with $A = (4n + 1)$, is already extinct, due to the relatively short half-life of its progenitor ^{237}Np ($t_{1/2} = 2.144 \times 10^6$ years). The most important isotope of this series is ^{233}U ($t_{1/2} = 1.592 \times 10^5$ years), which is, like ^{235}U, fissionable by slow neutrons. Some older sources give the final stable isotope as ^{209}Bi, but it was recently discovered that ^{209}Bi is an α-emitter with a half-life of 1.9×10^{19} years (deMarcillac *et al.*, 2003). The ending stable isotope of the neptunium series is therefore ^{205}Tl.

The parent of the thorium decay series is ^{232}Th ($t_{1/2} = 1.405 \times 10^{10}$ years), which is the longest-lived radioisotope among the thorium, uranium and plutonium isotopes. Its half-life is comparable to the earth's age and thus about half of the ^{232}Th is still present. The mass numbers of the radionuclides in the thorium decay chain can be divided evenly by four. The longest-lived member of this $4n$ chain is ^{228}Ra ($t_{1/2} = 5.75$ years). After 6 α- and 4 β$^-$-decays the series ends in the terminal nuclide ^{208}Pb.

The uranium-radium ($4n + 2$) (mass numbers divided by four leaving a residual of two) decay series has ^{238}U ($t_{1/2} = 4.468 \times 10^9$ years) as a parent and ends after 8 α- and 6 β$^-$-decays in ^{206}Pb. This series contains the longest-lived radium isotope, ^{226}Ra ($t_{1/2} = 1,599$ years). This series provides important isotopes of radon, polonium and radium for applications in industry, medicine and science (Choppin *et al.*, 2002).

The uranium-actinium ($4n + 3$) (mass numbers divided by four leaving a residual of three) decay chain begins with ^{235}U as the parent and ends, after 7 α- and 4 β$^-$-decays, in the stable isotope ^{207}Pb. The longest-lived isotope in this chain, ^{231}Pa ($t_{1/2} = 3.28 \times 10^4$ years), has been isolated on a multigram scale by processing uranium refinery residues. This decay chain contains the longest-lived actinium isotope, ^{227}Ac ($t_{1/2} = 21.772$ years).

Some of the naturally-occurring isotopes in these decay chains have useful applications in radiometric techniques used to determine the age of minerals. The uranium–thorium dating method uses ^{230}Th and its radioactive parent ^{234}U within a sample. This method has an upper age limit of about 500,000 years due to the half-life of 7.538×10^4 years of ^{230}Th and the accuracy at which we can measure the isotopic ratio. One of the oldest radiometric dating methods, which played a significant role in determining the earth's age, is the coupled geochronometer provided by the decay of ^{238}U ($t_{1/2} = 4.468 \times 10^9$ years) to ^{206}Pb and the decay of ^{235}U ($t_{1/2} = 7.038 \times 10^8$ years) to ^{207}Pb. This method covers age ranges of about 1 million years to over 4.5 billion years with routine precision in the 0.1–1% range (Parrish and Noble, 2003). In theory, the ^{234}U/^{238}U ratio could be useful in dating samples of ages between about 10,000 and 2 million years, but in practice, this dating method is almost never used, because unlike ^{230}Th/^{238}U dating it requires knowledge of the ^{234}U/^{238}U ratio at the time the material under study was formed. For those materials (principally marine carbonates) for which the initial ratio is known, ^{230}Th/^{238}U dating is a superior technique.

(c) The Oklo reactors

The ratio, as a function of geological times, of the naturally occurring uranium isotopes, ^{238}U ($t_{1/2} = 4.468 \times 10^9$ years) and ^{235}U ($t_{1/2} = 7.038 \times 10^8$ years), is determined by their relative decay rates. Due to its shorter half-life ^{235}U is more rapidly decreasing with time, and analyses of naturally occurring uranium generally show that the percentage of fissionable ^{235}U in natural uranium is close to 0.720%. In 1972 researchers at the French Commissariat à l'Energie Atomique in Pierrelatte measured mass spectrometrically a value of 0.7171 atom% of ^{235}U in one sample recovered from the Oklo mine in West African Gabon (Bodu *et al.*, 1972; Cowan, 1976; Zetterström, 2000). The lower ratio of 0.7171% indicated a small, but significant depletion in ^{235}U from the standard uranium samples. Highly concentrated uranium samples (up to 60% uranium by weight) from the ore body revealed even greater depletions, with ^{235}U concentrations as low as 0.29% (Naudet, 1975). In addition, other elements, such as neodymium, were found in isotopic compositions different from natural abundance (Hidaka, 2007). In the absence of a natural process that could fractionate ^{235}U from the more abundant ^{238}U, the missing ^{235}U had to be consumed by nuclear fission reactions in the uranium ore bodies (Fig. 32.3).

The Oklo site is a high-grade sandstone-hosted uranium deposit (Janeczek and Ewing, 1992). The reactors are small bodies in the uranium ores measuring 10–20 m in length and are less than 1 m thick and contain up to 80% uranium in the form of uraninite, UO_2 (Cowan, 1976; Smellie, 1995; Zetterström, 2000). To date, at least 17 such natural nuclear reactors have been discovered in the Oklo and the associated Okélobondo and Bangombé uranium ore deposits in the
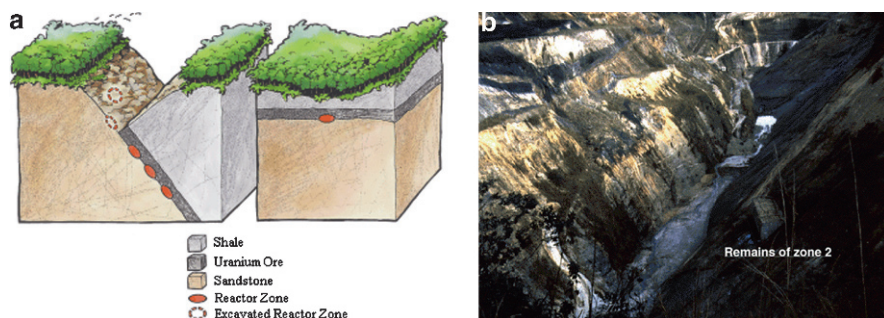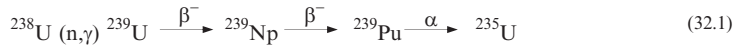

Fig. 32.3 *(a) Illustration of the reactor zone siting at Oklo. All reactor zones have existed where a layer of uranium-bearing sandstone has come into contact with an overlying layer of clay shale (SKB, 2002). The majority of the mined uranium existed as a layer of uranium ore, which covered the side of the pit. The reactor zones themselves were centimeter to meter thick layers of highly enriched uranium, buried within the uranium ore. (b) A view of reactor zone 2 at Oklo, fixed in concrete into the side of the mine pit to stop it from sliding down the slope of the pit (Loss, 2005), photo by courtesy of Prof. Gauthier-Lafaye.*

Republic of Gabon. The fuel of the natural reactors at Oklo stemmed mainly from fissionable ^{235}U, which had a five times greater abundance 2 billion years ago than today. The relatively high abundance of ^{235}U (about 3% of the total uranium) and the high concentration of uranium ore minerals supported nuclear fission reactions. Water in porous and fractured rocks of the Oklo reactors functioned as the neutron moderator slowing down the emitted neutrons from the fission of ^{235}U to be more readily absorbed by other ^{235}U nuclei, thereby sustaining fission reactions. Neutron poisons such as lithium and boron, that could stop the fission reactions by absorbing neutrons, were not present in sufficient quantities to inhibit reactor operations. The natural reactors reached criticality about 2 billion years ago and functioned for a period of about 600,000–1.5 million years (Cowan, 1976). During the operating period the reactors at Oklo produced actinide isotopes via neutron capture and subsequent beta and alpha decay:

$$^{238}\text{U (n,}\gamma\text{) } ^{239}\text{U} \xrightarrow{\beta^-} {}^{239}\text{Np} \xrightarrow{\beta^-} {}^{239}\text{Pu} \xrightarrow{\alpha} {}^{235}\text{U} \tag{32.1}$$

It is estimated that a total of 400,000 metric tons of uranium were deposited at Oklo (Cowan, 1976; Smellie, 1995) and an estimated 15,000 MWyr of fission energy was produced; temperatures ranged between 160°C and more than 360°C; and about 6 metric tons of fission products accumulated. The reactors also produced 2.5 metric tons of plutonium. Small amounts of the fissionable ^{239}Pu participated in fission reactions, while the majority of the ^{239}Pu decayed to produce ^{235}U, which added to sustain the fission reactions. In fact, about 45% of the total amount of ^{235}U consumed in fission reactions was produced by the decay of ^{239}Pu.

The reactors shut down naturally when the depletion of ^{235}U reached a level where nuclear reactions are no longer sustainable. Like these ancient natural reactors man-made reactors also generate radioactive wastes, some fraction of which will likely be disposed of in underground geologic formations. Although the geology at Oklo may differ from those at proposed nuclear waste disposal sites in deep geologic formations, the Oklo natural reactors provide an opportunity to observe how little actinides migrated away from their source over geologic time scales and thus serve as analogs for the storage and immobilization of man-made radioactive waste in modern repositories. Uranium ore deposits are also known in other geological formations of approximately the same age, not only in Africa but also in other parts of the world, particularly in Canada and northern Australia. To date, no other natural nuclear reactors have been identified.

(d) Uranium and thorium resources

Extensive information is available on uranium and thorium geology, mineralogy, mining and chemistry, including the earlier chapters in this work.

The *Gmelin Handbook of Inorganic Chemistry* contains comprehensive reviews of thorium and uranium ore deposits, mineralogy and geochemistry (Gmelin, 1972, 1978, 1979, 1990, 1991). Approximately 200 minerals contain uranium as a major constituent. The majority of such minerals include U(VI) forming extended structures, that can be described as polymerized uranyl(VI) polyhedra. A list, classification and description of these mineral phases are given in Burns (1999), Burns and Finch (1999), and Hill (1999). For more detailed discussions on the natural occurrence of uranium, its mineralogy, uses and applications, the authors refer to Chapter 5 of this work and also to other textbooks such as those of Burkart (1991), Bea (1999), and Burns (1999).

Uranium is present at about 2–4 ppm in the earth's crust and about 1–3 ppb in seawater (Burkart, 1991; Bailey *et al.*, 2002), and is thus more abundant than many other common elements, such as Cd, Ag, Hg, etc. The majority of coal used by power plants in the United States has a uranium concentration between 1 and 4 ppm (Bailey *et al.*, 2002). In general, igneous rocks with a high silicate content, such as granite, contain an above average uranium concentration. Typically, granite contains up to 15 ppm uranium and between 1 and 10 ppm uranium are found in sandstone, shale or limestone (Burkart, 1991). High-grade ore bodies can contain up to 20,000 ppm uranium (OECD/NEA, 2003). Sedimentary rocks generally contain below average uranium concentrations. The commercially most important uranium minerals are uraninite and pitchblende with a composition that varies from UO_2 to $UO_{2.5}$. Approximately 90% of the world's uranium resources are contained in unoxidized deposits of pitchblende and coffinite in arkasoic and quartzitic sandstones. Upon weathering, secondary minerals such as carnotite, tyuyamunite and uranophane are formed (Burns and Finch, 1999; OECD/NEA, 2008).

Resources of uranium are categorized based on the economics of uranium recovery from the ore body. The most common term is Reasonably Assured Resources (RAR), which refers to uranium in known mineral deposits of size, grade, and configuration such that recovery is within the given production cost ranges with currently proven mining and processing technology. Total RAR recoverable at costs of US$80/kg uranium, were estimated at about 3.5 million metric tons uranium (OECD/NEA, 2003). More recently, it has been estimated that roughly 5.5 million metric tons of uranium can be RAR recovered for less than US$130/kg (OECD/NEA, 2008). Australia, Kazakhstan, Russia, Canada and South Africa have the largest resources for low-cost uranium (Table 32.1). Extraction of uranium from more unconventional sources, such as phosphate deposits (22 million metric tons recoverable uranium) or seawater (up to 4,000 million metric tons uranium), would cost up to six times the US$80/kg price. Considering all optional uranium resources more than 35 million metric tons are available worldwide for exploitation (OECD/NEA, 2005).

Thorium is the most common actinide element, present in the earth's crust at about 10–15 parts per million, approximately five times more abundant than uranium (Burkart, 1991; Bailey *et al.*, 2002). There has been little demand for

Table 32.1 *Recoverable resources of uranium in kilotons (kt) at US$130/kg uranium* (*OECD/NEA*, 2008).

Country	kt	Percent of world	Country	kt	Percent of world
Australia	1,243	23	USA	342	6
Kazakhstan	817	15	Brazil	278	5
Russia	546	10	Namibia	275	5
Canada	423	8	Niger	274	5
South Africa	435	8			
Total worldwide: 5,469 kt					

Table 32.2 *Estimated resources of thorium in kilotons (kt) at US$80/kg thorium* (*OECD/ NEA*, 2008).

Country	kt	Percent of world	Country	kt	Percent of world
Australia	452	18	Norway	132	5
USA	400	16	Egypt	100	4
Turkey	344	13	Russia	75	3
India	319	12	Greenland	54	2
Venezuela	300	12	Canada	44	2
Brazil	302	12	South Africa	18	1
			Other	33	1
Total worldwide: 2,573 kt					

thorium for commercial nuclear applications. In 1996, the thorium consumption in the United States was only 4.9 metric tons. Consequently, there is no incentive for exact resource assessment and estimates of thorium reservoirs vary significantly. Table 32.2 shows the thorium resources by country estimated by the OECD (OECD/NEA, 2008). Some of the data are considered very conservative. There are claims that the United States thorium resource is as large as 3 million metric tons. Large thorium deposits exist in Idaho and Montana containing more than 100,000 metric tons ThO_2 (Ditz *et al.*, 1990; Gmelin, 1991; Hedrick, 2004). Other sources have estimated the worldwide thorium resources up to 4.5 million metric tons.

The most common commercial source is the rare-earth phosphate mineral, monazite, which generally contains between 1 and 10 wt% thorium (Bailey *et al.*, 2002). World resources of monazite are estimated to about 12 million metric tons, with large deposits in India and Australia. In granite, thorium is present up to 80 ppm (Burkart, 1991). Other minerals enriched in thorium are huttonite, $ThSiO_4$, and thorianite, ThO_2, with up to 80% thorium content (Oberti *et al.*, 1999). However, these minerals are not very common but could be

economically processed if the demand for thorium increased dramatically. The limited demand for thorium has created a worldwide oversupply of thorium compounds. Excess thorium not designated for commercial use was either disposed of as a radioactive waste or stored for potential use as a nuclear fuel or other applications. In 2005, the United States government authorized the disposal of over 3 million kilograms of excess thorium nitrate from the National Defense Stockpile (NDS) (Hedrick, 2004). For a more detailed discussion on the natural occurrence of thorium, its mineralogy and its technology and uses, the reader is referred to the *Gmelin Handbook of Inorganic Chemistry* (1988, 1990, 1991). A summary of the abundance, minerals, and geochemistry of thorium can be found in Krishnaswami (1999). More information can also be found in Frondel (1955), Hedrick (2004) and Clark *et al.* (2007). Chapter 3 of this work, which deals with the general properties of thorium and its compounds, also discusses the occurrence of thorium ores and the technology of their processing.

32.2.2   Anthropogenic actinide sources

With the exception of a few high local exposures the majority of radiation exposure to man worldwide is due to naturally occurring radiation sources. Natural sources include sources in the earth matter, such as food, water and radionuclides in building materials, cosmic rays from space, and atmospheric sources such as radon gas released from the earth and radionuclides formed by high-energy cosmic ray bombardment of atoms produced in the upper atmosphere. About 15% of the radiation exposure originates from the application of X-rays and radiopharmaceuticals for medical diagnostics and therapy. Only about 3% of radiation exposure originates from man-made sources such as industrial applications (i.e. smoke detectors), global fallout (from nuclear weapons testing), emissions from burning fossil fuels, releases from operating nuclear power plants, and from improper transportation, disposal, storage or recycling of radioactive materials.

(a)   Products from mining industry

The industrial scale exploration of natural uranium ores began with the development of nuclear weapons. Today, the demand for uranium in the commercial sector is primarily determined by the consumption and inventory requirements of nuclear power reactors. In March 1997, there were 433 nuclear power plants operating worldwide with a combined capacity of about 345 GWe (net gigawatts electric). Current projections show a steady growth in nuclear energy capacity to 446 GWe by the year 2010, representing a 30% increase. This increase will require 76,673 metric tons uranium by the year 2010, compared to 57,182 metric tons required in 1992 (OECD/NEA, 2003, 2008). For detailed reviews of uranium mining and fuel production activities the authors refer to the *Gmelin Handbook* (1972, 1979, 1981, 1988). Landa (2004) and Al-Hashimi *et al.*

(1996) reviewed the various aspects related to the impact of the storage of uranium mill tailings on the environment.

Historically, uranium has been recovered from ores by excavation or in situ leaching techniques. Deep uranium deposits require underground mining, while open pit mining has been used for deposits that are close to the surface. The latter technique requires the removal of much larger quantities of material and therefore has a much greater impact on the environment. Examples of open pit mining operations can be found in Canada and Australia. Probably the best known example of underground mining are the Cigar Lake and McArthur River mines in Canada with unusually high-grade uranium ores.

Most uranium is recovered by in situ leaching techniques. Acidic or alkaline solutions are used to dissolve and convert uranium in the porous ore body to water-soluble species. For acidic leaching most mills use H_2SO_4; sodium or ammonium carbonate is used in the alkaline leaching process that takes advantage of the very high stability of $UO_2(CO_3)_3^{4-}$ in solution. Residues and tailings, such as undissolved rock or unwanted dissolved materials, are returned to their underground location or are accumulated in settling ponds or trenches. During the milling or refining process the uranium is precipitated and calcined to obtain U_3O_8, generally referred to as yellowcake. The yellowcake contains 80–90% uranium by weight recovered from ores that have a uranium content as low as 0.03%. Since the yellowcake does not have the desired purity required for most nuclear applications, it needs to be refined to a high-purity product. The most common purification techniques are the extraction of uranium with tri(*n*-butyl) phosphate from nitric acid solutions or the conversion of the oxide to UF_4 and UF_6 followed by distillation of the latter. Additional details on uranium ore processing and separation can be found in Chapter 5 of this work.

Mining and milling operations create a substantial amount of waste because the uranium fraction is generally less than 1% of the ore. Processing 1 metric ton of uranium ore creates over 4 metric tons of liquid waste. Bradley reports the generation of over 2,000 m^3 of liquid waste waters per day from uranium ore processing in Russia (Bradley, 1997). In 2004, the inventory of uranium mill tailings in the United States was reported to be about 240 million metric tons (Landa, 2004). The tailings are about ten times more radioactive than natural granite and contain a large fraction of the ore radioactivity (particularly the long-lived ^{230}Th and ^{226}Ra) and toxic metals, such as manganese and molybdenum, which can leach into rivers and groundwaters (Fernandes *et al.*, 1996; Thomas, 1999). Health hazards arise from radioactive gas emanation, external exposure, and from the contamination of soil, surface and ground water. The isotopes ^{226}Ra, ^{230}Th, ^{210}Po and ^{210}Pb have been found in soils contaminated from untreated discharge of waste waters from uranium ore processing facilities. And water samples collected in the vicinity of tailing piles have shown levels of some contaminants at hundreds of times the acceptable level for drinking water. As an example, a survey of 60 radium and uranium mining sites in Portugal identified six sites that contain significant radioactive

components (Carvalho *et al.*, 2007). At these locations, up to 33,400 Bq kg^{-1} of ^{238}U were measured in sandy samples from mining waste heaps and up to 337 Bq kg^{-1} of ^{238}U are contained in soils collected from the areas around the mining sites. The Former Soviet Union exploited uranium ores in Germany and Czechoslovakia to meet their needs for uranium between 1945 and 1989. A total of 126,000 metric tons were mined in Saxony, Germany, leaving behind numerous tailings and large areas contaminated with uranium (Meinrath *et al.*, 2003). In 1977, an average of 2.9 mg L^{-1} uranium was measured in Saxonian lakes and small rivers close to sediment ponds and tailings. Such rivers may carry up to 300 kg U per year and uranium run-off still exposes the environment to significant amounts of legacy uranium.

(b)   Isotopically enriched actinides

In order to sustain a nuclear reaction in most commercial power plants, the ^{235}U needs be enriched to about 3–5%. Nuclear weapons and most research reactors worldwide use highly enriched uranium with over 90% ^{235}U. The mining and milling process raises the total uranium concentration, but the fraction of fissile ^{235}U remains 0.7%. Uranium enrichment can be achieved in many ways (Villani, 1979; OECD/NEA, 2003, 2008). Most techniques utilize the small mass difference between ^{235}U and ^{238}U. Gaseous diffusion and centrifugal isotope separation are the methods currently employed on an industrial scale. Two less economic enrichment technologies are electromagnetic separation and laser-based isotope separation.

A number of accidents have been reported in enrichment facilities involving UF_6, the most common feedstock for chemical conversion and enrichment processes. However, the majority of environmental contaminations by volume and mass stems from depleted uranium. Sources are armor-piercing conventional weapons, tank armor plating or residues from down-blending highly-enriched uranium to produce reactor fuel. The different applications of uranium in civil industrial applications are described by Betti (2003).

Different ratios of actinide isotopes are characteristic signatures to the origin of the material. Stratospheric fallout of the Northern Hemisphere is characterized by an averaged ^{240}Pu/^{239}Pu isotope ratio of 0.18 (Perkins and Thomas, 1980; Buesseler and Sholkowitz, 1987; Mitchell *et al.*, 1997) and an activity ratio of 0.03–0.05 for ^{238}Pu/^{239,240}Pu (Hardy *et al.*, 1973; MacKenzie *et al.*, 2006). Aged weapons-grade plutonium and reactor-grade plutonium have reported ^{238}Pu/^{239,240}Pu activity ratios of 0.019 and 1.66, respectively (Carson, 1993). Nuclear fuel exhibits a significantly higher isotope ratio depending on the degree of burn-up. A ^{240}Pu/^{239}Pu ratio of 0.42 was calculated for Chernobyl reactor fuel and an averaged (0.396 ± 0.014) was found in soils around Chernobyl (Boulyga and Becker, 2002). Also, emissions of actinides from nuclear reprocessing plants are characterized by a tenfold higher

^{238}Pu/^{239,240}Pu ratio compared to global fallout, such as 0.30 for releases at Marcoule in France (Lansard *et al.*, 2007).

(c) The light transuranium elements Np, Pu, Am and Cm

The discovery of plutonium and the development of nuclear weapons led to the accumulation of transuranium elements. Today, large quantities of the light actinides exist in nuclear weapons arsenals, stockpiles of fissionable uranium and plutonium, spent nuclear fuel stored at reactor sites, and in radioactive wastes from plutonium and spent fuel processing and research activities. Since the end of World War II nuclear reactors around the world have produced over 3,000 metric tons of plutonium and highly enriched uranium (HEU), of which about two thirds (1,750 metric tons HEU and 250 metric tons Pu) have been used for military purposes (Albright *et al.*, 1997). The vast majority of the plutonium produced, about 1,000 metric tons, is commercial-grade plutonium for reactor applications. The inventory of weapons-grade plutonium is unlikely to increase based on nuclear arms control treaties and blending down of stockpiled plutonium during the last 3 decades. However, the operation of the world's 439 nuclear reactors (by November 2007 (Schneider and Froggatt, 2008)) causes the inventory of reactor-grade plutonium to grow continuously. While most plutonium remains unprocessed in spent nuclear fuel, an estimated 200 metric tons of civil plutonium has been separated from spent nuclear fuel.

As mentioned earlier, only very minute amounts of transuranium elements can be found in nature. Larger quantities of transuranium elements have been generated in reactors by the irradiation of uranium fuel or in bomb-related debris. As an example, the short-lived ^{239}Np is produced during the event of nuclear explosions and the ratio of ^{239}Np/^{99}Mo can be used to characterize radioactive debris (De Geer, 1977). The majority of transplutonium elements are generated when irradiating uranium fuel with neutrons (Fig. 32.4, left).
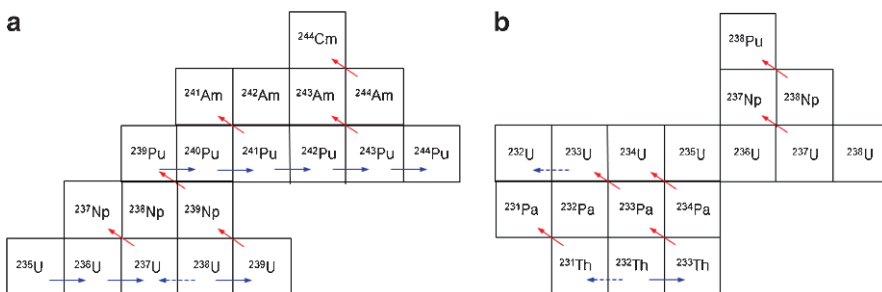

Fig. 32.4 *Charts illustrating the generation of actinides upon the irradiation of uranium (a) or thorium (b) nuclear fuel. The blue arrows pointing to the right indicate (n,γ) reactions, the diagonal red arrows indicate β⁻ decays, and the dashed arrows indicate (n,2n) reactions. Adapted from Brissot et al. (2001).*

Upon a series of neutron captures of ^{238}U and subsequent beta-decays some very long-lived actinides form, such as ^{239}Pu and ^{237}Np. When the fissionable fraction of ^{235}U in nuclear power plants is depleted the fuel rods are replaced and the residual spent nuclear fuel needs to be stored, reprocessed and disposed. Spent nuclear fuel contains roughly 96% uranium (the vast majority is ^{238}U), 1% plutonium, 0.1% minor actinides (neptunium, americium and curium) and 3% of fission products. Some actinides are formed by the decay of radionuclides present in spent nuclear fuel. For example, ^{241}Am is generated by the decay of ^{241}Pu and the fraction of ^{237}Np increases over time by the decay of ^{241}Am. These decay products determine the radiotoxicity of high-level radioactive waste beyond hundreds of thousands of years (see Section 32.4.3). In contrast to the uranium fuel cycle, the irradiation of thorium-based fuel generates far less amounts of cumbersome, long-lived actinides and thus reduces the long-term radiotoxicity of spent nuclear fuel (Demirbas, 2005). However, this route generates other radionuclides that may have a long-term environmental impact, such as ^{231}Pa, ^{229}Th and ^{232}U (Fig. 32.4, right). The generation of the relatively long-lived (about 27 days) ^{233}Pa and its ability to easily capture neutrons can affect the effective breeding efficiency and also require a longer cooling time for spent thorium fuel.

32.2.3 Actinide dispersions from nuclear weapons programs

Since the discovery of plutonium over 2,400 nuclear device detonations have been conducted worldwide. After the nuclear attacks on Hiroshima and Nagasaki in 1945, the predominant nuclear-weapons states, the United States and the Former Soviet Union, carried out a total of 1,054 and 715 nuclear weapons tests, respectively. An estimated 3,500 kg of plutonium has been released in atmospheric tests with an additional 100 kg released in underground tests.

In addition to the dispersion of radionuclides from nuclear weapons testing, transporting nuclear material around earth or into space poses the risk of accidental releases into the environment. Both the United States and Soviet Union space programs had accidents with their nuclear powered satellite systems. A total of about 4×10^{16} Bq ^{238}Pu was used by the United States space program. In 1964, a navigator satellite carrying the 6,300 GBq ^{238}Pu power unit SNAP-9A failed to stabilize in the earth orbit and re-entered the atmosphere at about 45 km over the Indian Ocean (SNL, 1964; Hvinden, 1978). The released ^{238}Pu, an estimated 17,000 Ci, was first detected 4 months later at an altitude of 30 km on particles with sizes ranging from 5 to 58 μm. The released ^{238}Pu activity was twice as high as the total activity dispersed by nuclear testing. This incident changed the ^{238}Pu/^{239,240}Pu ratio from about 0.024 to 0.034 in the Northern and to 0.20 in the Southern Hemisphere (Hardy *et al.*, 1973). In 1978, the Former Soviet Union Cosmos-954 satellite, containing kilogram quantities of highly enriched uranium, re-entered the earth atmosphere and disintegrated in large, radioactive fragments over Canada (Hvinden, 1978;

Krey *et al.*, 1979). The total amount of radioactivity released is estimated to be around 46,000 Ci (Bradley, 1997). In 1983, the Soviet RORSAT Cosmos-1402 satellite re-entered over the Indian Ocean and the core re-entered several days later over the Atlantic Ocean. The fuel containing highly enriched uranium disintegrated at high altitudes (Bradley, 1997). While no radioactive residues were found, the radioactivity released was estimated to be less than 15,000 Ci.

Some accidents of weapon-carrying airplanes reportedly resulted in the dispersal of weapons-grade plutonium into the environment. In 1960, a missile caught fire at the U.S. McGuire Air Force Base in New Jersey. The warhead partially melted and, although it did not explode, plutonium particles were dispersed during the fire into the environment (Lee and Clark, 2005). In 1966, considerable amounts of ^{239,240}Pu contaminated 2.26 km^2 of urban areas and farmlands near the Spanish village of Palomares upon the explosion of gunpowder in two hydrogen bombs that were released from a crashed airplane (Espinosa *et al.*, 1999; Aragon *et al.*, 2008). Contamination levels of above 1.2 MBq m^{-2} of alpha-emitting radionuclides in a 22,000 m^2 area were located in plants and soil to a depth of 10 cm. The site was remediated by soil removal. In January 1968, a US plane carrying four hydrogen bombs crashed on the sea ice near Thule, Greenland (McMahon *et al.*, 2000; Lind *et al.*, 2005); the aircraft and the chemical explosives of all four weapons exploded on impact. The detonation spread 10 TBq of plutonium on snow surfaces and an additional 1 TBq was estimated to be taken into ice. Measurable levels of plutonium were found at about 20 km from the crashpoint. It has been estimated that about 90% of the released plutonium was removed in clean-up operations. A residual of estimated 1 TBq ^{239,240}Pu remains in the seabed (Smith *et al.*, 1994).

Since the late 1960s no noteworthy accidental release of actinides during the transport of nuclear material has been reported. And since the late 1970s no releases from space power units are known to have occurred.

(a) Nuclear weapons testing

Historically, the major nuclear-armed states have been the United States, the former Soviet Union, France, China and the United Kingdom. Together, these countries performed 543 atmospheric nuclear weapons tests (UNSCEAR, 2000a). With 219 detonations, the former Soviet Union performed the largest number of atmospheric tests, followed by the United States with about 200 atmospheric tests between 1946 and 1962. France, China and the United Kingdom together carried out 88 atmospheric tests. The primary nuclear tests sites (Fig. 32.5) used by the United States were the Nevada Test Site (86 tests) and the islands in the Pacific Ocean, Christmas (24), Bikini (23) and Eniwetok (42); Semipalatinsk (116) and Novaya Zemlya (91) used by the Soviet test program; Lop Nor (22) for the Chinese tests; and Mururoa (37) in the Pacific Ocean used by the French testing program. These nuclear-induced explosions
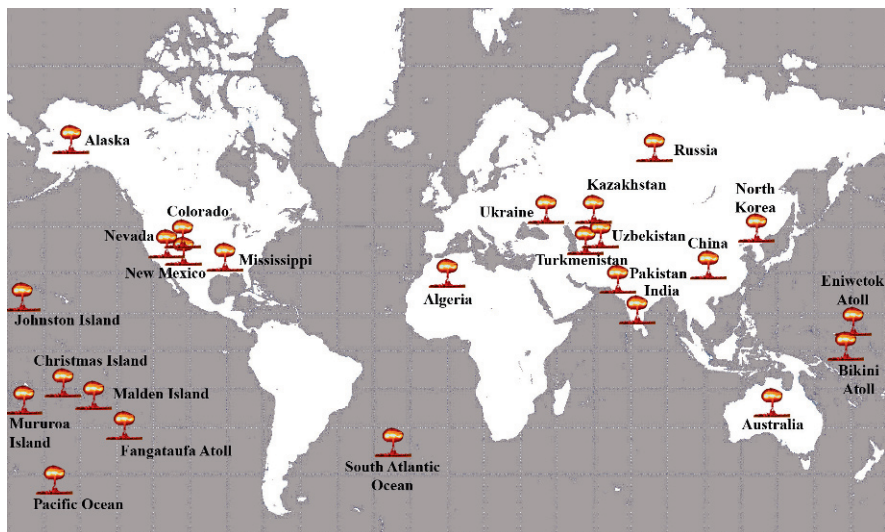
Fig. 32.5 *Locations of nuclear weapons test sites as listed in UNSCEAR* (2000a).

dispersed large amounts of radionuclides, primarily in the regions of their detonations, but also globally as fallout from the atmosphere. It has been estimated that these tests dispersed about 13 PBq of ^{239,240}Pu and 3.1 PBq of ^{241}Am into atmosphere and geosphere (Perkins and Thomas, 1980). About 40 TBq ^{237}Np were released globally by atmospheric nuclear weapons tests between 1945 and 1980 (Beasley *et al.*, 1998b).

The first injection of transuranium elements into the atmosphere occurred in July 1945 with the detonation of the first plutonium device at the Trinity Site near Alamogordo in New Mexico, USA. The device used about 6 kg of plutonium. The bomb dropped on Hiroshima on August 6, 1945 contained highly-enriched uranium and the second nuclear bomb detonated over Nagasaki 3 days later contained plutonium. Detonation events between 1945 and 1952 were low yield and contamination was confined to the troposphere. In 1952, a high neutron flux was created within the first thermonuclear fusion device (named *Mike*) on Eniwetok Island in the South Pacific, which yielded significantly more transuranium elements. Analysis of Mike debris showed that the ^{238}U in the device successively captured numerous neutrons to form the new isotopes of transuranium elements. At the time, ^{243}Pu was the heaviest known plutonium isotope, but ^{244}Pu and ^{246}Pu were found in the debris. Einsteinium and fermium were discovered and identified from daughter products in the debris (Ghiorso *et al.*, 1955). The largest detonation of a nuclear device was conducted in October 1961 by the Soviet Union on the island of Novaya Zemlya in the Barents Sea (Heylin, 1990; Khalturin *et al.*, 2005).

While large activities of radionuclides with mass numbers between 90 and 144 were produced by fission, very small amounts of the longer-lived actinide isotopes were dispersed. The United Nations Scientific Committee on the Effects of Atomic Radiation estimated the global release of plutonium isotopes in atmospheric nuclear testing to be 6.52×10^{15} Bq ^{239}Pu ($t_{1/2} = 24,110$ years), 4.35×10^{15} Bq ^{240}Pu ($t_{1/2} = 6,564$ years), and 1.42×10^{17} Bq ^{241}Pu ($t_{1/2} = 14.35$ years), compared to 6.75×10^{20} Bq of ^{131}I or 7.59×10^{20} Bq of ^{140}Ba (UNSCEAR, 2000a). The total effective doses from ^{239}Pu and ^{241}Am released in atmospheric testing are estimated at 18 and 15 μSv, respectively. Analysis conducted in 1989 suggested that global fallout from past testing accounts for only 1% of the annual mean dose of radiation exposure to humans.

After the atmospheric test ban treaty in 1963 the vast majority of underground testing was performed underground with 908 tests carried out by the United States, 750 tests by the former Soviet Union, and 160 tests by France (UNSCEAR, 2000a). Only France and China continued atmospheric testing until 1974 and 1980, respectively. Most nuclear weapons countries concluded their nuclear weapons test programs in the 1990s: the United States in 1992, the Former Soviet Union in 1990, the United Kingdom in 1991, and France and China stopped testing in 1996. Only India and Pakistan continued testing nuclear weapons up to 1998. The most recent nuclear test was announced by North Korea in May 2009. Most underground tests had a much lower yield than atmospheric tests, and the debris remained contained so that exposures beyond the test sites occurred only if radioactive gases leaked or were vented. Between 1951 and 1998 a total of 1,876 underground tests were carried out in seven countries (United States, Former Soviet Union, France, China, United Kingdom, Pakistan and India). Since the release of radionuclides from underground tests is very localized, the exposure dose has not contributed significantly to the total human exposure.

(b) Accidental releases from reactors

Windscale. The first significant emission of radioactivity after the discovery of plutonium occurred at Windscale in the United Kingdom. Two air-cooled graphite moderated reactors were constructed shortly after World War II and used between 1950 and 1957 to produce plutonium for the United Kingdom weapons program. The reactor fuel consisted of 180 metric tons of non-enriched uranium metal fabricated into aluminium-clad elements positioned within nearly 2,000 metric tons of graphite moderator. In 1952, two years after operations began, the release of excess Wigner energy trapped in the graphite caused a temperature increase in both reactors. Prior knowledge suggested that annealing graphite blocks would successfully release the energy. During an annealing procedure in October 1957 the reactor caught fire and extensively damaged the core. Both reactors were permanently shut down following the fire and the fuel was removed from both reactors (except for 15 metric tons of

damaged fuel in the core from reactor unit 1). This fire event is described in detail by Arnold (1995). The fire itself released an originally estimated 20,000 Ci of radioactive material into the nearby countryside and radioactivity was blown east over Belgium, Holland and Germany, and north over Scandinavia (Fig. 32.6). Recent re-analysis of air, grass and vegetation data suggested a higher release of radioactive material than previously estimated (Garland and Wakeford, 2007; Smith *et al.*, 2007). These studies confirmed that radioactive ^{131}I and ^{137}Cs were released, as well as ^{210}Po and a very small amount of plutonium. While there are sufficient measurements of ^{131}I, ^{137}Cs and ^{210}Po to establish emissions, fewer measurements for the actinides create a larger uncertainty on their emission estimates. It is reasonable to conclude that the magnitude of the release of irradiated uranium oxide particles from the Windscale fire is probably less than the value of 20 kg used in assessments of the impact of this release (Smith *et al.*, 2007). This conservative estimate is still only 1/1,000 of the amount of uranium involved in the fire, because the sintering of the uranium oxide fuel prevented the formation of fine, dispersable particulates. A revised estimate of the ^{239}Pu emission is 0.02 TBq (Garland and Wakeford, 2007; Jones, 2008). Most of the radioactive materials released have decayed and pose no ongoing risk, but small quantities of cesium and plutonium remain. Until Chernobyl (see below), this event, known as the Windscale fire, was considered the world's worst reactor accident releasing substantial amounts of radioactive contamination into the surrounding area.

Three Mile Island. The Three Mile Island accident had a very significant impact on public perception about the commercial nuclear power industry in the United States even though it did not lead to any deaths, injuries, or elevated cancer rates to plant workers or nearby communities. The Three Mile Island nuclear reactors consist of two pressurized water reactors. In 1979, Unit 2 of the nuclear power plants experienced a failure in the main cooling water pumps, preventing the steam generators from removing the generated heat. Due to inadequate cooling the nuclear fuel overheated and the fuel pellets began to melt, despite the fact that the reactor shut itself down. The partial core meltdown did not and could not lead to a breach of the containment building. An estimated 34,000 Ci of radioactive ^{85}Kr and about 16 Ci of ^{131}I were emitted from the fuel elements (NRC, 2007); actinides were not released in any significant quantities since they remained part of the intact and melted core. The Three Mile Island accident permanently changed both the nuclear industry and the Nuclear Regulatory Commission (NRC) regulations. In fact, the NRC has not approved an application to build a new nuclear power plant in the United States since the accident at Three Mile Island.

Chernobyl. The most serious accident and the most extensive release of radioactivity into the environment in the history of nuclear power occurred at the Chernobyl nuclear power plant, located approximately 100 km north of Kiev in the Ukraine. The reactor had been operated since 1983 and huge amounts of fission products had been stocked in the core. At the time of the
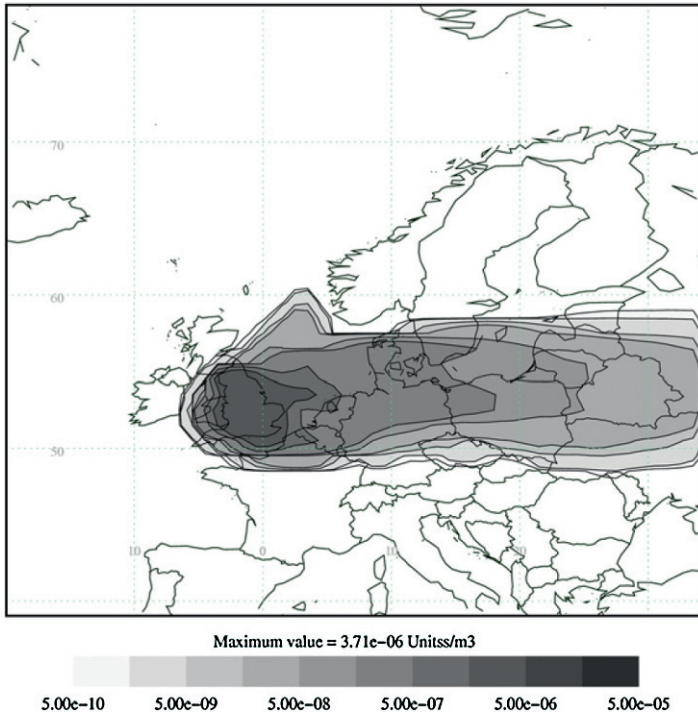
Fig. 32.6 *Modelled time-integrated* ^{131}I *radioactivity concentration* $(Bq\ m^{-3})$ *from October* 10 *to noon on October* 15, 1957. *The plume created by the Windscale fire covered England and Wales, Southern Scotland and extended to large areas of Western Europe* (*Johnson et al.*, 2007). *Reproduced by permission of Elsevier.*

accident about 5.37 MBq ^{238}Pu, 4.54 MBq ^{239}Pu, 6.33 MBq ^{240}Pu and 0.99 MBq ^{241}Am were inventoried in the reactor fuel per gram of UO_2 (Bogatov, 1998). On April 26, 1986 mistakes made by operating personnel during a low-power engineering test put Unit 4 of the reactor site in an unstable regime. Two explosions destroyed the reactor core and subsequent fires severely damaged the reactor building. The released energy shifted the 1,000 million metric ton cover plate of the reactor, and pieces of the core were ejected from the reactor. Large amounts of volatile radionuclides were released during the intense graphite fire within the first 10 days of the accident until the reactor core was contained in cement. About 96% of the transuranium elements (approximately 180 metric tons of irradiated UO_2 fuel with over 20 MCi total activity) were captured in the cement sarcophagus (Bradley, 1997). With the pillars of smoke and steam from the damaged reactor core tens of thousands of curies were emitted into the atmosphere in the form of gas and particulates. Wind carried the radioactive plume first north and then west/southwest. About 70% of the

radioactivity released was deposited in Belarus and an estimated 0.2 GBq of ^{237}Np and 1.5 TBq of ^{239,240}Pu were carried to the Baltic Sea (Holm, 1995). The increased radioactivity levels were first measured outside the Former Soviet Union 110 km north of Stockholm in Sweden.

The total releases are estimated to be about 1–2 EBq with ^{131}I, ^{134}Cs and ^{137}Cs as the main radionuclides (UNSCEAR, 2000b). Comparably much smaller amounts of transuranium elements reached the environment. An estimated 3% of the core inventory was released from the accident, carrying ^{239}Np (1.2 MCi), ^{238}Pu (800 Ci), ^{239}Pu (700 Ci), ^{240}Pu (1,000 Ci), ^{241}Pu (140,000 Ci), ^{242}Pu (2 Ci), and ^{242}Cm (21,000 Ci) into the environment (Bradley, 1997). The closest surroundings of the Chernobyl reactor were contaminated with particulates released from the fragmented reactor fuel formed from grains of UO_2 (Bogatov, 1998). These heavy particles (10–15 μm) were measured to contain ^{238}Pu (6.9 × 10^6 Bq per particle), ^{239,240}Pu (1.5 × 10^7 Bq per particle), ^{241}Am (5.0 × 10^6 Bq per particle), and ^{244}Cm (1.5 × 10^6 Bq per particle). In fact, the majority of the released plutonium was deposited in the near surroundings of the plant (Fig. 32.7). However, the deposition of nuclear fuel particles containing ^{239,241}Pu increased the radioactivity level to about three orders of magnitude higher in the 30 km exclusion zone around the reactor compared to normal environmental standards. Radioactivity levels for plutonium reached 2.3 Ci km^{-2} within a 1 km radius around the Chernobyl site, gradually decreasing to about 0.2 Ci km^{-2} within a radius of 15–30 km (Bradley, 1997). Recently, the contamination level of ^{239,241}Pu in soils was reported up to 7.4 × 10^5 Bq m^{-2} (Matsunaga *et al.*, 2004).

(c) Releases from processing plants

The anthropogenic actinides in the northern hemisphere mainly originated during nuclear weapons testing, fallout from the reactor accident at Chernobyl and intentional discharges of liquid waste streams from industrial-scale nuclear reprocessing facilities. The most prominent nuclear material processing plants have been: the Hanford, Rocky Flats and Oak Ridge sites in the United States, Sellafield in the United Kingdom, La Hague in France, and Mayak and Tomsk in the Former Soviet Union. Most of these facilities were established to process spent nuclear fuel for the separation of plutonium for weapons programs. Table 32.3 summarizes releases of actinides from major nuclear weapons material production and processing plants around the world. Most of the radioactivity releases reported in the open literature concern ^{137}Cs, ^{90}Sr, ^{24}Na, ^{131}I, and some other fission products, while reliable data on actinide releases remain fragmented. During early operations significant volumes of high-level wastes and highly contaminated solvents were discharged directly into ground or marine environments. For a detailed review of the releases of radioactivity into the environment in the former Soviet Union the authors refer to Bradley (1997).
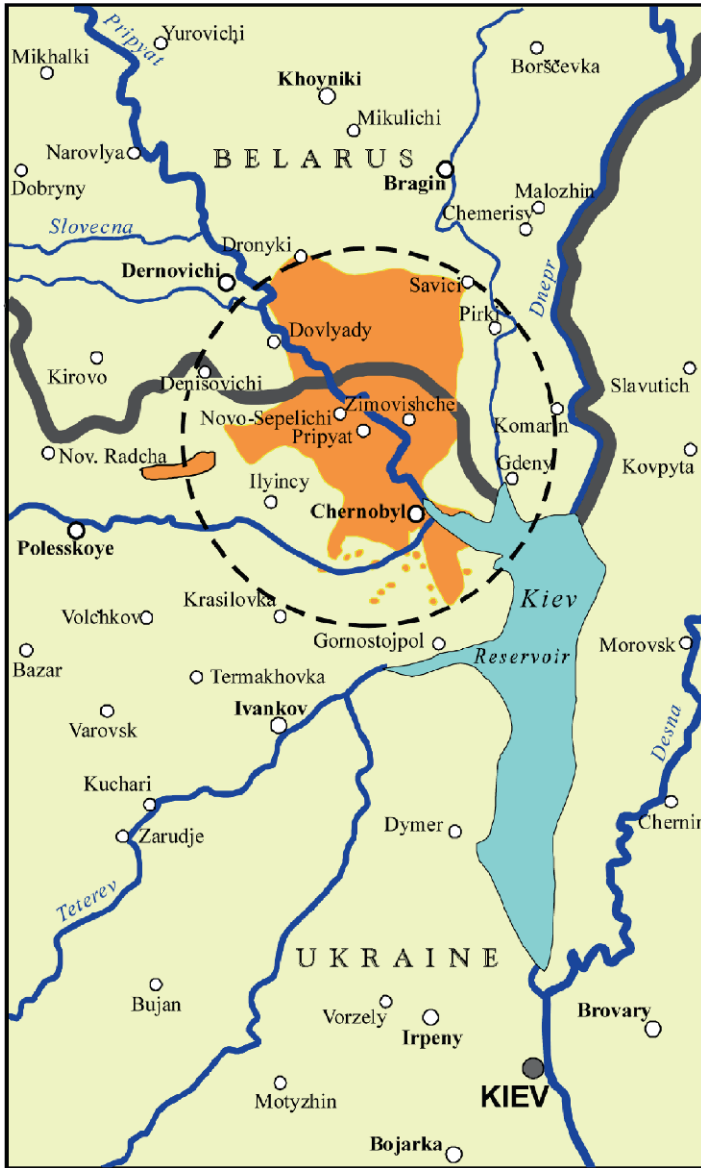
Fig. 32.7 *Plutonium contamination map of the vicinity of Chernobyl* (*UNSCEAR*, 2000b)*. The dashed circle represents the* 30 *km radius where plutonium contamination was measured above* 4 *Bq m^{-2}. Plutonium contamination was greatest within a radius of about* 2.3 *km around the reactor site.*

Table 32.3 *Actinide releases from nuclear weapons material production and fabrication plants (Bradley, 1997; UNSCEAR, 2000a; Choppin et al., 2002).*

Location	Release period	Airborne release (GBq)	Liquid release (GBq)
Fernald	1954–1980	50–150 GBq (U)	
Rocky flats	1953–1983 (Routine)	8.8 GBq (U), 1.7 GBq (Pu)	
	1957 (Fire)	1.9 GBq (Pu)	
	1965–1969 (Storage)		260 (Pu)
Hanford	1951		>7,000 kg U
Savannah River	1954–1989	140 GBq (Pu)	23 GBq (Pu)
Sellafield	1985–1994		15 TBq (^{241}Pu)
LaHague	1995–1999		21,800 GBq (^{241}Pu)
			310 GBq (^{241}Am)
Chernobyl	1986	2 GBq (^{242}Pu)	
Mayak[a]			74 Ci (Pu)
Tomsk-7[a]			20 Ci (Pu)
	1993	0.13–0.59 Ci (^{239}Pu)	
Krasnoyarsk-26[a]			51 Ci (Pu)

[a] Total amounts of radioactivity released from Russian nuclear weapons production sites released to rivers or lakes (Bradley, 1997).

La Hague and Marcoule, *France*. The COGEMA nuclear fuel processing plant in La Hague has been operating since 1976 and has a processing capacity of about 1,700 metric tons of spent nuclear fuel per year. In 2005 the plant processed 1,100 metric tons of spent nuclear fuel from several European countries. To date, more than 10,000 metric tons of light water reactor fuel have been processed at La Hague. The major concerns for radioactivity release into the environment are related to beta- and gamma-emitting radionuclides, such as ^{85}Kr, ^{3}H, ^{129,131}I or ^{14}C, and to a much lesser extent the actinides. For 2007, AREVA reported the release of liquid discharge containing 0.0213 TBq of alpha-emitting radionuclides compared to 12,000 TBq tritium, 1.4 TBq iodine isotopes and 1.0 TBq ^{137}Cs (AREVA, 2007). In comparison, reprocessing of nuclear fuel for defense purposes at Marcoule resulted in significant releases between 1961–1969 and 1975–1991. Annual discharges into the Rhone River of 0.7–4 GBq year^{-1} ^{238}Pu and up to 70 GBq year^{-1} ^{239,240}Pu in the 1960s and around 6 GBq year^{-1} ^{238}Pu and 20 GBq year^{-1} ^{239,240}Pu between 1978 and 1991 were reported (Lansard *et al.*, 2007). Between 1945 and 1998, the Rhone River received a total of 628 GBq ^{238,239,240}Pu, of which 85% (533 GBq) derived from liquid discharges. Accounting for only about 2% of the regional plutonium inventory, the releases from Marcoule resulted in the deposition of 2.8 GBq of plutonium close to the facility (Duffa and Renaud, 2005).

Seversk/Tomsk-7, Russia. The world's largest discharges of radioactive effluents into the environment have occurred at the Soviet reactor site 15 km northwest of the city Tomsk. The Siberian Chemical Combine (SCC), founded in 1954 and located in Seversk (formerly known as Tomsk-7), is Russia's largest plutonium production and processing complex with five reactor plants, several facilities for processing and enrichment, and storage facilities for radioactive waste. Tomsk-7 was established in 1949 to produce plutonium for the Soviet weapons program, but the reactors also provided 350 MW electric power for the site and the cities of Seversk and Tomsk (Bradley, 1997). Nuclear materials from both sites at Mayak and Tomsk were processed in the facilities at Tomsk. Inadequate management of liquid waste streams resulting from reprocessing spent nuclear fuel was the largest source for environmental contamination. Over 20 accidents have occurred at the SCC that resulted in significant releases of radioactivity to the environment. Since 1956, contaminated cooling water has been released into the Tom and Romashka rivers. Since 1963, an estimated 4×10^{19} Bq of long-lived radionuclides in liquid waste streams have been injected in 280–400 m deep boreholes about 20 km east of the Tom river (Lgotin and Makushin, 1998). The most serious accident at SCC occurred in 1993 when an explosion caused the rupture of the U/Pu extraction line of a storage tank that contained partially processed actinide salts, paraffin and tri(*n*-butyl) phosphate. The 34 m^3 storage tank had a reported inventory of 25 m^3 solution with 8,773 kg of uranium, and about 310 kg plutonium with a total radioactivity of 559 Ci (IAEA, 1998). Estimates of the total release of radioactivity caused by the explosion and fires accounted for up to 1,000 Ci of beta- and gamma-emitting radionuclides and up to 0.59 Ci of ^{239}Pu. The accident reportedly led to soil contamination between 10 and 13 Bq kg^{-1} at the time (Tcherkezian *et al.*, 1995). Highest contamination levels in topsoil reached up to 1,100 Bq m^{-2} at the time and the ^{238}Pu/^{239,240}Pu ratio of (0.35 ± 0.07) indicated that the source was partially burned nuclear fuel. Interestingly, official documents did not report any releases of ^{137}Cs or ^{241}Am. Gauthier-Lafaye *et al.* (2008) reported actinide inventories in soil that reached 5,900 Bq m^{-2} for ^{239,240}Pu and 1,220 Bq m^{-2} for ^{241}Am. The isotope signatures are in agreement with that of weapons grade plutonium material. The plants at Seversk and Mayak are thought to be the main sources for the massive contamination of many aquifer systems in Siberia and the Urals. Bradley (1997) estimated that together they released about 4.6×10^{19} Bq radioactivity into the Ob aquifer.

Kyshtym-Mayak, Russia. The Mayak plutonium production complex was established in 1948 with seven nuclear reactors and two reprocessing plants to produce plutonium for the Soviet nuclear weapons program. The site is located about 2,800 km from the Kara Sea near the city of Kyshtym and about 70 km north of the city Chelyabinsk in the southern region of the Ural in Russia, within the catchment of the Techa river. Routine and accidental discharges led to severe contaminations of Mayak's surrounding area. Several releases of large amounts of radioactive material occurred at the Mayak site. In 1957, a 300 m^3

tank containing radioactive waste exploded (Myasoedov and Drozhko, 1998). The explosion released about 90% (900 PBq) of the tank inventory, which was dispersed by wind to a 300 km area down-wind over the following 11 h. Although the explosion released about 44,300 Ci radioactive material, only trace amounts of ^{239,240}Pu were released (Jones, 2008). At least 130 MCi of radioactivity has been released directly to the environment around Mayak (Bradley, 1997). Christensen *et al.* (1997) provide an overview of the accidents and radioactive waste inventory at the Mayak reprocessing plants.

Sellafield, United Kingdom. Since its opening in 1952 the Sellafield reprocessing facility has intentionally released radioactive waste streams into the Irish Sea (Gray *et al.*, 1995). A large number of studies have investigated actinide concentrations in seawater, sediments and biota from the Irish Sea. The waste contained large quantities of ^{237}Np, various isotopes of plutonium and other radionuclides. As a result of the releases, the ^{237}Np in the Swedish–Danish waters are largely assigned to Sellafield's discharges. Between 1967 and 1999, 9.5 TBq of ^{237}Np (Beasley *et al.*, 1998a; Assinder, 1999) and a total of 120 TBq ^{238}Pu and 610 TBq ^{239,240}Pu (Jones and McDonald, 1994; Jones *et al.*, 1996) was estimated to have been released into the marine environment. Since the Enhanced Actinide Removal Plant was established in 1994 the ^{237}Np discharges decreased by a factor of 10, to roughly up to 1.5 mBq m^{-3}. The ^{237}Np activities decrease from north to the south due to the dilution of Sellafield discharges with water from the Baltic Sea (Lindahl *et al.*, 2005).

Rocky Flats, United States. From 1952 to 1989 the Rocky Flats Plant, located northwest of Denver in Colorado, fabricated uranium and plutonium components for the U.S. nuclear weapons program. During plant operations radioactivity was released into the environment on several occasions upon improper disposal of contaminated materials, leaking or ruptured pipes, or fires at processing facilities. Fires in 1957 and 1969 contaminated several buildings used to handle radioactive material and releasing radioactive plumes into the atmosphere. During the late 1950s and1960s improper storage of radioactive waste barrels caused radioactivity leaking from waste barrels into the soil, which partly became air-borne from the area. Much later, waste drums stored at the site leaked radioactivity, then wind and water carried plutonium and americium in a well-defined pattern to the east and southeast (Fig. 32.8). It was estimated that about 20 m^3 of plutonium-contaminated oil from machining operations containing up to 5 Ci of plutonium were released to the soil (Efurd *et al.*, 1993; Clark *et al.*, 2006). As a consequence, elevated levels of tritium, plutonium and americium were measured in air, soil and water around the site.

Hanford, United States. In 1943 the United States government chose the Hanford Nuclear Reservation Site to make plutonium for the atomic bomb. In both events in 1945, the first atomic explosion test at Alamogordo, New Mexico, in the United States and the bomb dropped on Nagasaki, Japan, contained plutonium that was made at the B Reactor at the Hanford site. Up to the cessation of plutonium production in 1987, more than 100,000 metric
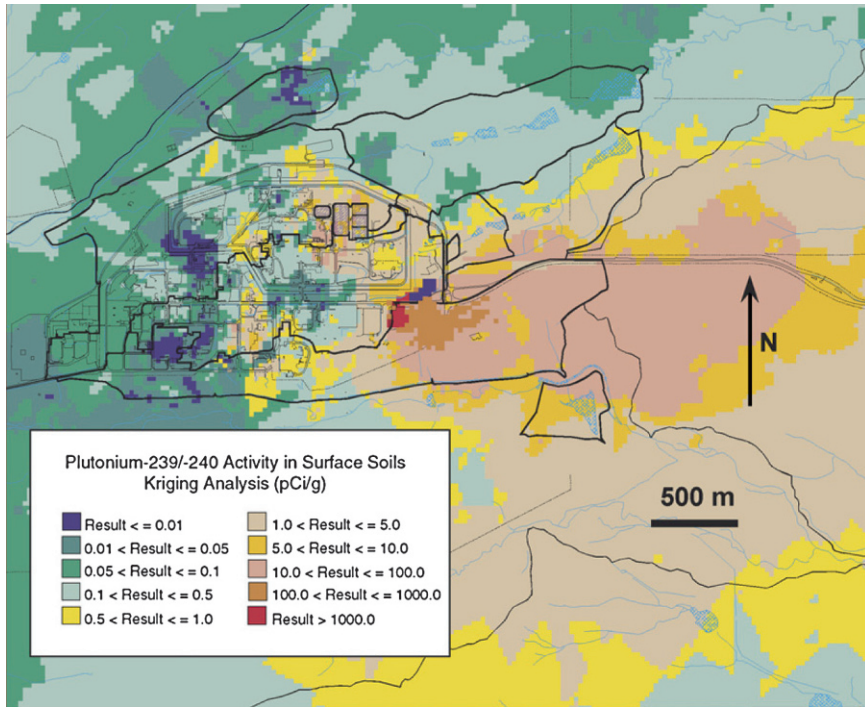
Fig. 32.8 *Estimated concentrations of plutonium contamination in surface soil at Rocky Flats, CO, now remediated (Clark et al., 2006a). A clear plume of $^{239/240}$Pu contamination tracks roughly with the prevailing winds from NW to SE is evident from the data. The "hot spot" of $^{239/240}$Pu with concentrations in excess of 1,000 pCi g^{-1} from leaking waste drums is shown in red. Reproduced by permission of the American Institute of Physics.*

tons of uranium spent fuel were processed at the Hanford site (DOE, 1999). Over 200 radionuclides were released into the air, water and soils at the site. Most of Hanford's air releases were during routine operations of the facilities to separate uranium from plutonium in used reactor fuel (DOE, 1999; Alvarez, 2005; Berkey and Zachry, 2005; McKinley *et al.*, 2007). The largest chronic air releases occurred before 1957 due to the absence of air filters on stacks of the separation plants. Large releases into the air during 1944–1972 were estimated for ^{131}I (740 kCi), ^{85}Kr (19 MCi), while only 1.8 Ci of ^{239}Pu was estimated to be air-released. The most significant air release occurred in December 1949, when between 7 and 12 kCi of ^{131}I were released during a secret United States Air Force experiment, referred to as "Green River". It involved processing of uranium fuel that had been cooled only for 16 days, compared to the usual 90–100 day cooling period, which would allow short-lived radionuclides to decay to lower levels.

There have been significant releases of radionuclides into the soil and water systems at Hanford. Early on, cooling water from the first eight nuclear reactors

carrying radioactivity was released to the Columbia River. Major radionuclides included ^{65}Zn (490 kCi), ^{24}Na (13 MCi) and also the short-lived ^{239}Np (6.3 MCi). The separation plants used large amounts of water to process used nuclear fuel and an estimated 1.66×10^{12} L of radioactive waste waters were dumped into the ground or in injection wells or shafts drilled deep into the ground. In 1951, a ruptured pipe caused about 350,000 L of alkaline waste, which contained a mixture of inorganic agents such as sulfate, phosphate, carbonate, and nitrate, to reach and contaminate the environment with more than 75,000 kg of uranium (McKinley *et al.*, 2007). Between 1943 and 1975 process ponds at the site received about 58,000 kg of uranium from which uranium could leach into the underlying aquifer and into the nearby Columbia River resulting in a groundwater plume that persists today (Fig. 32.9).

Presently, about 200 MCi in 204,000 m^3 of highly radioactive wastes from the early separation operations are stored in 177 tanks at Hanford. While over 96% of the radioactivity is from ^{137}Cs and ^{90}Sr, it also contains large inventories of protactinium (270 Ci), uranium (988 Ci), thorium (34 Ci), neptunium (133 Ci), plutonium (210 kCi), americium (143 kCi), and curium (444 Ci) (Alvarez, 2005).

Tricastin, *France*. Tricastin in south-eastern France is a large nuclear site with four power reactors, the Comhurex uranium conversion plant, the Eurodif enrichment plant and the Pierrelatte weapons facility. On July 7, 2008, about 30,000 L of stored decontamination solution containing 12 g L^{-1} of natural uranium were accidentally released due to an overflowing storage tank. Most of the solution was stopped by the holding tank's containment systems, but about 74 kg of natural uranium was released to the environment (AREVA, 2008; IRSN, 2008b). An immediate monitoring plan was implemented, which showed that the nearby rivers Gaffière and Lauzon contained elevated uranium levels and the radioactivity in ground and surface waters were found to be about 5% above the maximum allowed levels. In response, French authorities banned the use of water from the rivers Gaffière and Lauzon for drinking and watering crops. Measurements continued for about 2 weeks until the ban was lifted on July 22, 2008 subject to an extended monitoring plan (IRSN, 2008a). While this was the largest accidental release of actinides into the environment since Chernobyl, the released radioactivity level is orders of magnitude lower than previous incidents demonstrating the dramatic shifts in worldwide practices and environmental stewardship since the early 1980s.

(d) Releases from storage containment

Radioactive wastes created throughout the last 50 years have been stored in large tanks above and underground at sites worldwide. In the United States, highly alkaline wastes are stored in tanks at the Department of Energy sites at Hanford, Savannah River, Idaho, and Oak Ridge (OTA, 1991; Bearden and Andrews, 2007). Many of these holding tanks containing the actinides in large quantities from early separation processes were commissioned decades ago, and
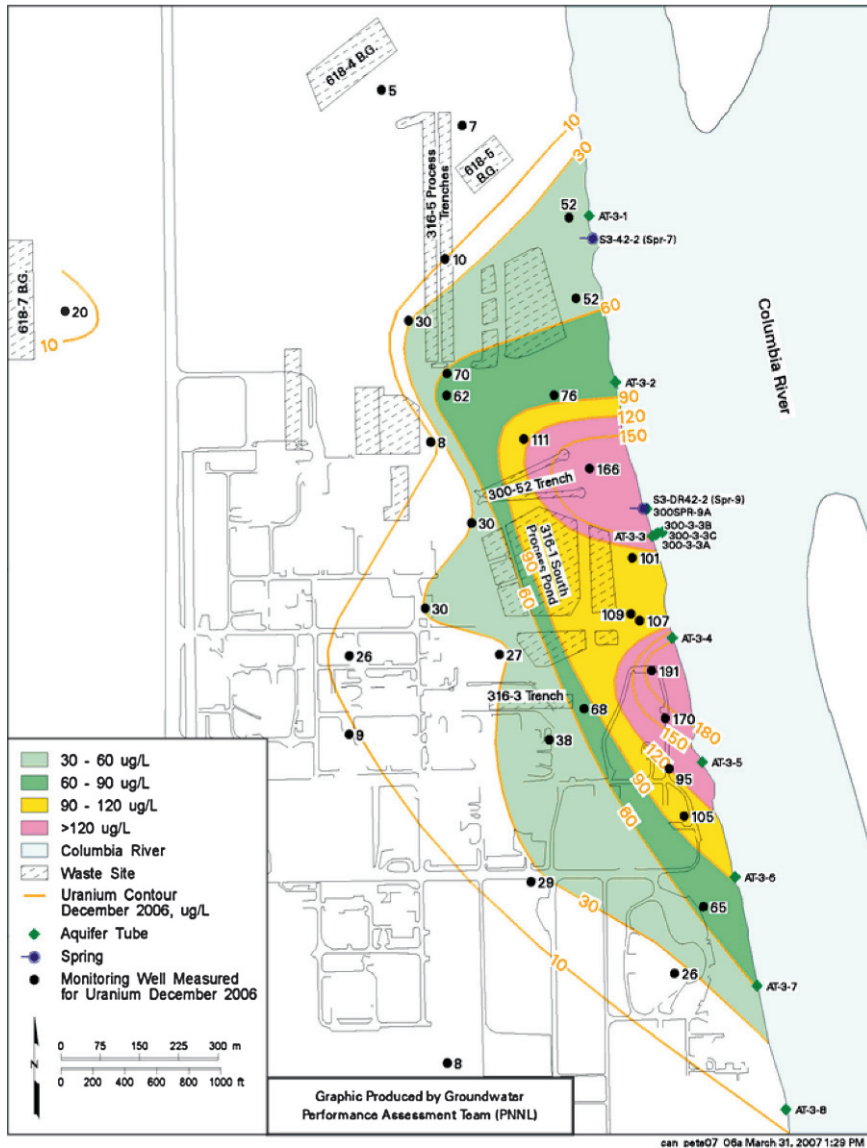
Fig. 32.9 *Illustration of the uranium contamination within the Hanford Site* 300 *area aquifer as of December* 2006 (*Wellmann et al.*, 2008). *Reproduced by permission of WM Symposia, Inc.*

are known or suspected to have leaked radioactivity into the environment and in nearby rivers. Most problematic is the situation at Hanford where 67 tanks are believed to have developed leaks.

Between 1949 and 1981, an estimated 2 kCi of actinides and ^{99}Tc in about 200 million liters of radioactive waste have been transferred into 149 single-shell and 28 double-shell storage tanks at the Hanford site, to contain between 540–860 kg of plutonium and 30 kg of americium (Agnew, 1995). The inventory of ^{237}Np in Hanford tanks is estimated to be between 50 and 100 kg. Over the years more than 4 million liters containing over 100 kCi have leaked into the Hanford soil. Some radionuclides still found in groundwater and soils at the Hanford site are ^{3}H, ^{106}Ru, ^{99}Tc, ^{129}I. Between 1954 and 1970 about 65,000 m^3 of transuranic solid waste was buried in the Subsurface Disposal Area at the Idaho National Engineering and Environmental Laboratory (Markham *et al.*, 1978). Approximately 4,000 m^3 of which is calcined solid waste stored in seven stainless steel tanks in massive underground concrete enclosements. An additional 4.5 million liters of acidic radioactive liquid waste is stored in 11 stainless steel tanks. At the Savannah River Site 140 million liters of actinide containing salt, salt solution and sludges are stored in 49 tanks.

High-Level radioactive wastes were also stored at Russian tank farms (Bradley, 1997). In 1991, an estimated 900 MCi of liquid high-level waste was stored in tank farms at the Russian Mayak site. More than 25,000 m^3 of liquid high-level waste have been accumulated over 40 years of processing. About 6,000–7,000 m^3 of wastes are stored in evaporated acid solutions in stainless steel tanks. Currently, 90 tanks exist at Mayak with 300–1,500 m^3 sludges and up to 12 MCi radioacticity each. Some tanks have wastes consistencies very similar to some existent at Hanford. At Krasnoyarsk-26, 36 stainless steel tanks are used to store underground 10,000 m^3 of high-level radioactive sludge. All the wastes stored in these tanks are acidic. As in the United States, many of these tank farms are aging and several tanks have been reported to leak radioactivity into the environment. A classification of wastes stored at Russian tank facilities can be found in Bradley (1997).

32.3   FATE AND TRANSPORT OF ACTINIDES IN THE ECOSPHERE

Nuclear weapons production yielded large actinide inventories and large volumes of wastes that were both intentionally and accidentally released into the environment, generating problematic contamination. That legacy contamination is slowly being addressed, site by site, differently in each country. The build-up of nuclear power plants worldwide depends on utilities and governments minimizing the environmental impacts of the fuel cycle – from uranium and thorium mining, to fuel processing, interim storage of byproducts, and final waste disposal.

Modern mining, enrichment, and fuel fabrication technologies have greatly reduced environmental releases of thorium and uranium isotopes relative to past practices that created large quantities of tailings and acidic byproducts. In many case large quantities of actinides leached into the environment.

Fuel processing will involve higher actinide inventories and a greater range of radionuclides in the future as traditional fuels are being burned longer and as fuels contain more neptunium and plutonium. Reprocessed fuels will contain heavier actinides and therefore produce greater quantities of fission products and neptunium, americium and curium. Nevertheless, modern processing technologies have not released significant quantities of actinides into the environment.

At the back end of the nuclear fuel cycle, spent nuclear fuel and separated byproducts are stored first in above ground or shallow repositories in the form of fuel or vitrified glass. Initially conceived to last a few to 50 years, it is now predicted that this interim storage will have to last for up to hundreds of years. Most countries intend to ultimately dispose of fission products and longer-lived actinides in deep geologic formations, and some countries may also dispose of spent fuel in the same repositories. The performance of longer-term storage and final disposal sites is defined by the retention of these byproducts for millions of years. Certification of the repositories depends upon effective retention of radionuclides from the near-field of the repository containing spent fuel, separated processed waste, or waste in vitrified glass, with or without added engineered barriers and backfill materials. Given the long time frames to be considered and the fact that these radionuclides are not found naturally, the behavior of actinides must be predicted from analog studies (such as the Oklo reactors), experiments and models that combine the properties of the actinides in the waste form, the characteristics of the repository and near field, the geologic, chemical and biologic nature of the near field and far field, and intrusion or other release scenarios. The same general approach is taken to predict the mobility of legacy environmental contamination.

32.3.1 General approach to predicting actinide mobility

The ability to predict the fate and transport of actinides in the environment is important both to address past contamination and to know the environmental impact of increasing nuclear energy generation. In general, reductionism is used to understand and predict the fate and migration of actinides in environmental systems. This begins by characterizing the geology and geochemistry of the contaminated site, fuel/waste repository site, or mining formation, and setting realistic boundary conditions derived from the site characteristics, e.g. rock fracture characteristics, predominant mineral compositions, extent of water saturation, pH range, dissolved gas concentrations, composition and salinity of the solution phase, etc. Then, processes and mechanisms that will affect the actinide solubility, speciation, and mobility are separately, quantitatively studied in laboratory settings, e.g. the solubility of the controlling actinide phases, the thermodynamic stability of binary and ternary actinide–ligand complexes, the absorption affinity and capacity of predominant mineral surfaces and particulates, etc. In addition, characteristics of the source term must be

considered. For example, dilute actinides in thousands of liters of strong acid solution leaked to unsaturated conglomerate rock 100 m below the surface will behave differently from small solid actinide particles released to surface soil and aquifers or to air during a very high-temperature fire. Ultimately, predictions of actinide mobility are generated from hydrogeochemical models. The models themselves are comprised of fundamental processes, input site characteristics, and physical and chemical parameters determined from laboratory-scale studies, and tested against field-scale observations.

The following sections present what most researchers and regulators believe are the most important processes and conditions that affect environmental actinide migration. Illustrative examples of simplified systems, discrete types of environments, and observations made at contaminated sites and aquifer systems worldwide are given. We also provide a brief description of general geochemical conditions, followed by fundamental properties and reactions of actinides that are relevant to the very diverse conditions present in the environment. Comprehensive reviews of the processes and data can be found in specialized reviews, book chapters, and books, including the extensive OECD/NEA critical review series (11 volumes to date) on chemical thermodynamics, and detailed descriptions of contaminated sites and proposed repositories.

32.3.2 Geochemical characteristics

The fate of actinides in the environment depends firstly on the geochemistry and geology of the site. The environment is a complex, elaborate system and the hydrogeological properties at the various sites, both contamination areas and disposal or storage sites, are quite diverse. For details on the mapping and unique, site-specific geologic characterizations of the many disposal sites in countries worldwide we refer to monographs such as that edited by Witherspoon and Bodvarsson (2001).

Water is recognized as the dominant transport medium for most elements in the environment (Stumm and Morgan, 1995) and it exhibits important boundaries that define allowable actinide oxidation states and the prevailing species. The physical and chemical properties of natural aquifers can be quite different. Compared with the extreme pH values and ionic strengths that can be adjusted in the laboratory, most natural waters are relatively mild, typically nearly neutral (pH 5–9) with a wide range of redox potentials (from -300 to $+700$ mV) and low salinities (ionic strength below 1 mol kg^{-1}) (Baas-Becking *et al.*, 1960). Although the method of Eh measurements and thus the accuracy of individual data points can be disputed, the trend clearly indicates higher pH values (6–9) for waters excluded from the atmosphere (Eh values below about 200 mV) and lower pH (about 4–8) for waters in contact with the atmosphere. Waters of high ionic strengths show an increased pH of about 7.4 for seawater and up to 10 for the most concentrated brines. A thorough discussion and

review of the redox chemistry of natural waters are given by Fish (1993), Langmuir (1997), Stumm and Morgan (1995), and Wanty (1999).

Bicarbonate or carbonate compete with hydroxide to complex actinide ions. In fact, at near-neutral conditions carbonate complexes of the actinides are found (i.e. $UO_2(CO_3)_3^{4-}$, $NpO_2CO_3^-$, and $Am(CO_3)^+$) to be stable in the absence of strong, multidentate, organic chelators. Most natural aquifers contain carbonate in the range between 0.1 and 10 mmol L^{-1} (Stumm and Morgan, 1995; Langmuir, 1997). As an example, the characterization of groundwaters from the German Gorleben site showed that the bicarbonate concentration ranges between 1 and 10 mmol L^{-1} (Kim, 1993). The (bi)carbonate concentration in groundwater varies with the CO_2 partial pressure (p_{CO_2}) and the pH as described in equations (32.2) and (32.3):

$$\log[HCO_3^-] = \log K^* + \log p_{CO_2} + pH \qquad (32.2)$$
$$\log[CO_3^{2-}] = \log K^{**} + \log p_{CO_2} + 2pH \qquad (32.3)$$

where K^* and K^{**} contain the Henry's constant and the proton dissociation constants. The average CO_2 partial pressure of about 0.01 atm as found in Gorleben goundwaters is significantly higher than the atmospheric CO_2 partial pressure of 3.5×10^{-4} atm. This translates to a carbonate concentration in groundwater that is sufficient to dominate actinide speciation. Detailed reviews of the carbonate chemistry in natural waters can be found in Stumm and Morgan (1995) and Langmuir (1997).

Many other inorganic ligands such as fluoride, sulfate, silicate, or phosphate can play a role by forming complexes with actinides, but outcompete hydroxide and carbonate only under exceptional site-specific circumstances. Among the many inorganic ions present in nature, chloride is most important because of its high concentrations in brines found around geological salt formations that have been proposed as radioactive waste disposal sites. Chloride can significantly alter actinide speciation by forming mixed chloro-hydroxo or chloro-carbonato complexes at near-neutral pH or by altering the nature of the actinide solubility-controlling solid. In moderately-high to high radiation fields the radiolytically-induced formation of oxidizing agents, i.e. hypochlorite, may affect the oxidation state stability of neptunium, plutonium or americium. The high ionic strengths of such brines also suppress the solubility of larger-sized humic colloids. Laboratory and simulated field studies have given ample evidence for the impact of chloride on actinide speciation and solubility (Magirius *et al.*, 1985; Büppelmann *et al.*, 1988; Choppin and Du, 1992; Pashalidis *et al.*, 1993; Neck *et al.*, 1995b; Runde *et al.*, 1996).

Organic chelating molecules are in the environment as small, molecular and macromolecular plant byproducts, ranging from molecular citrate and oxalate to macromolecular, polyelectrolytic humic substances. In addition, redox agents and complexing ligands, such as hydroxylamine, nitrilotriacetic acid (NTA), ethylendiaminetetraacetic acid (EDTA), dibutylphosphate (DBP), and tri(*n*-butyl) phosphate (TBP) used in plutonium processing are common to

coexist with the actinides in wastes effluents. Both the naturally occurring organics and anthropogenic chelators can complex the actinides. Depending on the charge and molecular weight of the resulting actinide–chelate complex and the ionic strength, particulate concentration, and surrounding mineral surface properties, the complex will precipitate, adsorb to surfaces, or persist in the solution phase. Oxalate and DBP are examples for agents that form less-soluble complexes (Keiling *et al.*, 1988; Keiling and Marx, 1991). The concentration of such small organic species is relatively low in natural systems, but could be at a higher level close to effluent outlets or in the near-field of radioactive disposal sites. Concentrations of organic carbon range from a few milligrams carbon per liter in fresh waters low in calcium and magnesium to up to 50 mg carbon per liter in bog or swamp waters (Kim *et al.*, 1990; Choppin, 1992; Moulin *et al.*, 1992a, 1996; NATO, 2005). Ocean concentrations of organic carbon range from 0.5 to up to 1.2 mg L^{-1} with higher concentrations at the water surface (Stumm and Morgan, 1995). In general, the complexation of actinides with hydroxide, carbonate and the macromolecular humic and fulvic acids dominate in natural aqueous systems.

Particulate matter is ubiquitous in natural waters, present up to 10^6 cm^{-3} in surface waters, groundwaters, oceans, and in interstitial soil and sediment waters (Stumm and Morgan, 1995). Suspended particles have a continuous particle size distribution (Fig. 32.10). Dissolved species are considered to have nanometer dimensions and for which a chemical potential can be defined. Colloids are operationally defined as having a dimension between 1 nm and 1 μm and are dynamic in that they are continuously generated, undergo compositional changes and can be continuously removed from solution. Studies
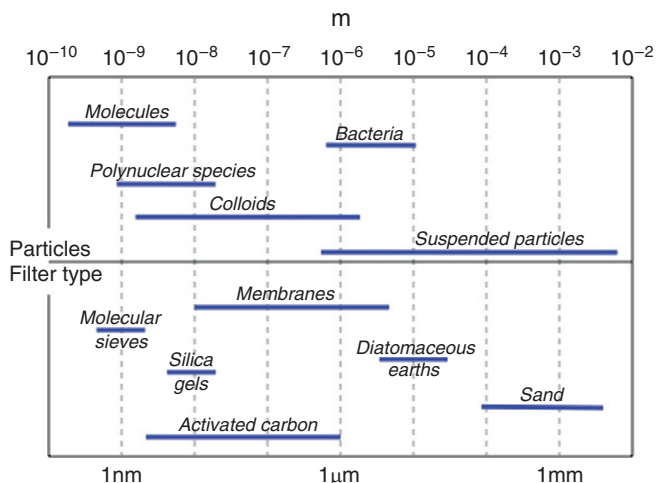

Fig. 32.10 *Dimensions of species present in natural waters and common filtration media used for particle separation. Adapted from Stumm and Morgan (1995).*

suggest that the colloidal fraction can be as large in mass as the sum of particles micron sized or larger. Colloids have the potential to greatly affect the environmental behavior of actinides because of their prevalence, reactive surface area, dynamic nature, and residence times that can vary by orders of magnitude.

32.3.3 Processes and mechanisms affecting actinide speciation

Without understanding the most pertinent geochemical interactions of actinides on a molecular scale, accurate prediction of the macro-scale processes in the field is extremely difficult. When actinides enter the environment they will undergo some key chemical reactions that will determine their fate and migration behavior. The actinide oxidation states may change if natural water conditions differ from the source material. Actinides will be more soluble or precipitate, depending on the inorganic and/or organic ligands present and on how the resultant actinide–ligand species adsorb onto or become incorporated into colloidal or surfacial mineral, chemical, or biological assemblages. The transport of the dissolved, suspended, and adsorbed actinide species then depends upon the local and site hydrology and geology. In the following sections we will provide an overview of these chemical processes that are most important for the fate of actinide in natural aquatic systems.

(a) Redox properties of the light actinides

The environmental fate of metal ions stems primarily from their oxidation states. The behavior of actinides that generally exist in a single oxidation state, such as Cm(III), is easier to predict than those that easily form multiple oxidation states, such as neptunium and plutonium. Multivalent actinides may exhibit a mixture of oxidation states for a given experimental condition. The coexistence of multiple oxidation states of an actinide is of particular importance for its transport characteristics. The solution Eh governs the general stability of actinide oxidation states, which then can be modified by complexing ligands or surfaces stabilizing a specific oxidation state. Pourbaix (Eh–pH) diagrams are useful tools to illustrate oxidation state stability as function of pH and ligand concentration from known thermodynamic data. Figure 32.11 illustrates the Pourbaix diagram of plutonium and the stability of its oxidation states in common natural waters.

Thorium is redox-inactive and exists as Th(IV) in aqueous media. Figure 32.12 shows the stability ranges for U(IV) and U(VI) solution species together with those of common natural redox-active species. Uranium(III) is unstable under most conditions and oxidizes easily to U(IV); and U(V) disproportionates to U(IV) and U(VI). Generally, U(VI) is predominant in surface and other oxidizing environments, while U(IV) is predominant in anoxic subsurface environments. The normal range of waters overlaps with the stability
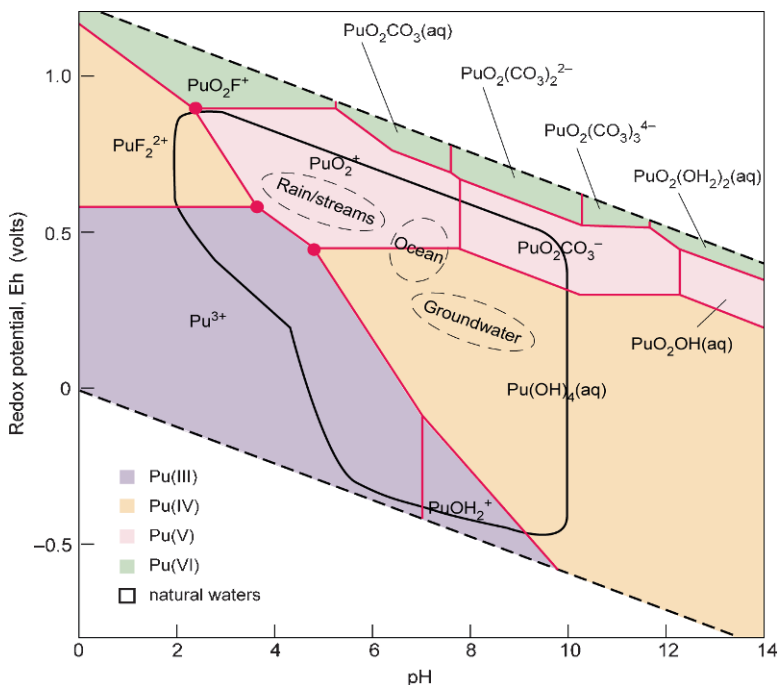
Actinides in the geosphere

Fig. 32.11 *Eh–pH diagram of plutonium, the most redox-active element in the actinide series. The circled area represent the range of conditions of common natural waters. The triple points indicate areas where multiple oxidation states of plutonium coexist in solution* (*Runde*, 2000).

fields of plutonium in the III, IV and V oxidation states (Fig. 32.11). Within this range, plutonium exhibits two triple points, where species in three oxidation states are in equilibrium. Plutonium(III) forms in natural waters only at very low redox potentials (below 300 mV at pH 5 and below 0 mV at pH 7). Plutonium(VI) species are stable in water only at highly positive potentials, and therefore Pu(VI) is unlikely to persist in most geochemical systems. At near-neutral pH, minor changes in the redox potential have a significant effect on the plutonium oxidation state and determine the relative concentrations of Pu(IV) and Pu(V) (Fig. 32.13). Specifically, a change from 400 to 500 mV at pH 7 corresponds to a major speciation change, from predominantly less-soluble Pu(IV) species to the much more soluble and mobile Pu(V) solution species. Besides plutonium, neptunium is the most redox-active elements in the actinide series and exists in its IV and V oxidation states under most natural conditions (Fig. 32.14). Neptunium(III) and Np(VI) are on the edges of the water stability region and can exist only under strongly reducing or oxidizing conditions, respectively. All other actinides have far more simple stability diagrams, because they exhibit only one or two stable oxidation states, and the number of
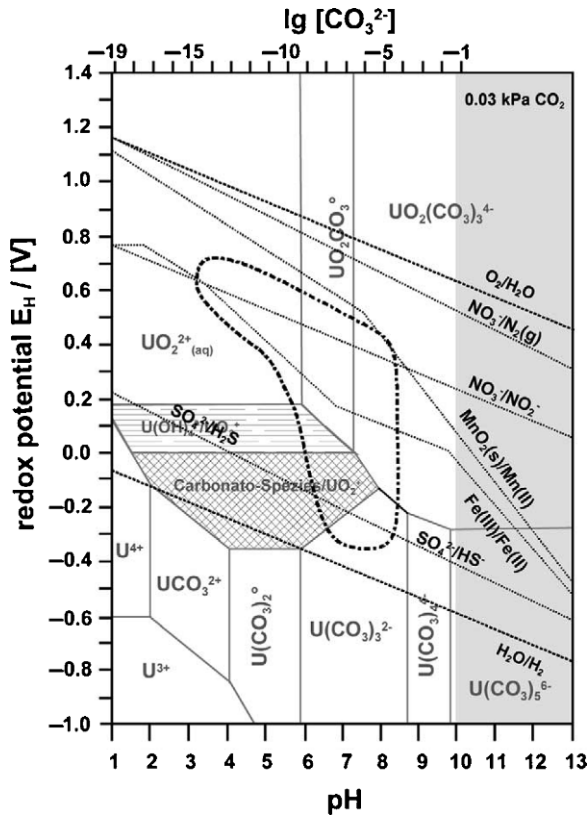
Fig. 32.12 *Stability areas for uranium oxidation states compared with environmentally-relevant redox couples (Meinrath et al., 2003). The circled area represents the conditions of common natural waters. Reproduced by permission of Elsevier.*

stable species they form is much smaller. Americium, as well as its neighbor curium, will be found mainly in the +III oxidation state under most environmental conditions.

Table 32.4 summarizes the oxidation states of the actinides and highlights the environmentally most relevant ones. In general, we expect to find Th(IV), U(VI), Np(V), Pu(IV), Pu(V), Am(III) and Cm(III) as the prevalent oxidation states in most ocean or groundwater environments. Other aqueous environments, such as anaerobic or organic-rich waters, stabilize the reduced oxidation states U(IV), Np(IV), and potentially Pu(III). In contrast, aerobic waters or brines can create oxidizing conditions that stabilize the higher oxidation states of the light actinides oxidizing Am(III) and Pu(IV) to Am(V) and Pu(V) and (VI), respectively. For more detailed information on the redox properties and
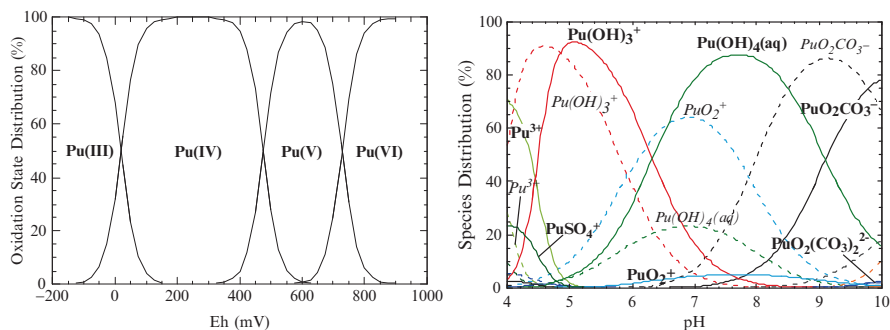
Fig. 32.13 (*left*) *Effect of the redox potential on the plutonium oxidation state distribution in natural water.* (*right*) *Plutonium species distribution at 400 mV (solid lines) and 500 mV (dashed lines) in low-ionic strength (J-13) water representative of conditions at Yucca Mountain (calculated for a closed system with constant carbonate concentration of 2.6 mmol L^{-1}) (Runde et al., 2002a). Reproduced by permission of Elsevier.*
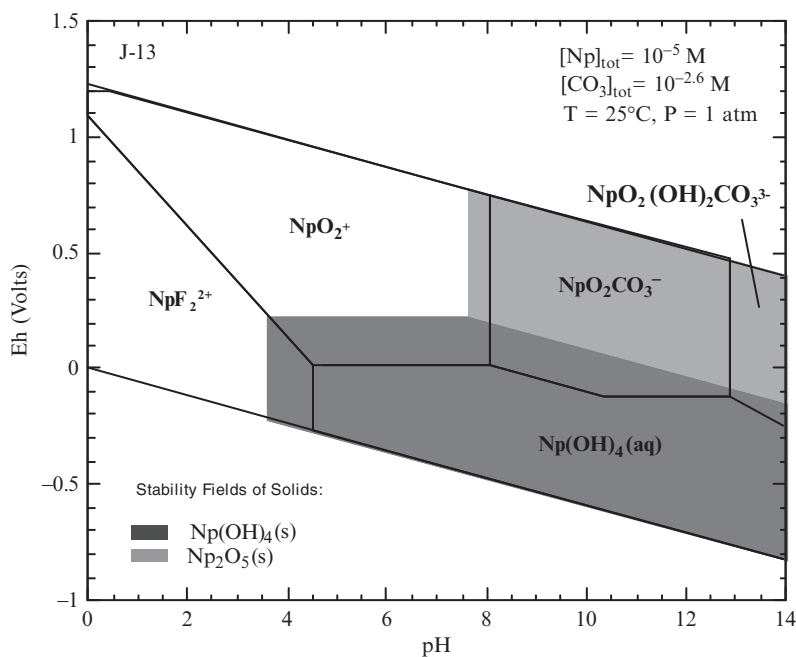

Fig. 32.14 *Eh–pH diagrams of neptunium. The shaded areas represent stability regions of solid phases that precipitate from a 10^{-5} mol L^{-1} neptunium solution. Solid lines represent the stability fields for solution species. The neptunium oxidation states are enclosed by the area of water stability (Kaszuba and Runde, 1999). Reproduced by permission of the American Chemical Society.*

Table 32.4 *Oxidation states of the light actinides.*[a]

Ac	Th	Pa	U	Np	Pu	Am	Cm
III	(III)	(III)	(III)	III	III	III	III
	IV	IV	IV	IV	IV	IV	(IV)
		V	V	V	V	V	
			VI	VI	VI	VI	
				(VII)	(VII)		

[a]The environmentally most important oxidation states are shown in bold, unstable species are placed in parentheses.

oxidation state stabilities of the actinide elements we refer to the Chapters 3, 5, 6, 7, 8 and 9 of this work.

In their lower oxidation states, the actinides form hydrated An^{3+} and An^{4+} ions, in solution. The highly charged cations in the V and VI oxidation states are unstable in aqueous solution and hydrolyze instantly to form linear *trans*-dioxo (actinyl) cations, AnO_2^+ and AnO_2^{2+}, respectively. Covalent bonding between the actinide and the two actinyl oxygen atoms enhances the effective charge of the central actinide ion to (2.3 ± 0.2) for AnO_2^+ and (3.3 ± 0.1) for AnO_2^{2+} (Choppin, 1983). The higher effective charge of An(VI) versus An(V) correlates with a shorter bond to the coordinated oxygen atoms, i. e. about 1.74 Å in Pu (VI) and 1.81 Å in Pu(V) (Conradson, 1998). The preference of actinide ions to form complexes generally follows their effective charges in the order:

$$An^{4+} > AnO_2^{2+} \geq An^{3+} > AnO_2^+.$$

Thus, tetravalent actinides form the most stable complexes and also form the least soluble solids; conversely, An(V) complexes are the weakest among the different oxidation states and An(V) solubilities are the highest. In general, the oxidized forms of the actinides, An(V) and An(VI), are relatively soluble and are of great concern to be mobile, molecular contaminants in natural systems. The linear *trans*-dioxo moiety of actinyl(V) and (VI) ions limits the structural variability and number of coordinated ligands compared to the potential coordination geometries of tri- and tetravalent actinide ions. For example, $Am^{3+}(aq)$ is coordinated by nine water molecules (Matonic *et al.*, 2001), while $UO_2^{2+}(aq)$ is bound by five water molecules in the equatorial plane perpendicular to the uranyl O=U=O axis (Allen *et al.*, 1997).

(b) Radiolysis of actinides

The isotopes of the actinide elements emit highly energetic alpha particles with energies around 5 MeV. The energy of these particles is absorbed in short dense tracks, producing electrons, ions and radicals. Most of the energy is converted to heat; but some of the energy deposited in the matrix can actually induce

changes in the solute, including actinide oxidation state distribution. Although the type of radiation appears to have little effect on the type of radiolysis products formed, the yield distribution of the primary radiolysis products depends on the different ionizing densities of the different radiation types. The more dense ionization tracks of alpha-particles cause an increased production of molecular species over radical species. A measure of radiation yields is the *G*-value, which is defined as the number of moles of radiolytically formed molecules or ions per joule of energy absorbed. As an example, the *G* values for the reduction of Pu(IV) or Pu(VI) in 1 M $HClO_4$, (0.36 ± 0.03) µmol J^{-1}, is found to be similar to that of Fe(II) $((0.53 \pm 0.03)$ µmol $J^{-1})$ or Ce(IV) $((0.33 \pm 0.03)$ µmol $J^{-1})$ (Spinks and Woods, 1990). The total energy deposited is the absorbed dose, expressed in grays (symbol Gy; in J kg^{-1}).

The radiation energy in dilute aqueous systems is absorbed mainly by water molecules, generating several highly reactive species, i.e. e_{aq}^-, H·, OH·, and H_2O_2. Hydrogen, H_2, is also a common radiolysis product of water, but it is generally less reactive. In the presence of oxygen additional radicals are also formed, i.e. O_2· and HO_2·, and the yield for radiolytically formed H_2O_2 increases. In contrast, the yield for the reducing species H· and e_{aq}^- decreases under those conditions. It is well established that alpha-particles, such as those emitted from actinides, have a larger linear energy transfer (LET of α (^{210}Po) is 700 eV pm^{-1} in water) than gamma-rays (2 eV pm^{-1} for γ(^{60}Co)). Thus, as mentioned above, the formation of molecular radiolysis products is favored in the radiolysis by alpha-particles, compared to radiolysis by gamma-rays and beta-particles, where the formation of radicals dominates (Hart, 1954).

The vast majority of radiolysis studies were done under acidic conditions that are not relevant to environmental systems. In these acidic systems auto-radiolytic reduction of Pu(IV) to Pu(III), or the oxidation of Pu(III) to Pu(IV) by using the radiation from ^{244}Cm is observed (Andreychuck *et al.*, 1990). The auto-radiolytic reduction of Pu(VI) is much more complicated and leads through the formation of Pu(V) to a steady state ratio of Pu(IV) and Pu(VI) concentration ratio that depends on the plutonium concentration (Newton, 2002). More environmentally-relevant studies concentrated on radiolysis in chloride-based brines. Such salt brines are simulants for conditions found at deep salt formations suitable for radioactive waste disposal. The most prominent examples are the Gorleben and Morsleben sites in Germany and the Waste Isolation Pilot Plant (WIPP) in Carlsbad, New Mexico, in the U.S. In contrast to dilute aqueous solutions, the ions of concentrated salt solutions interact with the radiation to form new reactive species, which leads to an increase of the redox potential of up to 900 mV, indicative of the radiolytic creation of a highly oxic environment (Pashalidis and Kim, 1992). Spectroscopic studies identified HClO and ClO^- as the main oxidizing species in chloride solutions of near-neutral pH responsible for oxidizing the actinides into their highest oxidation states V and VI (Büppelmann *et al.*, 1988; Pashalidis and Kim, 1992; Kelm *et al.*, 1999). Büppelmann *et al.* (1988) studied the radiolytic oxidation of

plutonium in chloride solutions and Pashalidis *et al.* (1993) proposed the interaction of hypochlorite with Pu(VI) and the formation of $PuO_2(OH)(OCl)$ and $PuO_2(ClO)_2$ being responsible for the stabilization of Pu(VI) in radiolytic chloride brines. The autoradiolytic oxidation of Am(III) to Am(V) was observed in the absence and presence of carbonate and the formation of Am(V) was spectroscopically verified (Magirius *et al.*, 1985).

Due to radiolysis, the reduction rates of Pu(VI) in 1 M H(Cl,ClO$_4$) solutions decreased with increasing chloride concentration. The autoradiolytic reduction of Pu(VI) by its own alpha radiation ceases at chloride concentration higher than 1 M (Rabideau *et al.*, 1958; Büppelmann *et al.*, 1988). Data indicate that the *G*-value for Pu(III) drops from 0.36 μmol J^{-1} in 1 M $HClO_4$ to 0.077 μmol J^{-1} in 0.5 M HCl–0.5 M $HClO_4$ (Rabideau *et al.*, 1958). Higher dose rates, induced by using the more radioactive isotope ^{238}Pu, show that Pu(IV) can be oxidized to Pu(VI) in concentrated chloride solutions. At chloride concentrations below 3 M and dose rates of 0.15 W L^{-1}, Pu(V) is the main product (Büppelmann *et al.*, 1988). An overview of the redox chemistry of plutonium in aqueous solution is given by Newton (2002).

Radiolysis also impacts the actinides' fate by decomposing solid phases to form secondary compounds. Ion beam (1.0 MeV Kr^{2+}) irradiations of U(VI) phases caused their degradation and the formation of UO_2 nanocrystals that are similar to those found in the vicinity of Oklo (Utsunomiya *et al.*, 2005). Those UO_2 nanocrystals can subsequently change in a paragenesis of alteration phases under oxidizing conditions (see Section 32.3.3 (d)). Multiple cycles of radiolytic formation of UO_2 and subsequent alteration to form U(VI) phases under oxidizing conditions can explain the loss of trace elements and the high purity of U(VI) alteration phases found in uranium deposits around the world.

(c) Solubility of actinides

The concentration of naturally occurring and contaminant actinides is generally low under most conditions. Key to assessing the safety of nuclear waste repositories or long-term storage facilities is the ability to predict the highest concentrations under site-specific conditions. The most pertinent property of an actinide to predict the concentration limits in environmental solutions is its soluble concentration or solubility (Stumm and Morgan, 1995). The solubility is related to the solubility product of the actinide-bearing solid phase. As an example, the solubility of americium over $AmOHCO_3(s)$ as the solid phase can be obtained from equation (32.4)

$$AmOHCO_3(s) \Leftrightarrow Am^{3+} + OH^- + CO_3^{2-} \tag{32.4}$$

corresponding to the solubility product

$$K_{sp} = [Am^{3+}][OH^-][CO_3^{2-}], \tag{32.5}$$

keeping in mind that under most environmental conditions, americium will be distributed over complexed species, besides Am^{3+}.

Clearly, evaluation of radionuclide mobility in geochemical environments proximate to nuclear waste repositories must consider soluble radionuclide concentrations that are controlled by the chemical potential of the system as well as the nature and solubility of relevant solid phases. The solid phase with the lower Gibbs energy, which translates ultimately into a lower soluble concentration, will over time control the solubility of the actinide. Generally, oxides and hydroxides, i.e. $An(OH)_3(s)$, AnO_2 and $An(OH)_4(s)$, or $AnO_2(OH)_2 \cdot nH_2O$, are the most important actinide solids to consider under natural conditions due to their low solubilities. However, at the carbonate concentrations of groundwater systems, the formation of mixed hydroxycarbonate solids, i.e. $AmOHCO_3(s)$ (Meinrath and Kim, 1991; Vitorge, 1992; Silva *et al.*, 1995) or $Pu(OH)_2CO_3(s)$ (Lemire and Garisto, 1989; Lemire *et al.*, 2001), and pure carbonates, i.e. $UO_2CO_3(s)$ (Grenthe *et al.*, 1992), is important. In fact, the latter compound is found in nature as the uranium mineral rutherfordine. High ionic strength, such as present at geologic salt formations, is critical for the formation of ternary actinide solids. As such, $NaNpO_2CO_3 \cdot nH_2O$ is the solubility-controlling solid at low carbonate concentrations (Fig. 32.15) and is also kinetically favored at increased carbonate, but over time it transforms to the thermodynamically stable phase $Na_3NpO_2(CO_3)_2 \cdot nH_2O$ (Neck *et al.*, 1995b; Runde *et al.*, 1996). $NaAm(CO_3)_2$ is expected to be the solubility-controlling solid americium phase at carbonated salt solutions of higher ionic strength (Felmy *et al.*, 1990; Silva *et al.*, 1995; Rao *et al.*, 1996) Under oxidizing conditions Am(V) follows the solubility of Np(V) (Fig. 32.15).

The solubility of actinide solids generally follows the effective charges of the actinide ions and their affinity for complexation. Thus, the precipitates of the strongly-complexing trivalent and tetravalent actinides are sparely soluble under environmental conditions, while solids of pentavalent and hexavalent actinides exhibit orders of magnitude higher solubilities. Oxide and hydroxide phases of tetravalent actinides primarily control actinide solubility under environmental conditions (Rai *et al.*, 1980; Rai, 1984; Lemire and Garisto, 1989; Neck *et al.*, 2007a). Although plutonium may exist in four oxidation states in water, conditions tend to favor one or two states, i.e. Pu(IV) and Pu(V). Solubilities of plutonium in most natural systems are controlled by Pu(IV) (oxy)hydroxides in the form of crystalline PuO_2 (or PuO_{2+x}) or amorphous $Pu(OH)_4$ (Rai, 1984). Aerobic conditions favor the formation of Pu(V) in solution over a Pu(IV) (oxy) hydroxide solid phase, thereby increasing the solubility. Similar redox changes occur with neptunium. Thermodynamic calculations identified crystalline NpO_2 to restrict the soluble neptunium concentration under reducing conditions to about 10^{-12} mol L^{-1} (Kaszuba and Runde, 1999). Similar concentrations have been determined for amorphous Th(IV) hydroxide (Neck *et al.*, 2003). In laboratory experiments, Np_2O_5, $Np(OH)_4(am)$ and crystalline NpO_2 have been identified as the confining solids (Nitsche *et al.*, 1993; Efurd *et al.*, 1998;
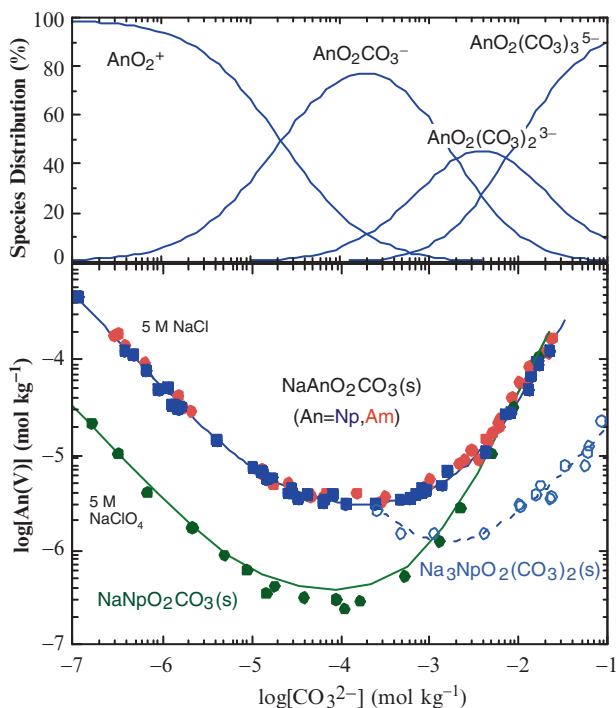
Fig. 32.15 *Species distribution (top) and solubility (bottom) of pentavalent actinides, Np(V) and Am(V), as a function of carbonate concentration. With increasing carbonate concentration the solid phase undergoes a solid phase transformation (Runde et al., 1996). The solution speciation (top) is calculated from thermodynamic data recommended by Lemire et al. (2001). Reproduced by permission of Elsevier.*

Neck *et al.*, 2001). At redox potentials below about 0.1 V, the Np(IV) solid is thermodynamically stable; more oxic conditions increase the fraction of Np(V) until the soluble Np(V) concentration reaches saturation and a solid phase transformation to Np_2O_5 occurs at Eh values above 0.35 V. In the intermediate range of about 0.1 and 0.3 V the total neptunium concentration in solution is controlled by the solubility of $Np(OH)_4(am)$ with varying concentration ratios of Np(IV)/Np(V) species in solution determined by the Eh and pH (Kaszuba and Runde, 1999). These studies illustrate that slight changes of the aquifer conditions can induce significant alterations in the actinide solubility and actinide oxidation state stability, especially for the most redox-sensitive actinides neptunium and plutonium.

The degree of crystallinity of the solid phase can also result in a range of solubilities over several orders of magnitude of concentration, with the amorphous phase being more soluble. As an example, crystalline oxides AnO_2, where An = tetravalent Th, Np and Pu, are calculated to restrict thorium, neptunium and plutonium concentrations at neutral pH as low as about 10^{-16} mol L^{-1}

(Kaszuba and Runde, 1999; Neck *et al.*, 2003, 2007a). In contrast, the corresponding amorphous hydroxides, $An(OH)_4(am)$ are calculated to be about seven orders of magnitude more soluble.

(d)   Secondary solid phase formation

Laboratory solubility measurements reach steady state as defined operationally by the actinide concentration in solution remaining constant for several weeks. However, over geological time scales precipitates may become less soluble as they recrystallize to form increasingly ordered solids with lower Gibbs energy (Fig. 32.16). Such a change may be kinetically controlled and not be observed in the experiment or in nature even after several years. Consequently, the solids formed in laboratory experiments may not represent the geologically most relevant, thermodynamically most stable solids with the lowest solubility. As an example, an investigation of spent nuclear fuel alteration found that several forms of hydrated $UO_3(s)$ formed at temperatures below 300°C and ultimately dehydrated schoepite, $(UO_2)O_{0.25-x}(OH)_{1.5+2x}$ where $0 \leq x \leq 0.25$, formed as a corrosion product (Finch and Ewing, 1990; Wronkiewicz *et al.*, 1992; Finn *et al.*, 1994). Within a period of 2 years of spent nuclear fuel corrosion in
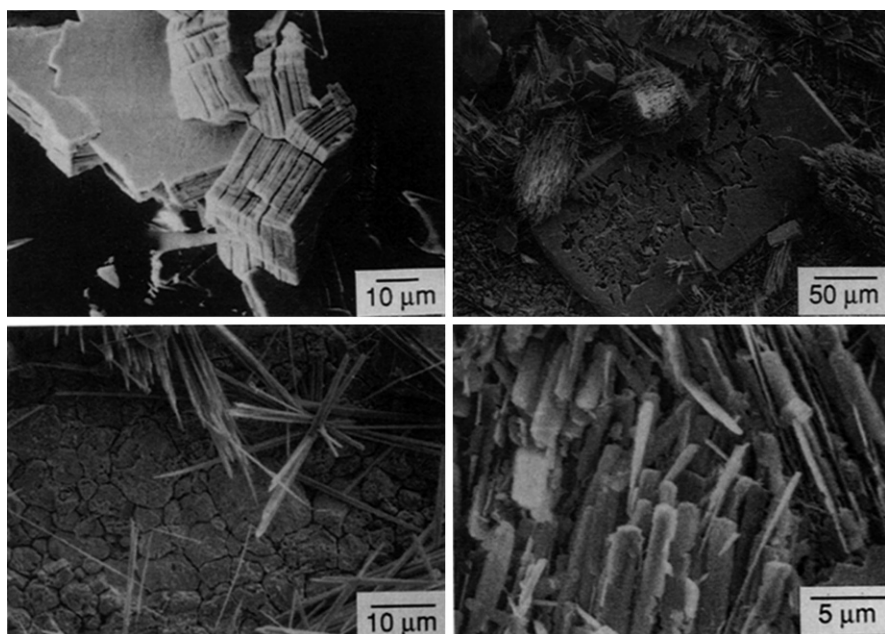

Fig. 32.16   *Scanning electron microscopy images of phases formed during the alteration of UO₂: (top left) schoepite crystals; (top right) becquerelite crystals; (bottom left) needles of uranophane; and (bottom right) soddyite crystals (Wronkiewicz et al., 1992). Reproduced by permission of Elsevier.*

water, the schoepite phases disappeared and peroxo phases formed, such as studtite $[(UO_2)(O_2)(H_2O)_2](H_2O)_2$ (Hanson *et al.*, 2005). In the presence of soluble silicate, a paragenetic sequence of U(VI) silicate minerals was found, i.e. soddyite, $(UO_2)_2(SiO_4)(H_2O)_2$, uranophane, $Ca[(UO_2)(SiO_3OH)_2](H_2O)_5$, and ultimately boltwoodite $(Na,K)[(UO_2)(SiO_3OH)](H_2O)]_{1.5}$ (Wronkiewicz and Buck, 1999). The silicates swamboite, $[U^{6+}(UO_2)_6(SiO_3OH)_6(H_2O)_{30}]$, and soddyite, $(UO_2)_2(SiO_4)(H_2O)_2$, are identified as terminal uranium phases in this paragenesis. At phosphate concentration above 10^{-4} M the formation of chernikovite, $(H_2(UO_2)_2(PO_4)_2•8H_2O$, has been observed, while no uranyl-phosphate secondary phases have been found at lower phosphate concentrations (Rey *et al.*, 2008). The introduction of binary U(VI) hydroxide phases to chloride brines resulted in their transformation to ternary oxyhydroxide phases. In the presence of 1 m $CaCl_2$ and KCl, $UO_2(OH)_2•H_2O$ spontaneously transforms to becquerelite, $CaU_6O_{19}•11H_2O$, and compreignacite, $K_2U_6O_{19}•11H_2O$ (Sandino and Grambow, 1994), respectively. However, schoepite is found to be a stable phase in 1 M NaCl.

A number of alteration phases were identified upon the oxidizing alteration of uraninite, UO_2, and UO_{2+x} by studying natural uranium deposits at Peña Blanca, Chihuahua, Mexico (Pearcy *et al.*, 1994) and at the Marshall Deposit in Colorado, USA (Deditius *et al.*, 2007), respectively. Uraninite, schoepite, uranophane, coffinite, calciouranoite and other uranium phases have been identified at the Colorado Plateau (Zhao and Ewing, 2000). Coffinite, $USiO_4•nH_2O$, can crystallize under reducing conditions and undergo subsequent alteration processes as observed at the upper Jurassic Morrison Formation in the Grants uranium region in New Mexico, USA (Fig. 32.17). The formation of

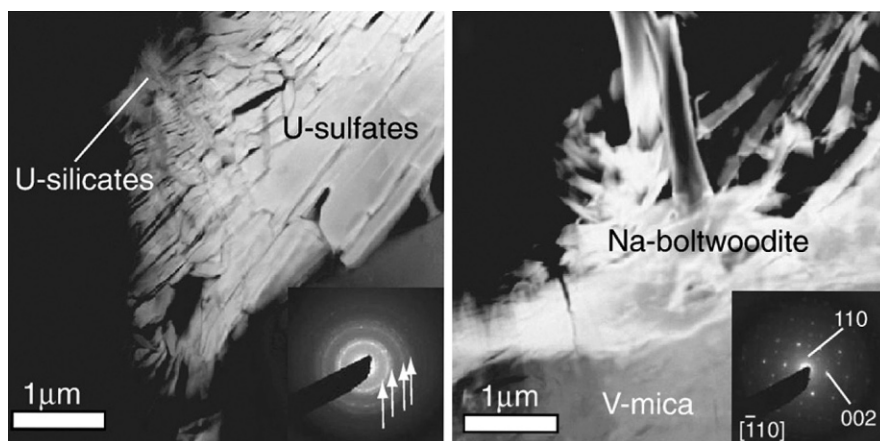**Fig. 32.17** *High-Resolution Tunnel Electron Microscopic images during the alteration of coffinite, $USiO_4•nH_2O$. (left) crystals of U(VI) sulfate intergrowths with U(VI) silicate on the surface of V-rich mica; (right) needle-shaped crystals of Na-boltwoodite precipitated on the surface of V-rich mica (Deditius et al., 2008). Reproduced by permission of Elsevier.*

calciouranoite, $(Ca, Ba, Pb)U_2O_7 \bullet 5H_2O$, suggests the interaction between the limestone host rock and uranium minerals (Zhao and Ewing, 2000). Along with the retention of uranium on aluminosilicates, mineralization of multiple secondary uranium phases have been reported at the Hanford site (Arai *et al.*, 2007; McKinley *et al.*, 2007). The alkaline nature of the leached waste caused reactions with the underlying geologic mineral and rock formation resulting in the formation of isolated uranyl silicate phases such as boltwoodite and uranophane. Low-soluble uranyl(VI) phosphates, i.e. metatorbenite $Cu(UO_2PO_4)_2 \bullet 8H_2O$ (Arai *et al.*, 2007) control the mobility of the contaminants (McKinley *et al.*, 2007). Incorporation of metal cations, such as MoO_2^{2+}, Ba^{2+}, WO_2^{2+}, AsO_4^{2+} or Sb^{5+} play an important role in stabilizing intermediate uranium phases. Burns *et al.* (2004b) synthesized several U(VI) phases (metaschoepite-formally $UO_3 \bullet 2H_2O$, β-$(UO_2)(OH)_2$, etc.) in the presence of Np(V). Incorporation of Np(V) was limited to few part per million in metaschoepite and β-$(UO_2)(OH)_2$, but was much greater in uranophane and Na-compreignacite, $Na_2[(UO_2)_3O_2(OH)_3]_2(H_2O)_7$ with over 400 ppm Np(V). Calculations indicate that the low solubility of uranophane entrapping trace amounts of neptunium can significantly reduce the neptunium concentration for long-term isolation (Murphy and Grambow, 2008).

These secondary phases may determine the subsequent release and mobility of key radionuclides. For example, formation of alteration phases during glass dissolution confirmed the uptake of fission products and actinides (Grambow *et al.*, 1997). And uranyl oxyhydroxide has been shown to incorporate neptunium into its structure (CRWMS, 2000a). Subsequent release of the neptunium from such metastable U(VI) phase may be assumed to be congruent to uranium by using a conditional solubility product of this secondary phase. On the other hand, the ultimately more stable silicate phases did not provide experimental evidence for neptunium incorporation to a significant degree. Hence, the release of neptunium from U(VI) oxyhydroxide is likely to be controlled by the infiltration rate and composition of infiltrating water and the corresponding solid phase conversion rates. Other actinides have also been shown to be sequestered by host phases, such as plutonium by perovskite ($CaTiO_3$) and zirconolite ($CaZrTi_2O_7$) (Begg *et al.*, 1998) or uranium by calcite (Sturchio *et al.*, 1998). The recent investigations illustrated that alteration phases that can sequester actinides from solution can be an important component for long-term nuclear waste isolation.

(e)   Complexation reactions

As illustrated by equations (32.4) and (32.5) the total concentration of soluble actinides in a solid–liquid phase equilibrium is determined from the solid's solubility product when the dissolved actinide cation remains uncomplexed in solution. In natural systems actinide ions will be exposed to a variety of complexing ligands. The presence of inorganic and organic complexing anions can

increase or reduce the soluble concentration via complexation of the actinide ion in solution. Indeed, detailed surface studies quantify how a specific ligand promotes dissolution by bonding with surface actinide atoms and then bringing them into solution. Actinide complexes in solution are described by the general equation:

$$m \, An^{x+} + n \, L^{y-} = (An)_m (L)_n^{mx-ny} \tag{32.6}$$
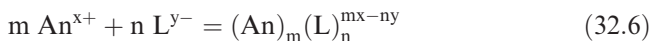
where m refers to the number of actinide ions complexed by n ligands. A value of $m \geq 2$ corresponds to the formation of polynuclear species, for example as found for U(VI) and Pu(VI) hydroxo complexes (Grenthe *et al.*, 1992; Reilly and Neu, 2006). The concentration of an actinide in solution can then be calculated as the sum of all solution complexes from both the complex formation constants and the solubility constant of the solubility-controlling solid phase. As an example, the soluble concentration of trivalent americium in an aqueous system as a function of the pH with $AmOHCO_3(s)$ as the solubility-controlling actinide solid phase and hydroxo and carbonato Am(III) solution complexes can be calculated by:

$$\begin{aligned}
[Am(III)]_t &= [Am^{3+}] + \sum \left[Am(CO_3)_n^{3-2n} \right] + \sum \left[Am(OH)_p^{3-p} \right] \\
&= (K_{sp} / [CO_3^{2-}][OH^-]) \left(1 + \sum \beta_n [CO_3^{2-}]^n + \sum \beta_p [OH^-]^p \right)
\end{aligned} \tag{32.7}$$

To model and predict solubilities, we must know both the composition and the solubility product of the controlling solid phase, the concentration of individual ligands and other cations that are competing for the ligand coordination or that raise the solution ionic strength, and the stability constants of the actinide–ligand complexes. Figure 32.18 illustrates the correlation between solubility-controlling solid phase and solution speciation for trivalent actinides (An = Am(III) or Cm(III)). In acidic solution, the aquo ion An^{3+} is stable and its concentration is governed by the solubility product of the solid phase. With increasing pH and ligand concentration – carbonate in the present example – subsequent complexation of the Am^{3+} aquo ion occurs to form Am(III) carbonato species, $Am(CO_3)_n^{3-2n}$. As the pH and carbonate concentration increase, the total An(III) concentration in solution increases due to the formation of anionic An(III) complexes, i.e. $Am(CO_3)_2^-$ and $Am(CO_3)_3^{3-}$. A similar trend can be seen in Fig. 32.15 for the complexation of Np(V) in carbonate.

Nature provides a variety of complexing agents capable of coordinating actinide ions. As hard "acids" the actinide ions form strong complexes with hard oxygen-donating ligands, i.e. OH^- and CO_3^{2-} or PO_4^{3-}, and less stable complexes with F^- and SO_4^{2-}, and only weak complexes with the monovalent anions Cl^- and NO_3^-. The affinity of actinide ions to form complexes with univalent or bivalent ligands follows the trends
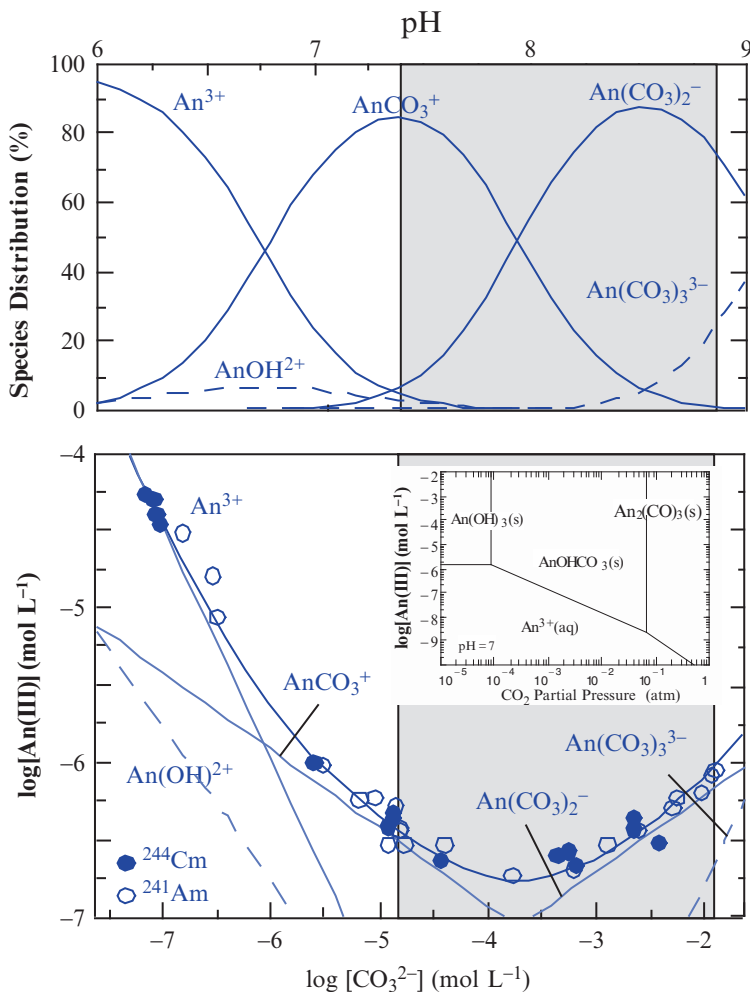
$$OH^- > F^- > NO_3^- > Cl^- >>> ClO_4^- \quad \text{and} \quad CO_3^{2-} > SO_3^{2-} > C_2O_4^{2-} > SO_4^{2-}.$$
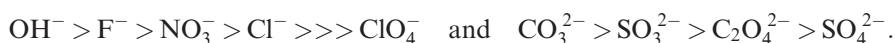
Fig. 32.18 *Correlation between solution speciation (top) and solubility of Am(III) and Cm(III) with $An_2(CO_3)_3 \bullet 2$–$3H_2O(s)$ as the equilibrium solid (bottom) (Runde et al., 2002b). Calculated concentrations for individual solution species are indicated by the straight lines that run tangent to the solubility curve. The partial pressure of CO_2 in natural waters spans about three orders of magnitude as indicated by the gray area. The stability diagram (inset) shows that the An(III) hydroxocarbonate, $AnOHCO_3(s)$, is favored in most natural waters (Vitorge, 1992). The solution speciation (top) is calculated from thermodynamic data recommended by Silva et al. (1995).*

Figure 32.19 illustrates the trend of first formation stability constants for actinides with various inorganic and organic ligands independent of the actinide oxidation state. Of special interest is the generally high stability of complexes with actinides in the tetravalent oxidation state.
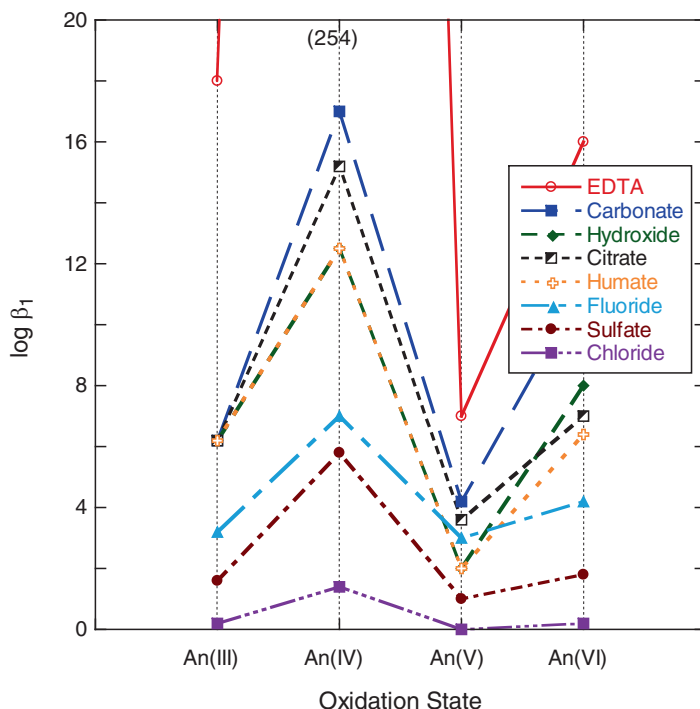
Fig. 32.19 *Comparison of stability constants of inorganic and organic complexes with actinides in their oxidation states III–VI. Stability constants taken from Grenthe et al. (1992), Silva et al. (1995), Lemire et al. (2001), and Hummel et al. (2005).*

(i) *Hydrolysis reactions*

Because of their omnipresence, hydroxide and carbonate are the most important ligands for actinide complexation in natural systems. The pH of natural waters is generally high enough to enable hydrolysis reactions of the actinide ions as:

$$m \, An^{x+} + n \, OH^- = (An)_m(OH)_n^{mx-n} \qquad (32.8)$$
$$m \, An^{x+} + n \, H_2O = (An)_m(OH)_n^{mx-n} + n \, H^+ \qquad (32.9)$$
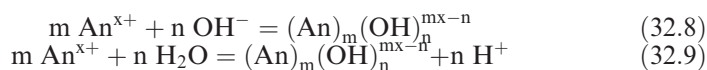
The onset of hydrolysis follows the effective charge of the actinide ion as described earlier. The interaction of actinide ions with hydroxide can generate monomeric and polynuclear solution species, as well as low soluble oxide, hydroxide, or oxyhydroxide colloids and solids. Actinide(III,IV) ions strongly hydrolyze at conditions of natural waters and form positively charged hydroxo complexes in solution, $An(OH)_n^{3-n}$ (where n = 1–2) and $An(OH)_n^{4-n}$ (n = 1–3), and An = Am(III), Cm(III); Th(IV), U(IV), Np(IV), and Pu(IV)

(Allard *et al.*, 1980; Grenthe *et al.*, 1992). At near-neutral and high pH, An(III) and An(IV) form the neutral hydroxo complexes, $An(OH)_3$ and $An(OH)_4$, respectively. Negatively charged hydroxo complexes of An(III) and (IV) have been proposed, but have not been experimentally verified. In contrast, the solid oxides and hydroxides of actinyl(V,VI) ions exhibit amphoteric character with increasing solubilities in alkaline solutions due to the formation of anionic hydroxo complexes, i.e. $NpO_2(OH)_2^-$ (Neck *et al.*, 2001). Uranium(VI) utilizes hydroxide as terminal and bridging ligands to form polynuclear complexes in solution, such as $(UO_2)_2(OH)_2^{2+}$ and $(UO_2)_3(OH)_5^+$ or $(UO_2)_4(OH)_7^+$ (Grenthe *et al.*, 1992). Figure 32.20 illustrates the hydrolysis of U(VI) as function of pH. Recently, the analogous dimeric complex of Pu(VI), $(PuO_2)_2(OH)_2^{2+}$, was spectroscopically identified (Reilly and Neu, 2006). In general, polynuclear solution species are highly stable and do not easily decompose back to structurally reduced building blocks. The actinide species that best illustrates this behavior is the highly stable Pu(IV) hydroxide, which can form soluble, polymeric hydrolysis species and can ultimately produce polymeric colloids. Based on spectroscopic studies and thermodynamic stability calculations the following hydrolysis species are the most relevant in near-neutral environmental conditions:

The monomeric hydrolysis species are:
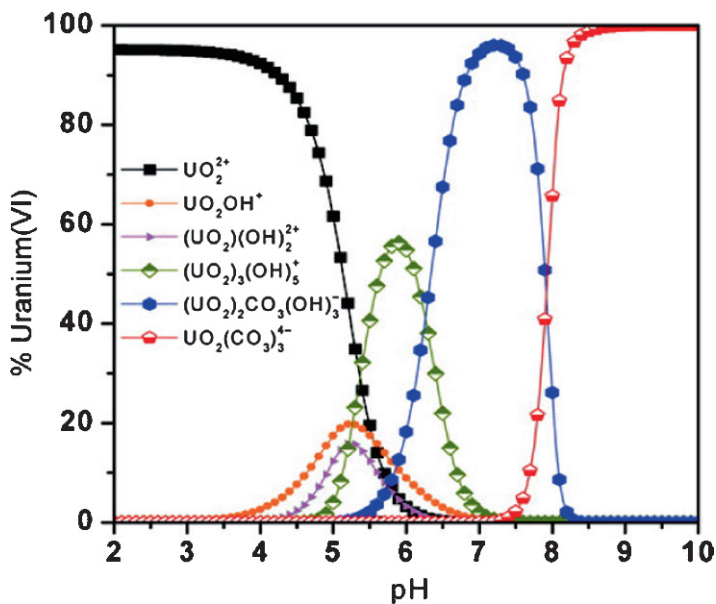

Fig. 32.20 *Major hydrolysis products of 20 μmol L^{-1} U(VI) in 0.1 M NaCl under atmospheric conditions (Müller et al., 2008). The U(VI) concentration is 20 μmol L^{-1}. Reproduced by permission of the American Chemical Society.*

An(III) (An = Am, Cm): An(OH)$^{2+}$, An(OH)$_2$$^+$ and An(OH)$_3$
An(IV) (An = Th, U, Np and Pu): An(OH)$_2$$^{2+}$, An(OH)$_3$$^+$ and An(OH)$_4$
An(V) (An = Np, Pu): AnO$_2$$^+$ and AnO$_2$OH
An(VI) (An = U, Np and Pu): AnO$_2$(OH)$^+$ and AnO$_2$(OH)$_2$
An(III) (An = Am, Cm): Am(OH)

and the polymeric species are Th$_6$(OH)$_{15}$$^{9+}$; (UO$_2$)$_2(OH)_2$$^{2+}$, (UO$_2$)$_3(OH)_5$$^+$, (UO$_2$)$_4(OH)_7$$^+$ and (UO$_2$)$_3$(OH)$_7$$^-$; and (PuO$_2$)$_2(OH)_2$$^{2+}$ at increased Th(IV), U(VI) and Pu(VI) concentrations, respectively.

(ii) Carbonate complexation

After hydrolysis species carbonate complexes of actinides are of major interest because of their importance for environmental behavior and industrial implications. As an example, the alkali leaching process used in mining and uranium decontamination utilizes the high solubility of UO$_2$(CO$_3$)$_3$$^{4-}$ for effective uranium recovery. The carbonate concentrations of groundwaters are controlled by dissolved CO$_2$, corresponding to about 10^{-2} atm (Kim, 1993) compared with the atmospheric partial pressure of about 3×10^{-4} atm. This relatively high carbonate concentration strongly influences the environmental chemistry of actinides in all oxidation states. For example, Fig. 32.21 illustrates the predominance of uranium(VI) carbonate species in a near-neutral natural mine water.
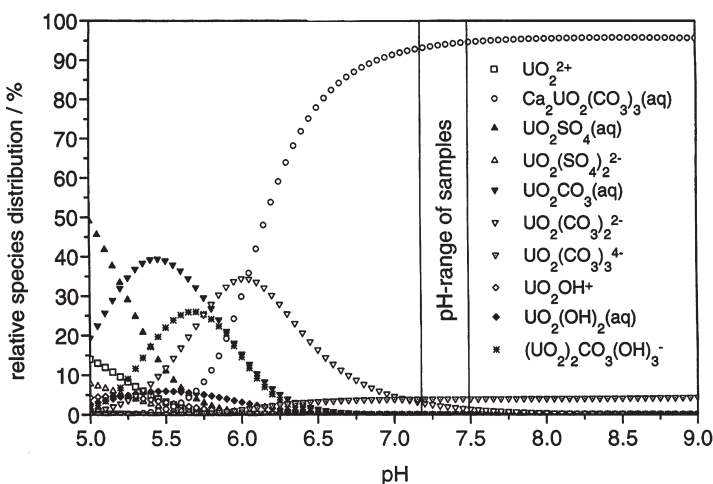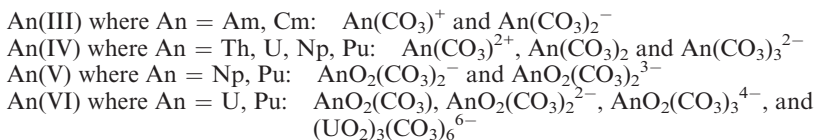

Fig. 32.21 *Speciation of U(VI) in uranium mine water from Schlema, Germany (Bernhard et al., 1998). The neutral mine water (pH 7.13) contained 3.9 mmol L^{-1} carbonate, 20.7 mmol L^{-1} sulfate and a uranium concentration of 21 μmol L^{-1}. Reproduced by permission of Elsevier.*

Carbonate generally bonds actinides in a bidentate fashion to form highly stable actinide carbonate compounds in solution and in the solid state. Solution carbonato complexes of trivalent actinides, $An(CO_3)_n^{3-2n}$, have been identified spectroscopically for Am(III) (Meinrath and Kim, 1991) and Cm(III) (Kim *et al.*, 1994; Fanghänel *et al.*, 1999) with n = 1–3, some in equilibrium with the carbonate solid, $An_2(CO_3)_3$. The An(IV) carbonates have not been well characterized in either the solution or solid state, probably because the An(IV) hydroxides are very stable and mixed hydroxo-carbonato species are likely to form. Analysis of solubility data and spectrophotometric or potentiometric titration studies suggest that $An(CO_3)_n^{4-2n}$, n = 1–3, form in aqueous solution (Lemire and Garisto, 1989; Lemire *et al.*, 2001). The limiting complex, $An(CO_3)_5^{6-}$, has been characterized structurally for Th-Pu; however, it is formed at very high carbonate concentrations (above 0.5 mol L^{-1}), which are not relevant to the environment. The actinyl(V) and (VI) ions may form three monomeric solution carbonate complexes of general formula $AnO_2(CO_3)_n^{x-2n}$ with n = 1–3 (x = 1 for An(V) and 2 for An(VI)) (Lemire and Garisto, 1989; Grenthe *et al.*, 1992; Silva *et al.*, 1995). These species are soluble up to millimolar concentrations, and even higher under ideal laboratory conditions, and form salts with alkali, alkaline earth, and other cations. At near-neutral pH, high carbonate and high An(VI) concentrations, An(VI) carbonate can polymerize to form polynuclear actinyl complexes. A highly symmetric uranyl carbonate, $(UO_2)_3(CO_3)_6^{6-}$ has been structurally identified and its formation constant suggests that it is an important environmental species at elevated U(VI) concentrations (Allen *et al.*, 1995). Based upon known formation constants, the following solution carbonato actinide complexes are most relevant under environmental conditions:

An(III) where An = Am, Cm: $An(CO_3)^+$ and $An(CO_3)_2^-$
An(IV) where An = Th, U, Np, Pu: $An(CO_3)^{2+}$, $An(CO_3)_2$ and $An(CO_3)_3^{2-}$
An(V) where An = Np, Pu: $AnO_2(CO_3)_2^-$ and $AnO_2(CO_3)_2^{3-}$
An(VI) where An = U, Pu: $AnO_2(CO_3)$, $AnO_2(CO_3)_2^{2-}$, $AnO_2(CO_3)_3^{4-}$, and $(UO_2)_3(CO_3)_6^{6-}$

These complexes may exist in rapid equilibrium with hydroxo complexes, depending on the solution conditions. Where hydroxide and carbonate concentration ratios accommodate for differences in complex stability of the binary species, mixed hydroxo-carbonato complexes have been proposed to exist. Both $(UO_2)_2CO_3(OH)_3^-$ and $(UO_2)(OH)_2(aq)$ are calculated to be the dominant equilibrium species at near-neutral pH when [U(VI)] = 10^{-5} mol L^{-1} (Grenthe *et al.*, 1992)). Analogous Pu(VI) complexes may form, but have not been characterized. For tetravalent actinides the mixed complexes $Th(CO_3)(OH)_3^-$ (Östhols *et al.*, 1994) and $Pu(CO_3)_2(OH)_4^{4-}$ (Yamaguchi *et al.*, 1994) have been proposed. Mixed hydroxo-carbonato complexes of An(III) can only form at low carbonate and relatively high pH, to compensate for the much higher stability of carbonate complexes compared to An(III) hydroxides. Mixed

complexes of general formula $Am(OH)_p(CO_3)_n^{3-p-2n}$ have been proposed (Bernkopf and Kim, 1984), but have not been verified experimentally. However, $AmOHCO_3(s)$ precipitates at low carbonate concentration and has been identified as a solubility-limiting solid phase at near-neutral pH (Felmy *et al.*, 1990; Meinrath and Kim, 1991; Vitorge, 1992).

(iii) Complex formation with secondary ligands

The vast majority of environmental actinide studies focus on the nature and thermodynamic stability of hydroxo or carbonato complexes because they will predominate in most common waters, unless there is a competing, "secondary" ligand present at a concentration sufficiently high to displace hydroxide and carbonate or form a mixed ligand complex. The most important secondary inorganic ligands in nature are silicate and phosphate. Chloride is important in saline waters, such as marine environments and brines at salt bed repositories. At high radionuclide inventories where radiolysis occurs peroxide and hypochlorite can form. Fluoride and sulfate complexes have been proposed to be present in rare environments.

Silicate phases comprise a large fraction of naturally occurring uranium minerals and a large number of synthetic U(IV) and U(VI) silicate compounds. In addition, studies of schoepite alteration show that secondary silicate phases are produced over time. Solution species have been identified at low pH; however, given the very low solubility of actinide silicates at near neutral pH, those species have not been characterized.

Phosphate may outcompete carbonate for U(VI) complexation when the phosphate to carbonate ratio exceeds 0.1 in solution (Sandino and Bruno, 1992). Indeed, the large resources of monazites, $(Ln,Th)PO_4$, and U(VI) apatite minerals for commercial mining illustrate the high stability and importance of actinide phosphates. In solution at neutral pH, the complexes $An(HPO_4)^+$ and $An(PO_4)$ are favored Am(III) species at phosphate concentrations above 0.01 mol L^{-1}. Due to their high stability and the low solubility of the corresponding solid phases, the actinide phosphate species in solution have not been studied in detail.

Natural waters from ancient salt formations, which are proposed to be or are now performing as disposal sites for nuclear waste, such as the Waste Isolation Pilot Plant (WIPP) in New Mexico, USA, or the Morsleben and Gorleben sites in Germany, are saturated with chloride salts. Chloride affects the solubility and speciation of actinides significantly compared to their chemistry in inert electrolyte solutions of similar ionic strengths. In addition, radiolytic formation of hypochlorite in chloride brines can alter both the oxidation state and speciation of actinides. For example, hypochlorite was shown to stabilize Pu(VI) (Büppelmann *et al.*, 1988; Pashalidis and Kim, 1992) and Am(V) in solution (Magirius *et al.*, 1985). Chloride also raises the Np(V) solubility by about one order of magnitude in acidic and near-neutral 5 M NaCl solution compared to

5 M NaClO$_4$ due of the effect of weak actinide-chloride interactions (Runde *et al.*, 1996). Actinide chloride complexes have been verified spectrocopically and several polynuclear chloro-hydroxo complexes of U(VI) have been characterized. Neptunium(V) and Pu(VI) have been shown spectroscopically to form multiple chloro complexes under acidic conditions (Neck *et al.*, 1995a; Allen *et al.*, 1997). At the higher pH of environmental systems, pure chloro complexes do not exist. However, since chloride can effectively replace coordinated water molecules (Allen *et al.*, 1997), mixed chloro-hydroxo and chloro-carbonato actinide complexes may be among the species formed in salt brines at near-neutral pH.

Hydrogen peroxide is a known radiolytic product in aqueous solution that can strongly complex the actinides. For example, studtite, $[(UO_2)(O_2)(H_2O)_2]$ $(H_2O)_2$, and metastudtite, $UO_2(O_2) \bullet 2H_2O$, have been identified in corrosion studies of spent nuclear fuels (Kubatko *et al.*, 2003; Hanson *et al.*, 2005). Both monomeric and polynuclear U(VI) peroxo-carbonato complexes, $UO_2(O_2)$ $(CO_3)_2^{4-}$ (Komarov, 1959; Goff *et al.*, 2008) and $(UO_2)_2(O_2)(CO_3)_4^{6-}$ (Goff *et al.*, 2008), respectively, have been identified. The molecular, dimeric Pu(IV) complex, $Pu_2(O_2)_2(CO_3)_6^{8-}$, was identified in solution and solid state (Runde *et al.*, 2007) further illustrating the high affinity of peroxide towards actinides.

(iv) *Organic complexes*

Natural organic compounds and those introduced to the environment are available to complex actinides. Synthetic ligands widely used in nuclear material processing and equipment and facility restoration are likely to bind actinides that are collocated in wastes and environmental contamination areas. Naturally occurring oxalate, acetate, malonate and industrial chelating agents such as acetate, EDTA or NTA are examples representative of these two large sets of organic ligands that coordinate actinides (Burns *et al.*, 2004a). Most of these chelating agents contain oxygen donor atoms that are anionic at near-neutral pH and are expected to preferentially bind An(IV). Consequently, the high thermodynamic stability of such Pu(IV) complexes creates a driving force for the reduction of Pu(V) and Pu(VI) and the oxidation of Pu(III) to Pu(IV). There is concern that resultant plutonium–ligand complexes of low and often negative molecular charges will be soluble, unreactive with mineral surfaces and other environmental materials, and therefore promote the long-range migration of plutonium (Hakem *et al.*, 2001; Oviedo and Rodriguez, 2003). As an example, transport of actinide–EDTA complexes has been reported at the Oak Ridge site (Cleveland and Rees, 1981). At near-neutral pH, mixed-ligand complexes of actinides are likely to form. Based on known thermodynamic constants $Pu(IV)(EDTA)(OH)_2^{2-}$ is the Pu-EDTA species predicted to be stable under most natural water conditions, unless there is a molar excess of EDTA present, in which case a bis-EDTA complex can form (Boukhalfa *et al.*, 2004). The coordination geometry of $Pu(IV)(EDTA)(OH)_2^{2-}$ is likely to be similar

to that of $Th(Ac)_4H_2O_n^{12-}$ with eight oxygen atoms at 2.52 Å from four bidentate acetate (Ac) groups, and two to three oxygen atoms at 2.37 Å attributed to solvating water molecules (Rao *et al.*, 2004). The stoichiometries, coordination numbers, and molecular charges for Pu complexes of NTA and EDTA degradation products, such as ethylendiaminetriacetic (ED3A), 2-oxo-1,4-piperazinediacetic acid (3KP), N,N′-ethylenediaminediacetic acid (N,N′-EDDA), iminodiacetic acid (IDA), and glycine should also be similar. NTA can form soluble complexes with both Pu(VI) and Pu(V), such as PuO_2NTA^{2-} (Al Mahamid and Becraft, 1995). NTA also reduces plutonium to its tetravalent oxidation state, while, in excess, this reagent inhibits the formation of Pu(IV) colloid and establishes the formation of a Pu(IV)–NTA solution complex.

Bacteria produce a range of potential ligands from their utilization and degradation of plant matter and other carbon sources, which are used for the acquisition of nutrients needed for growth (Atlas and Bartha, 1993; Ratledge and Dover, 2000). These ligands can influence the speciation of plutonium in the environment significantly, including unintended cellular accumulation. Among the large variety of ligands generated by bacteria plutonium complexation by siderophores and humic acids has received the most attention (Choppin, 1988; Moulin *et al.*, 1996; Artinger *et al.*, 2003). For a more detailed discussion of the microbial interactions of the actinides we refer to Chapter 33.

(f) Colloid formation

At the low actinide concentrations expected in surface and groundwater systems, the reactions of actinides with particulate surfaces most likely control the actinides' fate in the environment. Colloidal particulates occur naturally in most soils and groundwaters and can be produced by waste package degradation. The amount and stability of natural colloids differ for each site-specific ground- and surface water due to their varying chemical compositions and hydrogeochemical steady states (Degueldre *et al.*, 2000). The colloid stability in natural water primarily depends on the water chemistry, which is driven by the rock–water interactions. Decreasing concentrations of alkaline and alkaline earth ions and large concentrations of organics enhance colloid concentration and stability. Because of the large surface area of colloids, the extent of radionuclide interaction with colloidal matter is critical. Strongly sorbing radionuclides can easily form such pseudocolloids that can enhance the transport of strongly sorbing radionuclides along flow paths to the accessible environment. In order to understand the colloidal behavior of actinides in the environment, the characteristics and properties and composition of the colloids must be known.

The mobility of actinides in the environment is closely related to colloidal particulates in natural waters (Buddemeier and Hunt, 1989; McCarthy and Zachara, 1989). Every aquatic system contains suspended colloidal particles varying in nature, form and size. These particles can bond with actinides, especially when in the +III, +IV and +VI oxidation state, carry them away

from the source term and enter them into the geosphere. Two different types of actinide colloids can be defined: (1) real or *intrinsic* colloids produced by aggregation of hydrolyzed actinide hydroxide species (i.e. Pu(IV)), and (2) natural (inorganic or organic) colloids as the weathering products of soils, man-made materials (i.e. cement, glass), waste-forms, spent nuclear fuel, or cement. As being very small, colloids can act as carrier for actinides of high complexation and sorption capacities, such as Am(III) or Pu(IV), and thus enhance their migration. They also can add to the retention of actinides in waters of high ionic strength (Kessler, 1999). An overview of colloid formation, their fundamental properties and interactions in aqueous solutions can be found in Stumm and Morgan (1995) and Myers (1991).

(*i*) *Intrinsic actinide colloids*

Tetravalent and hexavalent actinides are such hard metal ions that they bind several inner-sphere water molecules and hydroxide to form dimeric, trimeric or polymeric species. The tetravalent actinide hydroxides can polymerize further and aggregate to form colloids, relatively low molecular weight species that can remain suspended. The formation of intrinsic colloids is initiated by stepwise hydrolysis and proceeds rapidly through a series of nucleation and polymerization processes. It has been well established that Pu(IV) forms such colloidal polymers in aqueous solution of sufficiently high plutonium concentration (Kraus and Nelson, 1950). The stability of such polymers increases with time probably due to further dehydration while approaching the thermodynamically enormously stable fluorite structure of crystalline PuO_2. The ultimate result is a quasi-stable species with a concentration in solution that can significantly exceed the thermodynamically calculated solubility of plutonium oxides or hydroxides significantly (Rai *et al.*, 1980; Neck *et al.*, 2007a) (Fig. 32.22). The intrinsic Pu(IV) colloids are inherently stable and are not destroyed by dilution, but can be altered by oxidation of the Pu(IV) or by heating an acidified colloid suspension. Depending on the conditions during the aging process the size distribution of Pu(IV) intrinsic colloids can vary ranging between one and hundreds of nanometers. Recent laser-induced breakdown spectroscopic studies showed that plutonium does not form significant amounts of colloidal Pu(IV) with sizes smaller than 400 nm when the total plutonium concentration is below 3×10^{-5} M (Knopp *et al.*, 1999). Structural characterization of intrinsic Pu(IV) colloids revealed a variety of structural features with some similar to that of PuO_2, such as the Pu–O and Pu–Pu near-neighbor distances of 2.33 and 3.84 Å, respectively (Neu *et al.*, 1997; Conradson, 1998). A number of Pu–O distances ranging between about 2.2 and 3.7 Å are suggestive of terminal Pu–OH moieties, oxo-bridged Pu atoms, and substantially varying structural subunits and terminal ligands. For a more detailed discussion of the nature, formation, size distribution and structural characterization of intrinsic Pu(IV) colloids we refer to Chapter 7 of this work.
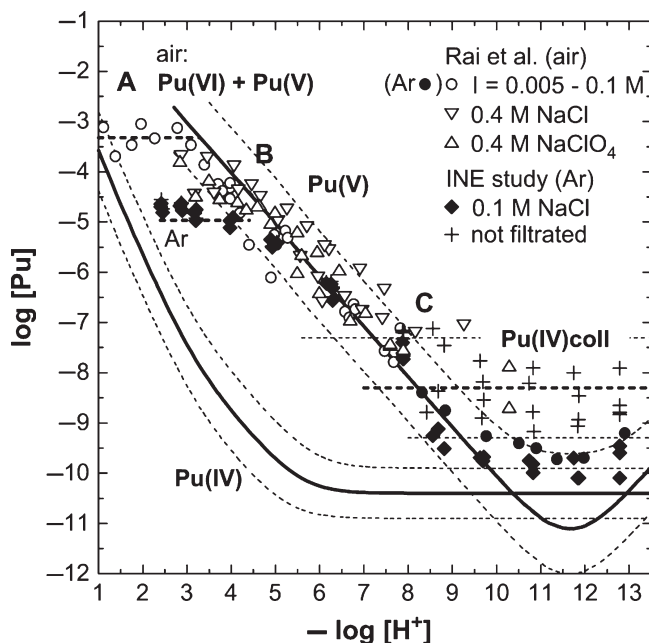
Fig. 32.22 *Impact of Pu(IV) colloid formation on plutonium solubility (Neck et al., 2007a). The formation of colloids can increase the fraction of plutonium in solution significantly, especially under near-neutral conditions. Solubility data referring to Rai et al. are taken from Rai et al. (1984, 1999, 2001), and INE study data are from Neck et al. (2007b). The solid lines show the predicted concentrations of Pu(IV) and Pu(V) as a function of pH. The total concentration of plutonium at high pH is significantly higher than predicted due to the formation of Pu(IV) colloids. Reproduced by permission of Elsevier.*

The intrinsic colloids of tetravalent actinides are of great concern because of their high stability at near-neutral pH, their resistance to disintegrate when diluted with water, and their ability to raise the actinide levels in solution and therefore enhance actinide mobility in aquifers. Even ionic strength and chloride concentration do not have an apparent affect on the stability of intrinsic colloids. These colloids have an integral part in actinide solution chemistry besides solid phase solubility, complexation reactions in solution and redox processes. For decades, the strong tendency of Pu(IV) to form intrinsic colloids have complicated thermodynamic hydrolysis studies and intrinsic Pu(IV) colloids have contributed to the large scattering of Pu(IV) solubility data (Neck *et al.*, 2007a). While most focus has been on intrinsic Pu(IV) colloids, similar generation of intrinsic colloids have been reported more recently for Th(IV) and Np(IV) and some studies suggest the formation of Am(III) colloids. Intrinsic Th(IV) colloids increased the total thorium solubility by two to three orders of magnitude (Altmaier *et al.*, 2004) and intrinsic Np(IV) colloids have

been found at neptunium concentrations exceeding the solubility limit of $Np(OH)_4$(s) (Neck *et al.*, 2001). Although it is unlikely that intrinsic colloids of tetravalent actinides will be generated in the far-field of an actinide waste disposal site, they can be part of the source and thus be transported into the environment. Discharge of acidic waste effluents into the neutral environment can easily produce intrinsic plutonium colloids that can persist for years. The near-neutral pH of natural waters favors the survival of intrinsic colloids and thus could provide a potential migration path away from a radioactive disposal site into the environment.

(*ii*)   *Natural inorganic actinide colloids*

The composition of inorganic colloids varies with the composition of the aquifer and the nature of the surrounding geological formations. Very common inorganic colloids are clay fragments, zeolithe, carbonate or iron(oxy)hydroxides. These colloids form via condensation reactions of smaller molecules or fragments or through the weathering processes of macromolecular rock or sediments. Some colloids may be formed during the weathering and alteration process of man-made materials. As an example, iron(oxy)hydroxide-based colloids may be produced by the corrosion of iron-based waste drum steels. Dissolution of high-level waste glass and spent nuclear fuel may generate clay (mainly smectite) and silica colloidal material (CRWMS, 2000a). The large surface area (10^4–10^5 m^2 kg^{-1}) and the high density of surface functional groups on inorganic colloids offer significant sorption capacities to easily adsorb actinides. Numerous studies have been performed with synthetic colloids in well-defined laboratory settings to investigate the fundamental behavior of actinide-bearing colloids. Colloidal iron(oxy)hydroxide sequesters plutonium nearly quantitatively in an irreversible uptake mechanism and may transport plutonium over long distances (Keeney-Kennicutt and Morse, 1985; Sanchez *et al.*, 1985). On the other hand, silica and montmorillonite can release adsorbed plutonium when exposed to a new environment to a significant fraction, thus potentially changing the transport mechanism with the water flow. Nagasaki *et al.* (1997) found a high stability of ^{241}Am and ^{237}Np montmorillonite colloids that transport through quartz columns. The plutonium that migrated at the Mayak site was associated with iron oxides as the vehicles for its transport (Novikov *et al.*, 2006; Kalmykov *et al.*, 2007).

   Plutonium(IV) has been shown to be quickly adsorbed to colloidal brucite, $Mg(OH)_2$ (Farr *et al.*, 2000). Sorption experiments of ^{239}Pu and ^{241}Am onto hematite, smectite, and silica colloids indicated that sorption of Pu(IV) and Am (III) is completed within hours to days and is quite faster than the desorption process which lasts over a period of months (Lu *et al.*, 2003). In addition, the sorption of Pu(V) is low, but increases with time probably due to redox reactions of the Pu(V) in solution or on the colloid surface. The latter observations emphasize the important relationship between solution speciation and surface

complexation. Precipitation of hematite in the presence of [241]Am led to the incorporation of Am(III) into the ferrihydrate structure and to an increased mobility in groundwaters in the presence of Pleistocene aeolian quartz sand (Schäfer *et al.*, 2003). The distribution of Am(III) and ferrihydrite colloids between groundwater and sediment remained in disequilibrium even after 1 month. This finding emphasizes the importance of kinetics on the distribution of actinides in natural water-sediment systems.

Only few studies are reported on the characterization of actinide pseudocolloids in natural aquifer systems. In groundwater near the Karachay Lake in Russia, which is contaminated with discharges from the Mayak site, [239]Pu and [241]Am were found to be associated with hydrous ferric oxide nanocolloids (Novikov *et al.*, 2006; Kalmykov *et al.*, 2007). Leaching spent nuclear fuel at 90°C with simulated groundwater at pH 4–7 generated schoepite and soddyite colloidal phases with varying amounts of actinides, indicating that the transuranium elements are not released congruently with uranium from the spent fuel (Finn *et al.*, 1994).

(*iii*)   *Natural organic actinide colloids*

The amount of organic particulates has a significant effect on their journey in the environment. Particulates of organic nature are formed by the degradation of plants and animals and are an abundant source for the hard actinide ions to adsorb on (Kim, 1991; Choppin, 1992; Moulin *et al.*, 1992a; Moulin and Moulin, 2001; NATO, 2005). Three groups of humic substances have been identified: (a) the humic acid, which is insoluble in acidic solutions, (b) the fulvic acid, which is soluble in acidic and alkaline solutions, and (c) humin, which is the solid fraction not extractable by acid or base (Kim *et al.*, 1990). Both humic acid and humin have a higher molecular weight than the fulvic acid, but all are structurally similar polyelectrolytes with aromatic carboxylic and phenolic groups being the dominant functional groups (Moulin *et al.*, 1992a; NATO, 2005). Natural waters contain generally fractions of both humic and fulvic acids where they are saturated with complexed metal ions. Fulvic and humic acids have been widely studied for their strong interaction potential with actinide ions and their redox properties (Kim, 1991; Choppin, 1992; Moulin *et al.*, 1992b; NATO, 2005).

Natural organic matter can significantly increase the mobile fraction of actinides due to the formation of organic complexes or pseudocolloids. The extent depends on the concentration of organic matter and the stability when contacted to various environments. As an example, only a small fraction of such americium complexes survived when contacted with boom clay (Maes *et al.*, 2006). Humic substances (humic and fulvic acids) appear in surface and groundwaters at concentrations between 0.5 mg L^{-1} in marine waters and up to 50 mg L^{-1} dissolved organic carbon (DOC) in swamp areas (Choppin, 1992). About 85% of waters from 100 sites across the United States had DOC contents

between 0.1 and 15 mg L^{-1}. Groundwaters from the German Gorleben site contained high concentration of humic matter with DOC up to 95 mg L^{-1} (Kim *et al.*, 1992). Large quantities of cations, including the actinides, can be bound by humic and fulvic acids via the functional groups, carboxylates, phenolates and amines. Non-specific binding via electrostatic interactions between cations and negatively charged groups within humates reportedly also accumulate a significant amount of plutonium (Choppin and Wong, 1998). However, the main and higher affinity interactions are through carboxylate and phenolate covalent complexation. Phenolate groups of natural and synthetic humic acids have been shown to significantly complex with U(VI) (Pompe *et al.*, 2000) and could also play a secondary role in chelating plutonium. Thorium(IV)-humate species display X-ray photoelectron spectra very similar to Th(IV) complexes with low-molecular weight carboxylates (Schild and Marquardt, 2000). The similarities between Th(IV) and Pu(IV) complexation behavior suggest that Pu(IV) will preferentially bind to the humate carboxylate groups. Pu(IV) is a harder ion (stronger Lewis acid) than Th(IV) and Pu(IV)-humate complexes might be stable at a lower pH than Th(IV)-humate compounds (Reiller *et al.*, 2002). Plutonium and americium were preferentially associated with dissolved organic matter of high molecular size (Matsunaga *et al.*, 2004). And calculations suggest that a DOC concentration of as low as 1 mg C L^{-1} could result in the interaction between actinides and organic matter. Humate complexes of uranium(VI) persist at pH below 5, but compete with strong ligands, such as carbonate and hydroxide, at higher pH (Fig. 32.23). Cm(III) humate complexes are predicted to dominate solution speciation in some German groundwaters that are rich in humic acids (Panak *et al.*, 1996; Zeh *et al.*, 1999).

Humates also can affect the oxidation state of redox-sensitive actinides. While trivalent actinides (americium and curium) and the hexavalent uranyl maintain their respective valencies, neptunium and plutonium can easily alter their valencies upon interaction with humic substances. It has been demonstrated that humic acid can reduce higher oxidation states of neptunium and plutonium to the more stable Np(IV) and Pu(IV) (Choppin, 1992; Zeh *et al.*, 1999), just as more simple organic chelators do. Humic acid is found to reduce Np(V) to Np(IV), especially when enriched in hydroquinone, and can coat mineral surfaces, such as goethite, to form actinide-scavenging aggregates (Kalmykov *et al.*, 2008). Plutonium(VI) and Pu(V) humate complexes have been observed to undergo progressive reduction to Pu(IV) at pH-dependent rates. The reduction of Pu(V) by humic acid has been shown to be affected by the concentration of humic acid, light, and the presence of divalent cations (André and Choppin, 2000). In the dark and at a high concentration of humic acid (10 ppm) up to 60% of Pu(V) was reduced to Pu(IV) after 2 weeks. The reduction rate was enhanced significantly by light exposure, and also by the addition of Ca^{2+} and Mg^{2+}. André and Choppin attribute the reduction of Pu(V) by humic acid in the dark to hydrogen peroxide, which is produced by
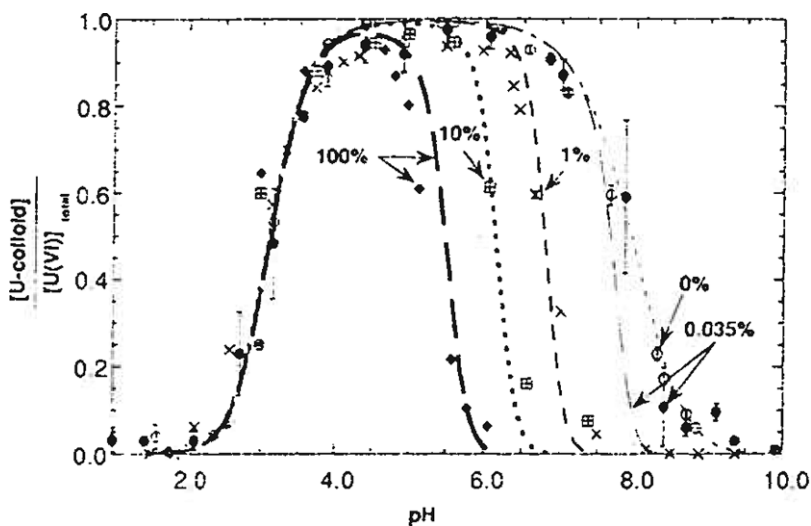
Fig. 32.23 *Impact of carbonate on U(VI) humate complexation (Zeh et al., 1997). The percentages refer to the CO₂ content in the atmosphere over the solution. At higher CO₂ partial pressure, carbonate outcompetes humate for uranium complexation and carbonate species dominate above pH 5 at 1 atm CO₂ (100%). Reproduced by permission of Oldenbourg Verlag.*

hydroxyquinone oxidation and catalyzed by Ca^{2+} and Mg^{2+}. The light-induced increase of the reduction rate is purported to be caused by hydrogen peroxide production from the disproportionation of superoxide, O_2^-, which is generated photochemically by humic acid-mediated reduction of oxygen. Humates can also serve as electron shuttles, receiving electrons from metal-reducing bacteria and delivering them to metal ions, including U(VI) and likely Pu(VI/V) to produce reduced An(III/IV) oxides.

At the near-neutral pH of natural systems, humate competes with hydroxide and carbonate for actinide coordination (Fig. 32.24). In the past, only binary actinide–humate complexes were proposed, while recent spectroscopic studies have provided evidence of ternary complexes. As an example, the ternary hydroxo–humate complexes, An(OH)HA and An(OH)₂HA where An = Am(III) or Cm(III) and HA = humate, have been identified using time-resolved laser fluorescence spectroscopy (Fig. 32.25) (Panak *et al.*, 1996; Morgenstern *et al.*, 2000)). At a humate concentration of 10.8 μmol L^{-1} and pH above 7, both ternary complexes dominate An(III) solution speciation in the absence of other strong ligands. The formation of ternary complexes also occurs in the presence of both humate and carbonate and Cm(CO₃)(HA) was observed to form at pH 6.5–9 when the dissolved organic carbon is at 5 mg C L^{-1} and the CO₂ partial pressure is below 1% (Panak *et al.*, 1996; Morgenstern *et al.*, 2000). The formation of such predominate ternary complexes at near-neutral pH
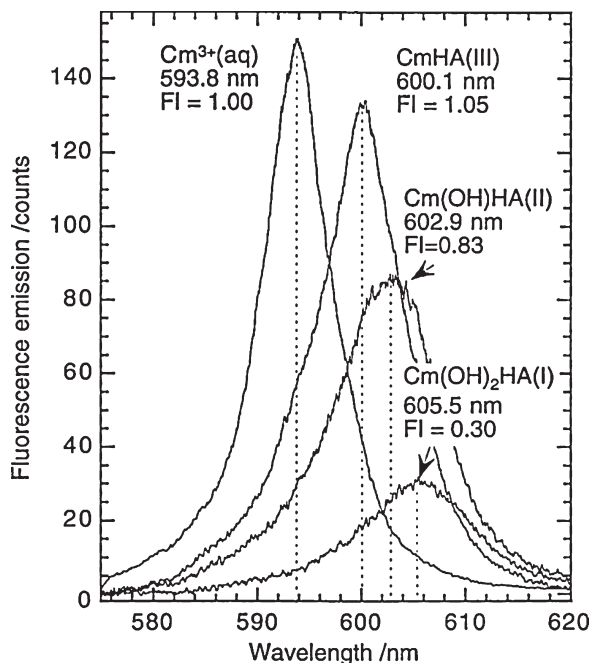
Fig. 32.24 *Spectroscopic characterization of ternary Cm(III) humate-hydroxo complexes (Morgenstern et al., 2000). The relative fluorescence emission factor (FI) decreases continuously from 1.1 at pH 6.2 to 0.3 at pH 10.2 indicating a change in Cm(III) humate speciation. Reproduced by permission of Oldenbourg Verlag.*

confirms that the speciation in natural systems is more complex than was previously thought (Fig. 32.25).

(g) Interactions with geologic matter surfaces

In the vicinity of a radioactive waste disposal site chemical processes such as radiolysis, solubility, and complexation reactions dominate the fate of the actinides, which may reach saturation upon water infiltration. When released and transported away from the source by infiltrating water, actinides are slowly being diluted and experience different environmental conditions. The formation of secondary macroscale solid phases of lower solubility and the sorption of actinides on solid geological material are key processes in the far-field that significantly change the actinides' fate and transport behavior. Nature is providing a wide variety of functional groups to coordinate the actinides in solution and on surfaces. Hydroxyl, carbonate, silicate and phosphate are probably the most dominant functional groups on rocks, sediments and minerals that can strongly bind actinide ions. The intimate contact between actinide
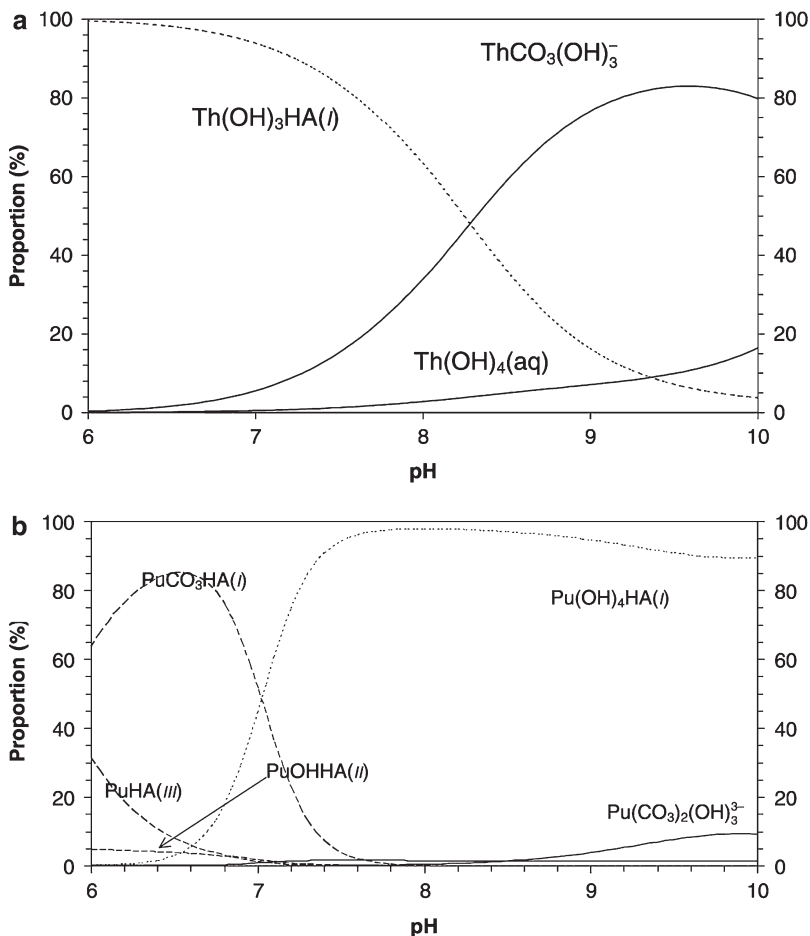
Fig. 32.25 *Predicted speciation of Th(IV) and Pu(IV) in the presence of humate, hydroxide and carbonate (Reiller, 2005). Reproduced by permission of Oldenbourg Verlag.*

ions and functional groups on rocks, sediments and mineral surfaces provide a dominant reaction path for their retention and immobilization. On the other hand, adsorption on mineral colloids has been recognized to be a transport path for actinides into the geosphere. The complex actinide chemistry, the large variety of surface groups on geological materials, and the dynamic reorganization of mineral surfaces create an inherently complex challenge for scientists to understand and to describe in mathematical models.

There is an enormous body of literature on the interaction of actinides with geologic material surfaces. Examples are found in Langmuir (1997), Triay *et al.* (1997), Jenne (1998), and Sterne *et al.* (1998); a review of the fundamental processes at the solid-water interface is provided by Stumm (1992). Actinide

ions can interact with solid surfaces in several ways: physical adsorption; reversible electrostatic adsorption via coulombic attraction between actinide ion and surface groups such as ion exchange; and chemisorption based on short-range interaction via covalent bonding or hydrogen bonding. As the actinide concentration in solution increases monomeric surface complexes may convert to polymeric and oligomeric surface species and ultimately form surface precipitates. Sorption isotherms are used to illustrate the correlation between the amount of species sorbed as a function of its concentration in solution (Stumm, 1992; Langmuir, 1997). The removal of actinide ions from solution by adsorption processes on surfaces is quantitatively expressed as the distribution coefficient, K_d, which is defined by

$$K_d = [\text{An}]_{\text{sorbed}} / [\text{An}]_{\text{solution}} \tag{32.10}$$

where $[\text{An}]_{\text{sorbed}}$ is the concentration of actinide adsorbed on the solid material and $[\text{An}]_{\text{solution}}$ is the concentration in solution. Often, K_d is expressed in L kg^{-1}. The K_d approach describes the distribution of the actinide ion between dissolved and solid phase and its removal from solution by all of the mentioned mechanisms combined. Its value depends on a number of parameters, such as the oxidation state of the actinide ion, the water conditions (such as Eh, pH), organic and inorganic ligand concentrations competing for actinide complexation, presence of microorganisms, and the nature of the sorbing solid phase. The measured K_d values are conditional constants valid for a given pH, solution and mineral composition, temperature, etc., and describe only the system in which they were measured. As such, each distribution coefficient represents a single point in a multidimensional space and contains little information for extrapolation to different conditions. Applying a single K_d value to predict the general removal of species that form strong complexes or precipitates or are subject to redox processes can lead to large errors of many orders of magnitude (McKinley and Alexander, 1993; Wilhelm, 2004). In fact, Rai *et al.* (1981) suggested that (Am(III)) sorption data, interpreted as K_d values, are more likely controlled by the solubility of an americium precipitate.

The presence of other ligands in solution may affect the uptake of actinides. In specific, strong correlations of U(VI) uptake have been observed in the presence of carbonate, phosphate, sulfate, and humate. Carbonate is known to reduce the uptake of actinides at high pH due to the high stability of anionic actinide carbonate complexes formed in solution. Humic acid reportedly moves the adsorption edge of U(VI) (and of Am((III)) on ferrihydrate and hematite to lower pH (Fig. 32.26) by forming a humic coating on the mineral surface (Ho and Miller, 1985), while formation of Am–HA complexes in solution reduces Am(III) uptake at higher pH (Moulin *et al.*, 1988; Moulin and Ouzounian, 1992). The presence of complexing ligands suppressed the uptake of Am(III) on silica in the order

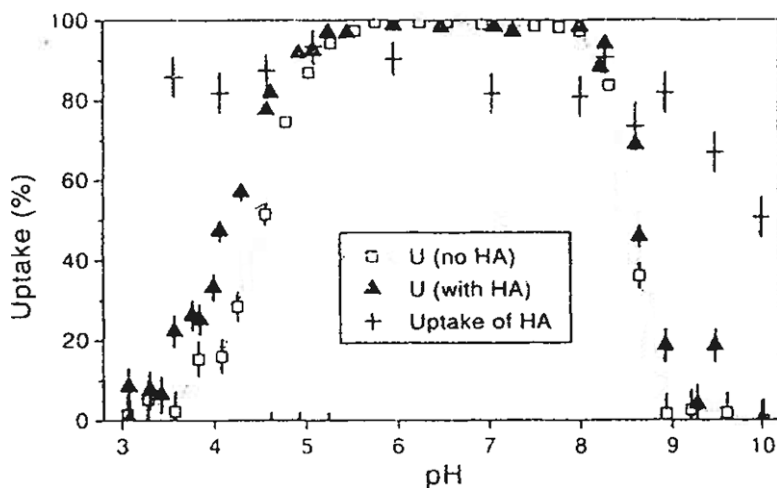EDTA > citrate > oxalate > carbonate (Pathak and Choppin, 2007).

Fig. 32.26 *Effect of humic acid (HA) on the uptake of U(VI) on hematite (Payne et al., 1996). The concentration of added HA is 9 mg L^{-1} and the total uranium concentration in solution is 10^{-6} mol L^{-1}. Reproduced by permission of Oldenbourg Verlag.*

The actinides exhibit common trends in their sorption behavior. The oxidation state of an actinide is paramount to its sorption behavior and is shifting the adsorption edge with pH, consistent with the effective charge of the actinide ion (Fig. 32.27). Similar to their high affinity for complexation, tetravalent actinides are affixed to solid surfaces at much lower pH than An(VI), An(III), or An(V). As an example, 50% uptake of Pu(IV), U(VI) and Np(V) on α-FeOOH was reported to occur at pH 3.2, 4.2 and 7.0, respectively (Turner, 1995). The uptake of oxidation state analogues was found to be similar on 12 different minerals and four rock types and a general K_d ratio of 500 : 50 : 5 : 1 was assigned for An^{4+}: An^{3+}: AnO_2^{2+} : AnO_2^{+} ions (Silva and Nitsche, 2002). Uptake of neptunium at pH 7 increased from K_d values below 10 to K_d values of about 1,000 when lowering the Eh from aerobic conditions to below +200 mV inducing the reduction of Np(V) to Np(IV) (Lieser and Mohlenweg, 1988). Similarly, the disproportionation reaction of Pu(V) to Pu(IV) and Pu(VI) was reported to form on the goethite surface (Keeney-Kennicutt and Morse, 1985). The latter is then slowly reduced to Pu(IV), leaving Pu(IV) as the dominant surface species. In contrast, Pu(V) oxidation to Pu(VI) on MnO_2 has been verified by EXAFS studies (Powell *et al.*, 2006).

There is a pronounced correlation between the sorption of actinides and the stability field of their hydroxo complexes in solution. Under acidic conditions, actinides may be adsorbed via ion exchange whereas the uptake of actinides via surface complexation is generally very low. With increasing pH and beginning of hydrolysis reactions sorption increases and reaches a maximum uptake in the
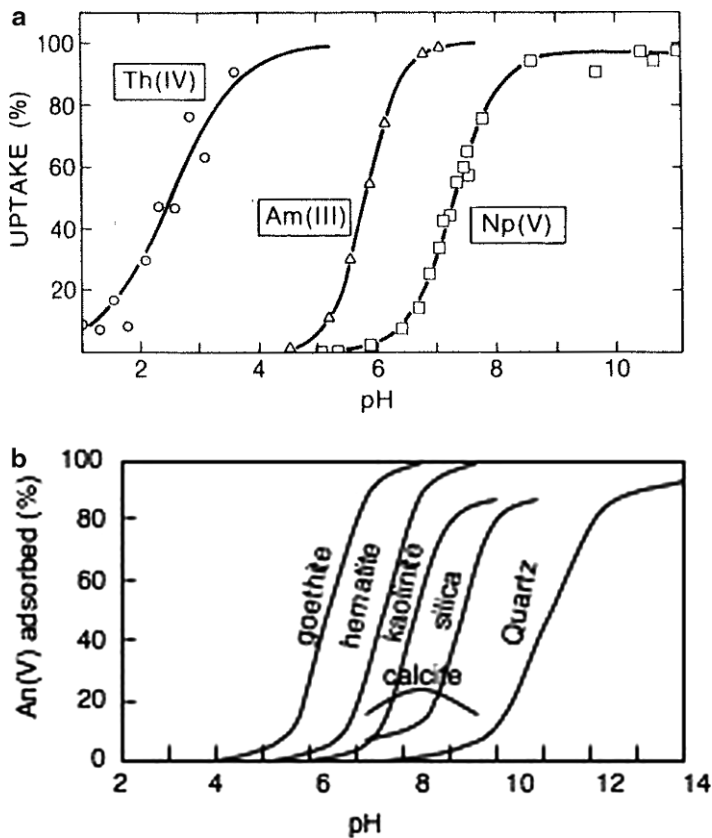
Fig. 32.27 *(a) Uptake of actinides in different oxidation states on Al_2O_3 (Righetto et al., 1988). The open circles are adsorption data for $2 \cdot 10^{-10}$ mol L^{-1} Pu(V) onto 10 mg L^{-1} γ- Al_2O_3. The solid lines refer to the uptake of Th(IV), Am(III) and Np(V). Reproduced by permission of Oldenbourg Verlag. (b) Adsorption of Np(V) (10^{-7} mol L^{-1}) on different minerals in 0.01 M NaClO$_4$ (after Langmuir, 1997).*

near-neutral conditions, usually around pH 6 (Figs. 32.27 and 32.28). Under basic conditions actinide uptake is reduced due to the formation of anionic hydroxo or carbonato actinide complexes in solution. Much lower impact of the surface charge on actinide sorption has been reported. Figure 32.28 illustrates the similar uptake behavior of U(VI) on the mineralogically different surfaces of silica, montmorillonite and clinoptilolite with a maximum uptake at near-neutral pH (Pabalan *et al.*, 1998). Temperatures up to 60°C did not significantly alter the strong uptake of U(IV), Np(IV) and Cm(III) on surfaces of bentonite, tuff and granodiorite (Baston *et al.*, 1997).

For decades, a large number of investigations have been conducted to understand the principal uptake mechanisms of actinides on single-phase minerals. The interpretation of sorption data especially of neptunium and
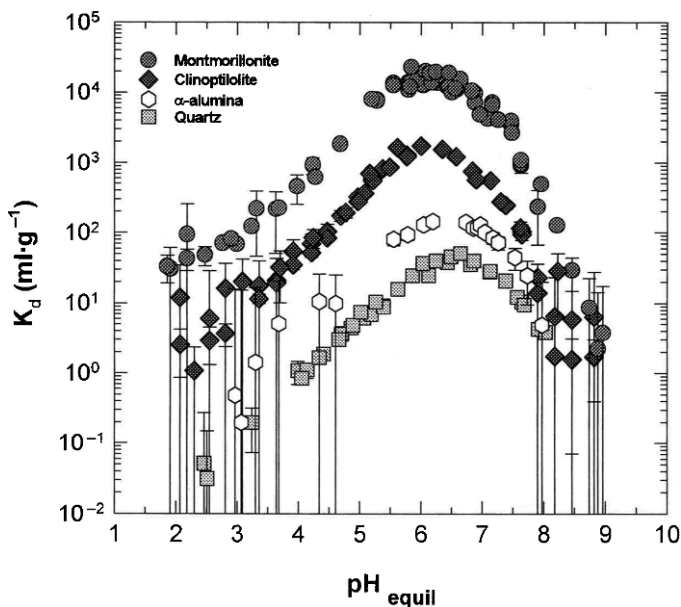
Fig. 32.28 *Effect of the pH on the uptake of U(VI) on silica, montmorillonite and clinoptilolite under atmospheric conditions pressure* ($p_{CO_2} = 10^{-3.5}$ *atm*) (*Pabalan et al.*, 1998). *Reproduced by permission of Elsevier.*

plutonium remains quite contradictory caused by their complex redox chemistries. In the past, the majority of actinide uptake studies have been to either determine batch distribution coefficients or to study column transport. Both methods were not designed to distinguish between different reaction mechanisms, such as bulk precipitation versus molecular surface complexation. Mineral types that are thought to be most important for actinide retention in natural systems are iron(oxy)hydroxides such as goethite, hematite and ferrihydrate; clay minerals such as montmorillonite, smectite, clinoptilolite; carbonate minerals such as kaolinite and calcite; phosphates such as apatite; oxides such as quartz; and model oxides such as alumina, titania and silica. Most studies have been performed with uranium and plutonium; fewer studies have focused on thorium, neptunium, americium and curium. Sorption data for plutonium demonstrated the strong ability of plutonium to adsorb on inorganic compounds with K_d values ranging between 10^3 and 10^5 L kg^{-1} (Yui *et al.*, 2001). A series of sorption experiments have been carried out for the actinides actinium to curium on bentonite, granodiorite and tuff and are summarized in (Berry *et al.*, 2007).

Clay minerals are known to retain actinides and are effective scavengers of the highly-charged f-elements. In fact, this process is observed at the Bangombé natural reactor in Gabon where the fissiogenic lanthanides neodymium,

samarium, and europium were trapped in the clay layer overlaying the uranium mineralization zone inhibiting their migration into the next black shale layer (Kikuchi *et al.*, 2008). Also, heavy metals may be retained in clay that is formed around mill tailings by intense weathering (Lin, 1997). Batch sorption experiments on clay resulted in K_d values that range between 15,000 and 210,000 L kg^{-1} for plutonium and between 15,000 and 80,000 L kg^{-1} for americium. Changing the geochemical conditions altered the uptake and the relatively low upper-limit K_d of 21,000 for plutonium may be indicative of the formation of Pu (V) (Lujaniene *et al.*, 2007). Uranium(VI) forms ternary hydroxo surface complexes on clay minerals in heterogeneous natural clay rock at pH above 9, and time-resolved fluorescence spectroscopy has revealed that Cm(III) exhibits multiple surface species on clay in the pH range 5–11 (Hartmann *et al.*, 2008). Stammose and Dolo (1990) observed an increase in Am(III) uptake on clay at pH above 5 with decreasing ionic strength.

   Thorium, plutonium and americium were found to strongly interact by adsorption and/or coprecipitation with both carbonate minerals, calcite and aragonite, with nearly quantitative removal from solution (Meece and Benninger, 1993). However, some 3–4% of the plutonium remained in solution, presumably in its V oxidation state. Uranium showed incorporation into aragonite and less into calcite (Reeder *et al.*, 2000) and natural coral appears to limit the uptake of uranium compared to laboratory experiments with synthetic carbonate minerals.

   Iron (oxy)hydroxides are very common minerals that have been shown to effectively adsorb the actinides even in their pentavalent oxidation state. Neptunium rapidly reacts with iron oxyhydroxides under neutral pH (Nagasaki *et al.*, 1998). Neptunium(V) was found to adsorb as an inner-sphere complex on the external sites of poorly crystalline ferric oxide. It is suggested that adsorbed neptunium subsequently diffuses through small pores in the oxide to occupy sorption sites on the internal surface (Nagasaki *et al.*, 1998). Sorption of Pu(V) on goethite occurs between pH 4 and 8, significantly higher than Pu(IV), which sorbs between pH 2 and 6 (Sanchez *et al.*, 1985). Uranyl(VI) strongly interacts with iron (oxy)hydroxides up to about pH 6 when desorption occurs due to carbonate complexation in solution (Waite *et al.*, 1994; Duff and Amrheim, 1996). Goethite adsorbed up to six times more U(VI) than a montmorillonitic soil from the San Joaquin Valley in California. Ferrihydrite is a strong sorbent for actinides and retains U(VI) strongly between pH 5 and 8.5. Phosphate can strongly bind to the ferrihydrite surface and increases U(VI) adsorption, probably via the formation of U(VI) phosphate complexes or surface precipitates (Payne *et al.*, 1996). Humic acid increased the uptake of U(VI) at pH below 7. As expected, Am(III) also strongly adsorbs on iron (oxy)hydroxide phases, such as hematite, ferrihydrate and ferrihydrate-coated silica (Stumpf *et al.*, 2006; Tao *et al.*, 2006). The degradation of ferrihydrate to hematite and goethite at 85°C and pH 8 in the presence of americium resulted in the incorporation of Am(III) into the degradation products hematite and goethite (Stumpf *et al.*, 2006).

Magnesium oxide is used at the WIPP site as backfill material. Brucite, $Mg(OH)_2$, and hydroxylated magnesium oxide, MgO (100), have been shown to effectively adsorb Pu(IV) and even incorporate the plutonium ions to a depth of at least 50 nm (Farr *et al.*, 2007). The presence of organic ligands, i.e. citrate, did not affect this behavior.

Traditional actinide uptake studies have been performed using single actinide and single mineral as a function of pH and carbonate concentration. The adsorptive properties of a single adsorbant may change when mixed with other mineral components. As an example, U(VI) is preferably adsorbed on ferrihydrate over kaolinite (Thompson *et al.*, 1998). Preferred sorption of plutonium to manganese oxide within a heterogeneous mixture has also been observed with Pu(V) and Pu(VI) (Duff *et al.*, 1999; Reilly *et al.*, 2003; Stout *et al.*, 2003).

In recent years, more sophisticated spectroscopic techniques, i.e. X-ray photoelectron spectroscopy, extended X-ray absorption fine structure (EXAFS) and grazing angle spectroscopies, laser-fluorescence spectroscopy, and Rutherford backscattering spectroscopy, have been applied to investigate the molecular aspects of interfacial reactions and have enabled the characterization of actinide surface complexes. As an example, laser-fluorescence spectroscopy was successfully applied to develop the surface speciation of Cm(III) on silica (Fig. 32.29). EXAFS spectroscopy has been widely used to interrogate the inner coordination sphere of the adsorbed metal and actinide species (Grown and Sturchio, 2002). In general, actinides are bound on mineral surfaces as inner-sphere complexes. A transition from an outer-sphere cation-exchange uptake of U(VI) on montmorillonite at low pH to monomeric, bidentately
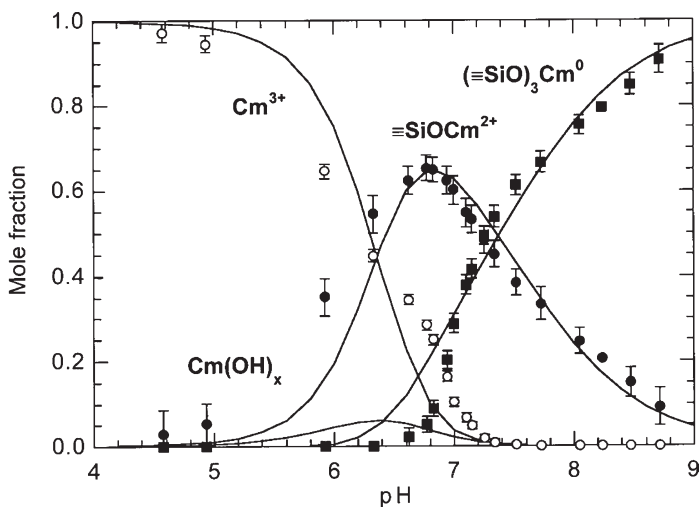

Fig. 32.29 *Cm(III) sorption and speciation on silica (Chung et al., 1998). Reproduced by permission of Oldenbourg Verlag.*

coordinated inner-sphere surface complexation at near neutral pH is reported (Sylwester *et al.*, 2000). In most cases, the U(VI) surface complex is found to be coordinated in a bidentate fashion (Waite *et al.*, 1994; Sylwester *et al.*, 2000) as observed in carbonate, phosphate or nitrate solution complexes. The linear $O=U=O^{2+}$ structure remains intact when adsorbed on mineral surfaces. Structurally distinct monomeric and monodentate U(VI) surface species interacting with multiple surface sites were characterized on montmorillonite at pH 3.5 (Chisholm-Brause *et al.*, 1994). The formation of oligomeric inner-sphere U(VI) surface species on silica at pH of about 6 was proposed with a U–Si distance of 3.1 Å and a U–U distance of about 4.0 Å (Sylwester *et al.*, 2000). However, the observation of a U–U distance could also be indicative of a surface precipitate of a U(VI) silicate phase. Mononuclear U(VI) species are also found on kaolinite at pH between 6 and 7, while polymerization occurs at pH 7–7.5 (Thompson *et al.*, 1998).

Actinides can also be embedded into the host structure. As an example, U^{4+} ion is found to substitute Ca^{2+} in natural calcite without significant distortion of the overall structure (Sturchio *et al.*, 1998). Different coordination geometries of U(VI) are observed in the two most common carbonate polymorphs, calcite and aragonite (Reeder *et al.*, 2000). Incorporated into aragonite, U(VI) is present in similar environment as in the solution species $UO_2(CO_3)_3^{4-}$. A change in the U(VI) coordination is required for its incorporation into calcite resulting in a less ordered and less stable coordination environment. Consequently, calcite is less effective for the long-term sequestration of U(VI). However, scavenging radionuclides by incorporation into a mineral structure can provide a valuable retention mechanism that may become critical for long-term actinide mobility and bioavailability assessments.

(h)   Interactions with biomolecules

Bacteria are ubiquitous in nature. They exist in the environment as isolated cells, or much more commonly in biofilms of single or mixed strains and species. The abundance of bacterial species is highly variable and is determined by the availability of nutrients, water, carbon sources, terminal electron acceptors, and temperature. For example, organic-rich, temperate soils may contain up to 10^{10} cells g^{-1}, while Antarctic sandy sediments may contain only 10^6 cells g^{-1} (Weinbauer *et al.*, 1998). Certain conditions may lead to the pervasiveness of a particular family or class of bacteria, which in turn will determine the local conditions and prevailing biogeochemical processes at that site. These microorganisms naturally influence the environmental behavior of the major elements that they utilize for cell survival and population growth, including C, N, P, S, and transition metals such as Mn and Fe. In many micro-environments fluxes and cycling of metal ions are controlled exclusively by biological activity (Fletcher and Murphy, 2001). Actinides have no known biological utility, yet they have the potential to interact with bacterial cellular and extracellular

structures that contain metal-binding groups, to interfere with the uptake and utilization of essential elements, to interact with bacterial by-products, and to alter cell metabolism as described in the following references (Lovley *et al.*, 1991; Banaszak *et al.*, 1999; Neu *et al.*, 2002; Lloyd, 2003; Gadd, 2004). A detailed review of actinide interactions with bacteria and microbial matter is provided in Chapter 33.

These interactions can transform actinides from their most common forms, solid, mineral-adsorbed, colloidal, or ligand-complexed to a variety of biogeochemical species that have much different physico-chemical properties. For example, organic acids that are extruded products of cell metabolism can solubilize actinides and then enhance their environmental mobility or in some cases facilitate metal transfer into cells. Phosphate- and carboxylate-rich polymers associated with cell walls can bind actinides to form mobile biocolloids, or more likely, actinide-laden biofilms associated with mineral solids. Bacterial membranes, proteins or redox agents can produce strongly reducing electrochemical zones and generate low-valent molecular actinide species or "biomineralized" oxide particles. Alternatively, they can oxidize actinides to form soluble complexes. The most common and predominant mechanisms are shown schematically in Fig. 32.30. Bacteria and biomolecule interactions have been studies with the actinides in their oxidation states, III, IV, V, and VI. Most research has been done with uranium or plutonium, so other actinide states will
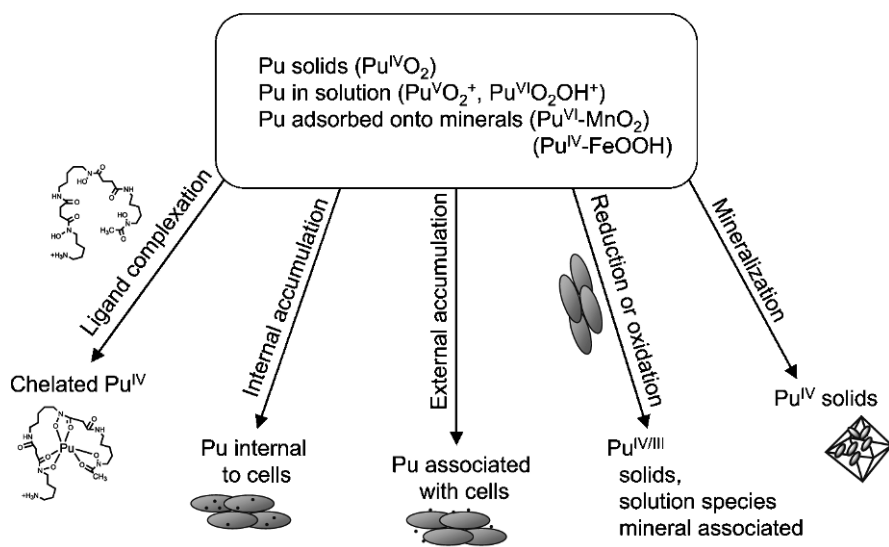

Fig. 32.30 *Illustration of the most common interaction mechanisms between microbes and plutonium (Neu et al., 2005). Reproduced by permission of Oldenbourg Verlag.*

be discussed only to highlight specific processes and transformations of prevalent forms, such as the bioreductions of Np(V).

The most common oxidation states of uranium and plutonium, U(VI) and Pu(IV) are generally favored in the presence of biomolecules and by most common aerobic bacterial processes. As discussed earlier, plutonium is stabilized in natural waters in its IV and V oxidation states by the formation of soluble complexes and as suspended Pu(IV) colloids. Plutonium solubility can also be enhanced by anthropogenic and bacterially-produced organic ligands (O'Boyle *et al.*, 1997; Ruggiero *et al.*, 2002). Similarly, americium adsorption onto quartz was found to be significantly reduced by chelators produced by *pseudomonas fluorescens*, *pseudomonas stutzeri* and *shewanella putrefaciens* (Johnsson *et al.*, 2006). The most effective biomolecules for dissolution and complexation of actinides are arguably the siderophores. Siderophores are a class of biogenic ligands that have been well studied for their actinide binding (White *et al.*, 1988; Bouby *et al.*, 1999). These low molecular weight organic chelating agents are produced by aerobic and facultative anaerobic bacteria and have a high specificity for iron (Neilands, 1981). Siderophore-promoted dissolution of Pu(IV) hydroxides has been demonstrated (Brainard *et al.*, 1992; Ruggiero *et al.*, 2002). Among the chelators tested, enterobactin and other catecholate-based ligands (like Tiron) are more effective at solubilizing plutonium than any other ligands tested, by up to a 1,000 times for enterobactin. There is some evidence that hydroxamate type siderophores attach to the surface of iron and plutonium (hydr)oxides and may in fact inhibit subsequent dissolution by other ligands.

Among the solution species that could result from dissolution and desorption Pu(IV) and U(VI) complexes are the most favored. For example, hexadentate siderophores like the tri-hydroxamates, desferrioxamine E (DFE) and desferrioxamine B (DFB), form stable 1:1 Pu(IV) : siderophore complexes in solutions of pH < 2.5 (Neu *et al.*, 2000). The stability constant for the Pu(IV)-DFB complex was estimated from measurements in acidic media and Gibbs energy correlations to be log β = 30.8 (pH < 2.5) (Jarvis and Hancock, 1991). At higher pH, the complex hydrolyzes to form mixed-ligand compounds of the form Pu(IV)-siderophore(OH)$_n$. However, if the siderophore is present in molar excess, then the Pu(IV)(siderophore)$_2$ complex may form (Boukhalfa, *et al.*, 2007). The resulting chelate-complex could then be mobile as a soluble species or adsorb to a mineral or bacterial surface by mechanisms as described in previous sections. An alternative process is that the chelated actinide can be internalized into the cell.

Direct uptake of metals by bacteria can occur by passive or active transport across the membrane(s). The large size and charge of actinide ions favor surface binding and makes their transport across the cell membrane unlikely. Anion binding or chelation by siderophores, which are specifically recognized by membrane proteins, can make actinides more susceptible to trans-membrane channel. Thorium (IV) and Pu(IV) have been shown to be taken up, but U(VI) not taken up by this process (John *et al.*, 2001).

In addition to complexation by biomolecules and accumulation inside the cell, bacteria can also take up actinides via external complexation and adsorption. Biomass, cells and/or extracellular material, provide surfaces for adsorption and can strongly influence the metal speciation and mobility (Gillow *et al.*, 2000). Metal ions can be specifically or nonspecifically bound by cell walls and extracellular polymers, or can be sequestered within biomass/mineral matrices (Haas *et al.*, 2001). Detailed characterization of bacterial cell walls and extracellular polymers, or exopolymers, which are produced by bacteria to create a selective barrier between the cells and the environment, has revealed complicated structures containing multiple functional groups. Binding groups with soft donor atoms like sulfhydryls, thioethers, imidazols, amines, and amides provide high affinity binding sites for soft metal ions, but are unlikely to have an effect on actinides. Functional groups with harder donor atoms such as sulfonates, hydroxides, carboxylates, phosphonates, and phosphodiesters can covalently complex most hard metal ions, including actinides, to form highly stable species. Among these, anionic glycerol–phosphate groups, which cover most of the microbial cell envelope, and exopolymer carboxylate and hydroxide groups are likely the most significant actinide chelators. These same chelating groups are in biofilm, and can bind actinides outside of individual cells. The bioaccumulation or bioadsorption of plutonium onto bacterial cells has been proposed to both immobilize plutonium (Dhami *et al.*, 1998) and mobilize plutonium (Gillow *et al.*, 2000) in subsurface environments. Extracellular polymeric compounds isolated from *clostridium* sp., *pseudomonas fluorescens*, and *shewanella putrefaciens* were found to complex Pu(IV) in a 1:1 stoichiometry with carboxylic groups being the primary binding units (Harper *et al.*, 2008).

Several XAFS studies of U(VI) biosorption have shown that uranium preferentially complexes with phosphate functional groups at the cell surface, which was supported with theoretical predictions (Fowle *et al.*, 2000; Haas *et al.*, 2001). Pu(VI) has also been shown to be taken up, specifically via complexation by phosphate groups (Panak *et al.*, 2002). Batch-type studies with isolated exopolymers demonstrate that large quantities of uranium are taken up by these molecules (He *et al.*, 2000).

Another broad class of mechanisms by which bacteria interact with actinides is direct enzymatic and indirect redox changes. Dissimilatory metal reducing bacteria (DMRB), which derive energy by using oxidized metals as terminal electron acceptors in respiration, may play an important role in actinide speciation in anoxic environments, as they do for iron and manganese (Fig. 32.31). Metal-reducing bacteria have been shown to reduce U(VI), Pu(VI), Np(V), and Pu(V) (Lovley *et al.*, 1991; Lloyd *et al.*, 2000) and under certain conditions also Pu(IV). Bacterial reduction of U(VI) to U(IV) with the subsequent precipitation of U(IV) oxide has been well characterized in the laboratory and even recently demonstrated in the field (Anderson *et al.*, 2003). The resultant biogenic U(IV) precipitate in laboratory studies has been identified by XRD as being very fine

E_h(pH 7) in V

+1.2

PuO_2^{2+}/Pu^{3+} PuO_2^{+}/Pu^{3+}
$\{$ Pu^{4+}/Pu^{3+} , pH = 1
+1.0 — PuO_2^{2+}/PuO_2^{+}

1/2 O_2 + 2H^+/H_2O
+0.8 — Fe^{3+}/Fe^{2+} , pH = 0
$PuO_2^{+}(10^{-24}$ M)/PuO_2(s)

Aerobic heterotrophic respiration
Heterotrophic denitrification

+0.6

$Fe(OH)_3$(s)/Fe^{2+}

NH_4^+/NO_2^-
+0.4 — Nitrate/Nitrite

$Pu^{4+/3+}$EDTA, pH = 2   Cytochrome a

UO_2^{2+}/U^{4+} Cytochrome c
+0.2 —

$Fe^{3+/2+}$EDTA, pH = 2

0 —   Quinone

Iron sulfur proteins

PuO_2(s)/$Pu^{3+}(10^{-6}$ M)
−0.2 — SO_4^{2-}/HS^-

a-FeOOH(s)/$FeCO_3$(s)
                                 $NAD(P)^+/NAD(P)H$
−0.4 — H_2 Oxidizing
                                 methanogenesis

−0.6

Fig. 32.31 *Correlation of iron, uranium, and plutonium redox potentials with those of microbial organisms (Neu et al., 2005). Reproduced by permission of Oldenbourg Verlag.*

grained uraninite, UO_2 (Gorby and Lovley, 1992). The U–U distance was slightly shorter in biogenic uraninite than in bulk uraninite, which according to the authors creates a surface stress that increases the solubility of biogenic uraninite 10^9 fold over the solubility of well crystallized uraninite (Suzuki *et al.*, 2003). Nearly all studies of the bacterial reduction of actinides have been initiated from An(VI) or An(V) species and proposed or verified that the product was a solid An(IV) (hydr)oxide. A reductive dissolution of Pu(IV) hydroxide has also been demonstrated, although with NTA present (Rusin *et al.*, 1994).

   If the actinide is present at a sufficiently high concentration, then the reduction product can be an amorphous or crystalline biomineral. This process can be

achieved by direct electron transfer or by the bacterial metabolism saturating the solution around the cell with a ligand that forms an insoluble precipitate with the actinide. These processes could transfer uranium, neptunium or plutonium from solution species into stable oxides or phosphates minerals. Macaskie *et al.* used immobilized phosphate-producing bacteria to precipitate plutonium, as well as other actinides as biogenic phosphates (Macaskie *et al.*, 1994; Yong and Macaskie, 1998).

Metal-reducing bacterial can indirectly affect actinide speciation by producing reductants, such as Fe(II), Mn(II), and sulfide (Nash *et al.*, 1986; Newton, 2002). It has been shown that reducing bacteria can use redox-active humic substances and hydroquinone, a common experimental humic functional analog, to shuttle electrons (Royer *et al.*, 2002). The addition of an electron shuttle increases the reduction rate of iron in these studies, but the shuttle is also an indiscriminant reductant that can reduce actinides as well. A study reported the reductive dissolution of PuO_2 by both Fe(II) and hydroquinone (Rai *et al.*, 2002).

(i) Geochemical modeling

Several geochemical codes have been developed to model laboratory data and to predict the behavior of the actinides at extended field scales. Past versions were limited to basic thermodynamic data, such as solubility products and complex formation constants, and non-specific, empirical data such as K_d values. Modern codes attempt to better reflect real systems and reduce the uncertainties by defining thermodynamic parameters in surface complexation models. In addition, complex interactions of the actinides in high-ionic strength media are modeled using the more simple specific ion-interaction theory (SIT) (Ciavatta, 1980; Grenthe *et al.*, 1992; Grenthe and Puigdomenech, 1997) or the more elaborate Pitzer activity coefficient model (Peiper and Pitzer, 1982; Harvie *et al.*, 1984; Pitzer, 1991). Advances are being made by including more components requiring charge balance, and linking molecular, micro- and field scales. An overview of geochemical modeling can be found in Grenthe and Puigdomenech (1997) and in the many issues of dedicated journals and conference proceedings.

32.3.4 Actinides in environmental zones

(a) Global fallout

Worldwide fallout of radioactive debris, particles and gases from atmospheric nuclear weapons testing has been the major source of anthropogenic radioactivity dispersed in the marine and terrestrial environments. Approximately 76% of the fallout accumulated in the Northern Hemisphere and 24% in the Southern Hemisphere. The extreme conditions of a nuclear detonation, high pressure and high temperatures up to tens of millions of degree Celcius, and the location of the

detonation – atmospheric, ground or water – produce radioactive fallout particles of different size and properties. The particle composition depends on the interaction between bomb materials vaporized in the fireball and surface materials swept up by the atmospheric turbulence (Adams *et al.*, 1960). Weapons detonations near the ground contain large amounts of swept-up surface materials in the cooling fireball and fallout particles consist of melted soil (silicate) particles carrying radionuclides. In contrast, detonations at high altitude generate much smaller, oxide particles from the reaction between vaporized and condensating bomb material (mainly iron) and radionuclides. With about 80% of the total fallout, global (stratospheric) fallout of fine particles less than 10 μm in diameter is predominant. Their atmospheric residence time can span several years, long enough to mix with hemispheric air to be distributed worldwide (Perkins and Thomas, 1980). As an example, deposition of radioactive fallout in Japan decreased after Chinese atmospheric nuclear testing ceased in 1980 indicating a stratospheric residence time of about 1 year (Hirose *et al.*, 2008). Local fallout (12%) and tropospheric fallout (10%) is material that is too heavy to participate in atmospheric mixing and thus is deposited rather quickly contributing to the radioactivity levels close to the testing site (Hamilton, 1963). Tests conducted at or near the ground generate substantial tropospheric fallout with a mean residence time in the global atmospheric circulation of about 30 days.

The isotopic signatures of nuclear weapons tests can be used as geochronological indicators for marine processes and allow us to distinguish between different sources and events (Koide *et al.*, 1985; Izrael *et al.*, 1994; Mitchell *et al.*, 1997). Holleman *et al.* (1987) compiled information on plutonium fallout and 7300 data of plutonium obtained from stratospheric, atmospheric and surface samples. An estimated 2×10^5 PBq of fission products with about 13 PBq (360 kCi) of ^{239,240}Pu and smaller amounts of other man-made transuranium isotopes were deposited on the earth's surface by nuclear weapons testing (Perkins and Thomas, 1980; Essien, 1991). This deposition of plutonium is more than one order of magnitude lower than that of ^{90}Sr (about 151 PBq) and ^{137}Cs (about 225 PBq). The maximum annual deposition occurred in 1963 after the large-scale atmospheric testing in 1961 and 1962 (Hirose *et al.*, 2008). The largest source of stratospheric fallout, which peaked in 1962, is characterized by a ^{240}Pu/^{239}Pu ratio of (0.18 ± 0.01), as found in marine sediments of the Northern Hemisphere (Perkins and Thomas, 1980; Buesseler and Sholkowitz, 1987; Mitchell *et al.*, 1997). The ^{237}Np/^{239}Pu ratio is determined to be about 0.45 in the Northern Hemisphere and about 0.35 in the Southern Hemisphere (Krey *et al.*, 1976; Yamamoto *et al.*, 1996; Beasley *et al.*, 1998b; Kelley *et al.*, 1999). The second source is tropospheric fallout with a lower ^{240}Pu/^{239}Pu ratio of 0.035 and is proposed to originate from surface-based, low-yield testing at the Nevada Test Site (Perkins and Thomas, 1980; Buesseler and Sholkowitz, 1987). In particles of the latter fallout plutonium appears to be more tightly bound by the silicate carrier than in particles of the global fallout. Therefore, it is not

participating in the plutonium solid/solution exchange reactions and is rapidly accumulated at the sediments of the North Atlantic.

Hardy *et al.* (1973) provided baseline data about the dispersal of fallout plutonium from weapons testing based on 65 soil samples collected around the world. The minimum baseline level of plutonium contamination in the northern hemisphere is between about 0.04 and 0.15 Bq m^{-2} of fallout ^{239}Pu. The ratio of ^{239,240}Pu/^{238}U has been measured to vary between 0.0001 and 0.24, compared to about 10^{-12} in uranium minerals (Essien, 1991). The global integrated deposition of ^{241}Pu is about 440 Bq m^{-2} with an air concentration of about 0.8 Bq m^{-3} (Choppin *et al.*, 2002). The global fallout of ^{237}Np is estimated to be about 1.5 metric tons (Beasley *et al.*, 1998b). By 1974, the ^{241}Am activity accounted for 22% of the total ^{239,240}Pu activity, and it will continue to increase via the decay of ^{241}Pu until reaching a maximum in 2037 with 24% of the ^{239,240}Pu activity (Perkins and Thomas, 1980). Holm and Persson (1978) used the secular equilibrium of ^{242m}Am and ^{242}Cm in 5–16 year aged samples of the lichen *cladonia alpestris* to determine the ^{242m}Am/^{239,240}Pu ratio to be about 0.03% in global fallout. Only minute amounts of curium isotopes were produced in the nuclear test explosions.

The fallout isotopes can also be used as tracer for geochemical studies, such as sediment mixing or scavenging processes in water and sediment columns (MacKenzie *et al.*, 2006). Investigations of ocean water, sediments and corals provided insight into the fallout signature. As an example, plutonium particles that matched the signature of 1954 tests at Bikini atoll in the Marshall Islands were found in Japanese waters (Gauthier-Lafaye *et al.*, 2008). Particles from the Marshall islands with a ^{240}Pu/^{239}Pu ratio of less than 0.065 were traced back to low-yield tests conducted at Runit Island (Jernström *et al.*, 2006). Both pure plutonium and Si/O rich particles carrying actinides were found and investigated. Traces of ^{137}Cs were only found in the silicon-rich particles suggesting minor fission of ^{239}Pu. Debris from the *Bravo* test at Bikini atoll collected in 1954 was measured to contain (0.43 ± 0.03) Bq mg^{-1} ^{239,240}Pu and (0.22 ± 0.02) Bq mg^{-1} ^{241}Am at time zero (Hisamatsu and Sakanoue, 1978). Adams *et al.* (1960) investigated the compositions and structures of fallout particles collected at the Nevada and the Eniwetok test sites. Most of the radioactivity was found on particles smaller than 100 μm in diameter and no intrinsic, pure actinide particles were identified. Several types of particles from Eniwetok were identified with some consisting of $Ca(OH)_2$ and $CaCO_3$ cores covered with radioactive dicalcium ferrite and radioactive magnetite; particles from the Nevada Test Site consisted of transparent radioactive glass with dark-colored outer layers.

The nuclear accidents at Palomares (Spain), Thule (Greenland), Chernobyl (Russia) and at the McGuire Air Force Base in New Jersey (USA) generated fallout that differs from global fallout. Analysis of hot particles sampled at Thule and Palomares exhibited quite lower ^{240}Pu/^{239}Pu atom ratios of (0.056 ± 0.003) and (0.056 ± 0.0012), respectively (Mitchell *et al.*, 1997). Similar low ratios have been found for the low-yield nuclear weapons detonation at

Mururoa Atoll (0.032 (Vintro *et al.*, 1996)), the Nevada Test Site (0.035 (Krey *et al.*, 1976)) or in the Nagasaki area (0.042 (Komura *et al.*, 1984)). Hot particles collected in soil from the Palomares area contained uranium, plutonium and americium as main radioelements (Aragon *et al.*, 2008). The highly fragile, granulated particles had activity ratios of ^{238}Pu/^{239,240}Pu of (0.017 ± 0.001) and ^{241}Am/^{239,240}Pu of (0.24 ± 0.02). Interestingly, the Thule samples were isotopically heterogeneous suggesting that the weapons damaged in the Thule accident contained different nuclear materials. Uranium and plutonium were found to be homogeneously distributed in 20–40 µm size particles collected in Greenland (Lind *et al.*, 2005). EXAFS studies revealed a mixed U/Pu oxide with uranium present in the IV oxidation state and plutonium appearing as a mixture of Pu(III)/Pu(IV). The lower ^{240}Pu/^{239}Pu atom ratios are indicative of a low burn-up plutonium consistent with weapons-grade plutonium. The accident at Chernobyl caused dispersion of fuel components with highest actinide depositions close to the reactor facility. Activity levels for ^{239,240}Pu vary heavily depending on the distance from the reactor and soil type. Muramatsu *et al.* (2000) reported the ^{240}Pu/^{239}Pu atom ratio of (0.408 ± 0.003) in surface soil samples from forest sites within the 30 km zone around the Chernobyl reactor, characteristic for Chernobyl-derived plutonium in the environment. Based on the almost equal distribution of plutonium between organic and mineral layers Muramatsu *et al.* (2000) suggested that plutonium is redistributed in forest soil by migrating from the organic to the underlying mineral layers. The missile fire and release of plutonium at the McGuire Air Force Base created submicrometer-sized hot particles and single large particles. The ^{240}Pu/^{239}Pu atomic ratio of 0.057 is indicative of weapons-grade plutonium (Lee and Clark, 2005). Americium-241 was present at levels up to 1.08 Bq g^{-1} soil from the decay of ^{241}Pu. However, the theoretic ingrowth of ^{241}Am was calculated to be 1.81 Bq g^{-1} suggesting that some of the ^{241}Am could have migrated from the site and was not trapped in the high-fired plutonium matrix. Radiolytic damage and amorphization of the plutonium particle may have contributed to this effect.

(b) Aqueous environments

Sources of radionuclides in the world's aquifers span from the fallout from nuclear weapons tests, releases from accidents during transportation of radioactive material, accidents involving nuclear submarines, to accidental and intentional injection from processing plants, and the intentional dumping of radioactive waste into surface and groundwater.

(i) Marine and surface waters

The majority of weapons tests dispersed actinides into ocean and aquatic systems. Perkins and Thomas (1980) estimated the deposition of about 16 PBq of plutonium isotopes in the world's oceans. The measured oceanic

concentration, however, is orders of magnitude lower because of the removal of actinides by sediments, marine corals and the biosphere. Hamilton (2004) estimated that the total activity of the natural marine radiation environment, including the upper few meters of deep-sea sediment, exceeds 5×10^7 PBq.

Surface waters of the North Pacific Ocean sampled between 2001 and 2002 contained between 1 and 10 mBq ^{239,240}Pu m^{-3} (Hirose *et al.*, 2006). Ocean water and sediments from the North Pacific exhibit a wide range of ^{240}Pu/^{239}Pu ratios (0.19–0.34). A characteristically higher ^{240}Pu/^{239}Pu atom ratio of up to 0.28 was found in corals. Water samples from the central and western North Pacific Ocean was indicative of global and tropospheric fallout that originated from testing in the Marshall Islands in the 1950s (Buesseler, 1997). Higher values were observed in subsurface waters and sediments and in the deep waters close to the Marshall Island. At Bikini, the highest levels of transuranium isotopes were found in the 1970s with 4.44 Bq ^{239,240}Pu g^{-1} and 2.85 Bq ^{241}Am g^{-1} in surface sediments in the northwest part of the lagoon (Donaldson *et al.*, 1997). The ratio in soil samples from Bikini Atoll was around 0.3 (Muramatsu *et al.*, 2001), very similar to the ratios (0.318–0.338) found in debris from the *Bravo* thermonuclear test on Bikini Atoll in 1954 (Komura *et al.*, 1984). The continuous circulation and exchange of water with the open ocean resulted in the removal of 111 GBq year^{-1} for ^{241}Am and 222 GBq year^{-1} for ^{239,240}Pu. Today, tens of TBq of ^{239,240}Pu remain distributed in sediments at Bikini and Eniwetok at different depths (Robison and Noshkin, 1999).

The actinides exhibit quite different abundance in open waters reflecting their characteristically different chemistries. The concentration of ^{232}Th in seawater is very low at about 1.7×10^{-7} Bq L^{-1}, slightly increasing with depth (Krishnaswami, 1999). Neptunium is a widespread contaminant in the Irish Sea, while only low activities are found in sediments. The activity pattern of ^{237}Np in the water samples indicate its transport from the Sellafield reprocessing plant via the Norwegian Coastal Current to the North Atlantic Ocean. In contrast, plutonium shows the opposite behavior and its soluble concentration decreases with the distance from the discharge location. The ^{237}Np/^{239}Pu atomic ratio (3.5–85) is up to 50 times higher than observed in Sellafield discharges (1.69) or in weapons test fallout (0.48) (Lindahl *et al.*, 2005). The low amounts of ^{237}Np found in marine sediments indicate its high mobility as soluble Np(V) in seawater. The common divalent cations in seawater, Ca^{2+} and Mg^{2+}, also appear to lower the retention of Np(V) (McCubbin and Leonard, 1995). The large fraction of neptunium in seawater exists as a mixture of NpO_2^+ and $NpO_2(CO_3)^-$. The ^{239,240}Pu inventory in the western Mediterranean waters is reported to be about 25 TBq and about 40 TBq in the underlying sediments (Vintro *et al.*, 1999; Vintro *et al.*, 2004). Originally about 69 TBq were deposited from fallout.

The waters around the Russian test site for nuclear weapons Novaya Zemlya islands in the Russian arctic, exhibit significant levels of radioactivity (Fig. 32.32). About 130 nuclear explosions resulted in the estimated release of up to about 60 TBq ^{239}Pu into the Chernaya Bay, which feeds into the Barents Sea (Bradley,
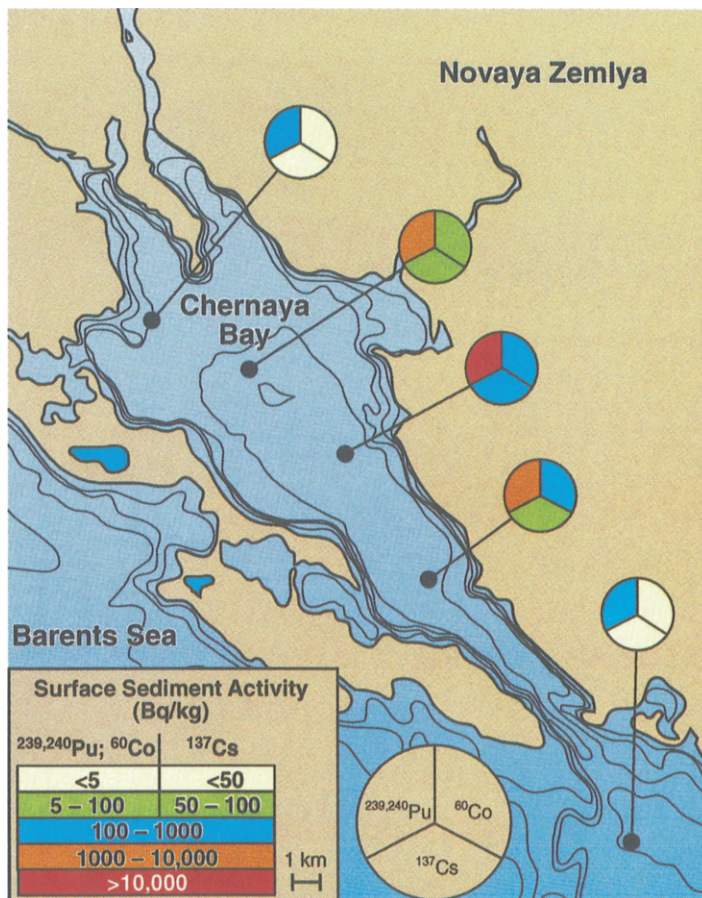
Fig. 32.32 *Distribution of some radionuclides in Chernaya Bay from nuclear weapons tests at Novaya Zemlya in the Former Soviet Union (Bradley, 1997). Reproduced by permission of Battelle Memorial Institute.*

1997). Past discharges of estimated 120 MCi from the Mayak processing plants into the Lake Karachi resulted in 5.7×10^{-6} Ci L^{-1} radioactivity, containing (0.0212 ± 0.0104) MBq L^{-1} of ^{239}Pu, (0.0193 ± 0.013) MBq L^{-1} of combined ^{238}Pu and ^{241}Am, and (0.0196 ± 0.0111) MBq L^{-1} of uranium isotopes. The inventory of plutonium in the reservoirs at Mayak is estimated to a minimum of 40 TBq (Vorobiova *et al.*, 1999). Between 1949 and 1951 about 76 million cubic metres of liquid radioactive waste were discharged into the Techa river. The total activity released directly to the Techa river is estimated to be about 100 PBq with about 2 TBq of actinides (Myasoedov and Drozhko, 1998). Underground nuclear explosions at the Semipalatinsk site created a network of fractures that enabled contaminants to reach the surroundings. In 2002,

radiation levels of up to 113 Bq L^{-1} ^{239,240}Pu have been reported in waters connected to the Ouzynboulak river in Kazakhstan (Hrkal *et al.*, 2006).

Rivers carry isotopic signatures of actinides from fallout and from nuclear processing plants. Sediments from the Columbia River, USA, had trace amounts of ^{243,244}Cm as potential remnants from nuclear weapons testing (Beasley and Ball, 1980). Plutonium and ^{241}Am were detected in 2006 in the Rhone river downstream of the Marcoule site (Eyrolle *et al.*, 2008). Discharges at the Hanford site left a legacy of large groundwater contaminations behind and some of the contamination has reached the adjacent Columbia River (Wellmann *et al.*, 2008). The ratios of the uranium isotopes ^{235}U and ^{238}U and its decay daughters ^{234}Th and ^{234}Pa have been used to distinguish contaminant origin and identify a spill in 1951 as the main cause for the uranium plume at the Hanford site (Christensen *et al.*, 2004, 2007). Millions of curies of radioactivity have been discharged into the rivers around the Tomsk-7 and Krasnoyarsk-26 sites. An estimated total radioactivity of 4 GBq ^{232}Th, 4 GBq ^{238}U, and 22 GBq ^{239,240,241}Pu have been released from Tomsk-7 into the Tom river valley (Waters *et al.*, 1999). The radionuclides ^{232}Th (1.1 Bq kg^{-1}) and ^{237}Np (up to 776 Bq kg^{-1}) have been found in fish from the Tom river. However, Waters *et al.* (1999) state that despite the large releases into the Tom and Yenisei Rivers over the past several decades, extensive contamination is not present. A summary of radioactivity inventories in Former Soviet Union water systems is provided by Bradley (1997) and Waters *et al.* (1999).

The actinides injected into marine waters do not only affect the soluble phase but also transfer to sediments, coral and fish. The majority of plutonium, americium and curium are contained in sediments close to coastlines near the effluent injection. As an example, ^{241}Am discharges into the Irish Sea from Sellafield, UK, were rapidly adsorbed on particles and fine-grained sediments (Warwick *et al.*, 1996). Traces of ^{242}Cm and ^{244}Cm have been measured in sediments from the Scottish coast believed to result from the transport of radioactive sources in the Irish Sea (Schneider and Livingston, 1984). A recent analysis of sediments collected in the vicinity of Sellafield showed significant activities related to the actinides (Tavcar *et al.*, 2005). In an intertidal sediment from the Cumbrian coastline 6.45 Bq kg^{-1} for ^{241}Am were measured. The plutonium in natural sediments from the Cumbrian coast was primarily associated with iron and manganese (oxy)hydroxides and organic matter (McDonald *et al.*, 2001). A sediment taken from the tidal zone of the river Ribble contained 1.72 Bq kg^{-1} of ^{237}Np, 32 Bq kg^{-1} of ^{238}Pu, 187 Bq kg^{-1} of ^{239,240}Pu, and 288 Bq kg^{-1} of ^{241}Am. Inhomogeneous agglomerates of ^{241}Am on particles were detected in sediments taken from the Irish Sea with a high activity layer at 26–28 cm depth (Perna *et al.*, 2005). Agglomerates of much smaller hot particles were found to be associated with iron and manganese phases. These observations suggest a preferential removal of Pu(IV) and Am(III) via adsorption on particulates. Over time, ^{241}Am will decay to the more mobile ^{237}Np and thus continuously increase the ^{237}Np concentration in oxidizing

aquifer systems, such as surface waters. Waters and soils around uranium mill tailings have shown significant radioactive contaminations. For instance, several U(VI) solution species have been identified spectroscopically in mining-related waters from Saxony, Germany: $Ca_2UO_2(CO_3)_3(aq)$ in carbonate and calcium-containing mine water at pH 7, and $UO_2(CO_3)_3^{4-}$ in calcium-poor tailing water at pH 9.8 (Bernhard *et al.*, 1998). $UO_2SO_4(aq)$ was found in acidic mine water at pH 2.6.

(*ii*) *Groundwaters*

Subsurface waters around the world have actinide contaminations primarily due to the intentional waste disposal approaches in the past. However, detailed reports on the characterization and speciation of the contaminants remain rare. As an example, plutonium was found in low concentrations in groundwater close to the chemical processing plant of the Idaho National Laboratory. The waters are characterized by high nitrate contents, but low in organic molecules and dissolved organic carbon. One well water contained ^{238}Pu up to 2.9 mBq L^{-1}, of which more than 75% of the plutonium was found to be present as species smaller than 0.05 μm (Cleveland and Rees, 1982). Oxidation state analysis indicated that nearly all plutonium was present in the IV oxidation state as predominantly soluble species.

Organic molecules in waste effluents can have profound implications on actinide solubility and speciation. At the Maxey Flats radioactive waste disposal site in Kentucky up to 0.5 ppm plutonium was found 100 m from the site dissolved in solution complexed primarily by EDTA (Cleveland and Rees, 1981). Ferric hydroxide did not retain the plutonium as expected in the absence of EDTA. The higher concentration of soluble plutonium in waters at the Maxey Flats site illustrates the impact of chelating organic ligands on the stabilization of plutonium in solution.

In some groundwaters, enrichment of plutonium isotopes was observed after migrating from the injection site. At the Savannah River Site the transplutonium radionuclides ^{243}Am, ^{244}Cm, ^{245}Cm and ^{246}Cm migrated away from the seepage basin and decayed in situ down-gradient to yield progeny plutonium isotopes (Kaplan *et al.*, 1994; Dai *et al.*, 2002). The migration of original plutonium isotopes contributed less to the elevated $^{240}Pu/^{239}Pu$ atom ratios about 30 m downstream and thus remained close to the fringe of the seepage basin. Only less than 4% of the $^{239,240}Pu$ was found as colloids, which was used to explain the high abundance of plutonium in its V and VI oxidation states. Groundwaters around the Chernobyl site had increased levels of ^{238}Pu, $^{239,240}Pu$ and ^{241}Am with activity ratios similar to those calculated for the spent fuel in the unit 4 of the Chernobyl power plant (Odintsov *et al.*, 2007). Concentrations of up to 0.076 kBq m^{-3} ^{238}Pu, 0.18 kBq m^{-3} $^{239,240}Pu$ and also 0.23 kBq m^{-3} ^{241}Am were measured in groundwater sampled north of the Chernobyl power plants (Odintsov *et al.*, 2007).

(c) Subsurfaces and sediments

Plutonium contamination levels and ratios of plutonium isotopes, in specific that of ^{239}Pu/^{240}Pu, have been measured worldwide in a huge variety of soil and sediment samples. Some examples are: plutonium deposited from fallout in the volcanic ash soil in Korea has been characterized to be more mobile compared to other Korean sites (Lee and Lee, 1999); in soil from the Swiss Alps up to 2.8 Bq kg^{-1} americium and plutonium were measured due to fallout (Froidevaux *et al.*, 1999); and in the soil of grass lands and spruce forests in southern Bavaria, Germany, up to 100 Bq kg^{-1} fallout ^{239,240}Pu was found in the top 10 cm below the surface (Bunzl and Kracke, 1994). Significant activity levels of ^{239,240}Pu and ^{241}Am (5–10 kBq kg^{-1}) have been found in surface gley soil from west Cumbria with the actinides enriched in the organic fraction (Livens and Singleton, 1991).

The accident in Chernobyl left hundreds of square miles contaminated with plutonium, americium and curium. The majority of the actinides appear to be confined within the top sections of the soils. In 1998, a study of Kapachi soil depth profiles measured the total activity of 177 kBq m^{-2} for ^{241}Pu, 8.6 kBq m^{-2} for ^{238}Pu, 17.1 kBq m^{-2} for ^{239,240}Pu, 13.7 kBq m^{-2} for ^{241}Am and 2 kBq m^{-2} for ^{244}Cm in the top 5 cm, which indicates a very slow vertical movement of the actinides in that soil type (Mboulou *et al.*, 1998). The authors note that ^{241}Am is observed to migrate faster than the plutonium isotopes.

Surface soils sampled in the early 1970s from outside the Subsurface Disposal Area perimeter at the Idaho National Engineering and Environmental Laboratory contained transuranium contaminations that averaged to 0.03 Bq g^{-1} for ^{238}Pu, 1.4 Bq g^{-1} for ^{239,240}Pu, and 1.9 Bq g^{-1} for ^{241}Am (Markham *et al.*, 1978). The highest activities were contained in the top 0–3 cm soil layers with an average ^{239}Pu concentration of 23 Bq kg^{-1}. The largest fraction (37%) of the plutonium was associated with hydrous oxide coatings of soil particles, such as iron or manganese oxide phases (Ibrahim and Morris, 1997). About 22% of the total ^{239}Pu was associated with soil organic matter and 21% were associated with refractory silicates and clay minerals. Under the conditions at the Idaho site, only little amounts of plutonium (3.8 %) were available for water-soluble mobilization from the soil.

Areas at the Rocky Flats Environmental Technology Site (RFETS) have shown plutonium contaminations in soil caused by various releases during fire events, acid splashes or leaking storage containers. EXAFS and XANES studies of 13 samples from different areas at the RFETS found plutonium in its IV oxidation state (LoPresti *et al.*, 2007). Soil from a waste storage pad and painted-over concrete sample exhibited Pu–O (2.38 and 2.32 Å, respectively) and Pu–Pu (3.83 and 3.84 Å, respectively) distances that are very similar to those found in PuO$_2$. This is to be expected, if the plutonium was dispersed as oxide particles during the plant fires in 1957 and 1969. In contrast, XANES

identified Pu(VI) in a concrete floor surface that was exposed to HNO_3 accidentally released from a PUREX separations line.

(d)   Colloidal transport

The first evidence for actinide transport as pseudocolloids was obtained 11 years after the *Cheshire* nuclear test in 1976, when colloid-associated actinides were detected in a well 300 m to the southwest of the detonation site at the Nevada Test Site (NTS) in the United States (Buddemeier and Hunt, 1989; McCarthy and Zachara, 1989). Two examples that received more recently heightened attention are the migration of plutonium at the NTS and at the Mayak site in Russia. At the NTS, where over 150 atmospheric and underground nuclear tests were conducted between 1951 and 1962, plutonium concentrations of up to 0.23 Bq L^{-1} were detected at the NTS's ER-20-5 well complex 1.3 km away from the source (Kersting *et al.*, 1999). Almost all plutonium was exclusively associated with colloids composed of silica, zeolites, and clays. The unique $^{239/240}$Pu ratio indicated that the plutonium detected originated from the *Benham* nuclear test 40 years ago in December 1968. Underground detonations perturbated and fractured the underground rock formations creating enhanced transport pathways in the saturated zone. Plutonium was promptly injected and integrated into a melted rock zone. Consequently, the transport mechanism of plutonium injected by nuclear weapons testing may differ significantly from colloid-facilitated actinide transport at processing plants or nuclear waste repositories. The observation of actinide pseudocolloid migration at the NTS remains under dispute. Sampling techniques and the impact of the explosion on plutonium transport are the focus of the concerns raised.

At the Mayak site, plutonium has been detected in groundwater (0.16 Bq L^{-1}) three kilometers away from the source (Novikov *et al.*, 2006; Kalmykov *et al.*, 2007). Between 70% and 90% of the plutonium was associated with small colloids between 1 and 1.5 nm in size. However, up to approximately 30% was declared as "soluble" plutonium species with sizes smaller than 1 nm. The nature of these species could be polynuclear, mononuclear or plutonium sorbed on nanoparticles of very small size.

In modern geochemical modeling, colloidal transport contributes significantly to the release of actinides from waste repositories. Risk assessment calculations for the Yucca Mountain site, a potential site for geologic repository for high-level radioactive waste in the United States, assign 25% of the total dose released at 100,000 years to colloidal ^{239}Pu (CRWMS, 2000b). The speciation of uranium in five natural waters from the German Gorleben site, a proposed salt repository for radioactive waste, showed that over 75% of the uranium is associated with colloids (Zeh *et al.*, 1997). These groundwaters contain substantial amounts of dissolved organic carbon of which over 60% is humic acid. Clearly, in such humic-rich waters the fate of the actinides is closely associated with the migration behavior of humic colloids.

(e) Natural analogues

Elemental and isotopic distributions of actinides at natural analogue sites are useful to examine the geochemical history of radionuclides and to predict the performance of proposed man-made nuclear waste repositories (McKinley and Alexander, 1993). There are several natural uranium ores worldwide that can be studied to understand the long-term behavior (millions to billions of years), of uranium and by extension other actinides. Examples for natural analogue sites are: the Morro do Ferro sites at Pocos de Caldas, Brazil (Waber *et al.*, 1991); the Nopal I uranium deposit, Peña Blanca, Mexico (Leslie *et al.*, 1999); the granite-based uranium ore mineralization system of El Berrocal, Spain (Perez del Villar *et al.*, 1993; Bruno *et al.*, 2002); the uranium-thorium deposits at Palmottu, Finland (Haveman and Pedersen, 2002; Blyth *et al.*, 2004); the granite-hosted uranium deposit in southern China (Min *et al.*, 1998); the uranium deposit at Koongarra, Australia (Payne *et al.*, 1992; Yanase *et al.*, 1998); the alkaline environments at the Khushaym Matruk site in Central Jordan in an argillaceous sedimentary formation (Techer *et al.*, 2006); and the prominent Oklo-Okélobondo and Bangombé natural nuclear reactor zones in Gabon (Mathieu *et al.*, 2001).

Among the most studies natural analogues are the natural reactors and uranium deposits at Oklo (see also Section 32.2.1 (c)). The natural reactors provide the opportunity to analyze a 1–2 billion year containment of nuclear waste and to determine how underground rock formations contained the waste. Remarkably, the highly radioactive waste generated by the Oklo reactors billions of years ago never moved far from its origin and was held in place by the granite, sandstone, and clays surrounding the reactors (Berzero and D'Alessandro, 1990). Minerals, such as chlorite and illite, exhibit significant amounts of adsorbed uranium, thorium and rare earth elements (Janeczek and Ewing, 1992; Bros *et al.*, 2003). Plutonium has moved less than 10 ft from where it was formed almost 2 billion years ago, without the elaborate containment we use today on nuclear power plant waste. Numerous fission products have been found in the immediate vicinity of the reactors with many being retained in the reactor itself and in adjacent rock formations (Bros *et al.*, 1993; Hidaka, 2007). Rare earth cations (Ce, Sm, La, Pr, Nd, Gd) are retained in the uraninite of the reactor. Fission products and other species incompatible with the structure of uraninite, such as Tc, Ru, Rh, Mo, Pb, Pd and Bi, are still retained in metallic inclusions or insoluble precipitates (i.e. PbS) found in close proximity to the uraninite (Bros *et al.*, 1993). In fact, solid graphitic carbonaceous matter around the reactor acts as a barrier to the migration of U, Pu, Pb and a number of other fission products. Isotopic studies of clay minerals from argillaceous rocks neighboring one of the reactors exhibited depletion of ^{235}U with $^{235}U/^{238}U$ ratios as low as 0.56% (Bros *et al.*, 1993). One sample, however, revealed an enrichment of ^{235}U to 0.7682%, which is explained as a result of ^{239}Pu production according to equation (32.1) and migration

away from the reactor core, followed by its decay to ^{235}U. The formation of secondary uranium phases has been recognized to have a retaining effect on uranium migration. These same phases also may incorporate fission products and therefore serve as a barrier against migration. As an example, the initially mobile plutonium appears to have been incorporated into apatite and clay minerals around the reactor zone (Hidaka, 2007). Some fission products, such as Ba, Sr and Cs, have been lost in large quantities, primarily because they are highly soluble and readily transported by aqueous solutions in geologic environments.

32.4 CURRENT AND POTENTIAL FUTURE ACTINIDE INVENTORIES AND MANAGEMENT

32.4.1 Nuclear weapons stockpiles and cold war legacies

There still exists a great inventory of uranium and plutonium in nuclear weapons arsenals in the United States, Russia, China, France and the United Kingdom. However, arms control agreements and unilateral decisions led to a significant decrease of the nuclear arsenal. By the end of 2006, 26,854 warheads were reported to exist in nuclear weapons states, well down from its peak of about 70,000 in 1986 (Norris and Kristensen, 2006). Disassembling nuclear warheads creates secondary waste streams besides large amounts of plutonium that has to be isolated from the environment. The largest nuclear weapons states, the United States and Russia, have each declared about 50 metric tons of excess plutonium to its military requirements, most of it as part of the former weapons program (Albright, 2004). Three metric tons are already scheduled for disposal in the Waste Isolation Pilot Plant in New Mexico, USA, while 37 metric tons are scheduled to be used in mixed-oxide (MOX) fuel. However, most of the separated and stored plutonium cannot be employed for reuse in MOX fuel without further reprocessing. This is mainly due to the ingrowth of ^{241}Am from the decay of ^{241}Pu.

The weapons era left behind large contamination at many sites and cleanup efforts will require future generations. For example, in the United States remediation efforts are ongoing at the former plutonium production and reprocessing sites at Hanford and have been completed at Rocky Flats (Clark *et al.*, 2006). In 1996, 640,000 metric tons of contaminated soil and sediment were removed from the bottom of the uranium process pond at Hanford. In 2001–2002, additional layers of contaminated sediments were removed to reduce the uranium contamination level (McKinley *et al.*, 2007). Some of the remediation efforts in the United States, remedial technologies, monitoring and sensing, and underlying scientific projects to identify and characterize subsurface contaminants are discussed by Berkey and Zachry (2005).

32.4.2   Renaissance of nuclear energy

While the inventory of weapons-grade plutonium is unlikely to increase, reactor-grade plutonium and minor actinides, neptunium, americium and curium, will accumulate due to the growth of nuclear power reactors. There is a clear prospect of an increasing demand of nuclear energy worldwide. In 2008, 439 reactors were operating worldwide (WNA, 2009) and many are being built worldwide, with the majority in Asia (Hasan, 2007). With this increase of nuclear power plants comes the continuing accumulation of spent fuel rods and waste effluents from mining, fuel fabrication and reprocessing. To meet the demand of nuclear energy in the future, the natural uranium resources are not long-term sufficient and advanced technologies have to be developed to better utilize existing uranium stockpiles in spent fuel rods. Table 32.5 summarizes the dominant countries and their production of uranium in 2007. The total production of about 39,600 metric tons of uranium in 2006 accounted for only 59% of the total uranium of 66,815 metric tons required for all reactors around the world (WNA, 2008b; 2009). During the past years the required uranium to meet the demands from the operating reactors worldwide stayed almost flat and was reported to be 68,357 metric tons uranium in 2005 and 65,405 metric tons in 2009 (WNA, 2009). Estimates for world reactor requirements reach up to 86,070 metric tons by the year 2020 (OECD/NEA, 2003). The shortfall between fresh production and reactor requirement is expected to be filled by several sources, including stocks of civilian and military inventories of natural and enriched uranium, nuclear fuel produced by reprocessing of spent reactor fuels and from surplus military plutonium, and uranium production by re-enrichment of depleted uranium tails.

Substantial global growth of nuclear energy is expected for this century carrying the responsibility for proper management of spent nuclear fuel. Historically, reprocessing of spent nuclear fuel was the preferred option, but due to technological hurdles, proliferation concerns, public acceptance and economics some countries have adopted a wait-and-see strategy. Recently, an

Table 32.5 *World uranium production* (*in metric tons of uranium*) *by country in* 2007. *Data are compiled from WNA* (2008b).

Australia	8,611	Namibia	2,879
Brazil	299	Niger	3,153
Canada	9,476	Pakistan	45
China	712	Romania	77
Czech Republic	306	Russia	3,413
France	4	South Africa	539
Germany	38	Ukraine	846
India	270	United States	1,654
Kazakhstan	6,637	Uzbekistan	2,320
Total worldwide: 41,279 t			

international partnership GNEP (Global Nuclear Energy Partnership) has been formed to promote the peaceful use of nuclear power and to pursue technical cooperations. In principle, some nations ("fuel supplier nations") would provide enriched uranium fuel to and take back spent fuel from nations that operate nuclear power plants. Meanwhile, over 20 countries are participating. There is agreement to close the fuel cycle and to reuse the separated plutonium in MOX fuels providing a sustainable technology for the future while reducing nuclear waste and the risk of nuclear proliferation.

Spent fuel reprocessing technologies have evolved significantly with growing industrial experience and substantial research and development programs in multiple countries. Recent developments focus on recycling uranium and plutonium and partitioning the minor actinides neptunium, americium and curium, such as the TRUEX or UREX+ processes (Lagus, 2005). The long-lived minor actinides could be vitrified and disposed of or transformed into fission products by irradiation in Fast Breeder Reactors. Recycled plutonium in MOX fuel has partly been transmuted in French power reactors, which reduces the volume of high-level nuclear waste by a factor of 6. Figure 32.33 shows that for the first 100 years the toxicity of uranium-based spent nuclear fuel is dominated by the fission products cesium and strontium, while the long-lived actinides dominate after about 100,000 years. Although transmuting actinides will reduce the volume of High-Level Wastes (HLW) significantly, wastes from this technology will still need to be disposed of in geologic repositories. Reducing the fraction of the long-lived actinides will significantly decrease the long-term radiotoxicity of HLW. Information on the spent fuel treatment strategies in France, Russia, India, Japan and the United States is available in IAEA (2008).

The thorium fuel cycle is of interest for the expansion of nuclear energy. Natural reserves of thorium are more abundant than those of uranium, providing an excellent fuel source for sustainable nuclear power. Two primary benefits associated with thorium fuels are enhanced proliferation resistance and lower radiotoxicity from the resulting spent fuel (Loiseaux *et al.*, 2002; Dekoussar *et al.*, 2005). The formation of ^{232}U during fuel use provides intrinsic proliferation resistance (Galperin *et al.*, 1997). From a waste management perspective, fewer plutonium and minor actinides are produced and the spent fuel has a lower radiotoxicity, relative to the uranium fuel cycle (Fig. 32.34). A longer succession of neutron capture reactions is needed to create americium and curium isotopes when starting from the lighter ^{232}Th isotope compared to ^{238}U (see Fig. 32.34). However, thorium fuels will require longer short-term storage due to the formation of the intermediate ^{233}Pa ($t_{1/2} = 27.0$ days). The cooling time of thorium-based spent fuel will be longer than uranium-based fuel, which is dominated by the intermediate ^{239}Np ($t_{1/2} = 2.35$ days). Mixed thorium–plutonium oxide fuels have been proposed for the transmutation of transuranium elements, as these fuel cycles are sustainable and result in a much reduced production of these elements (Todosow *et al.*, 2005).
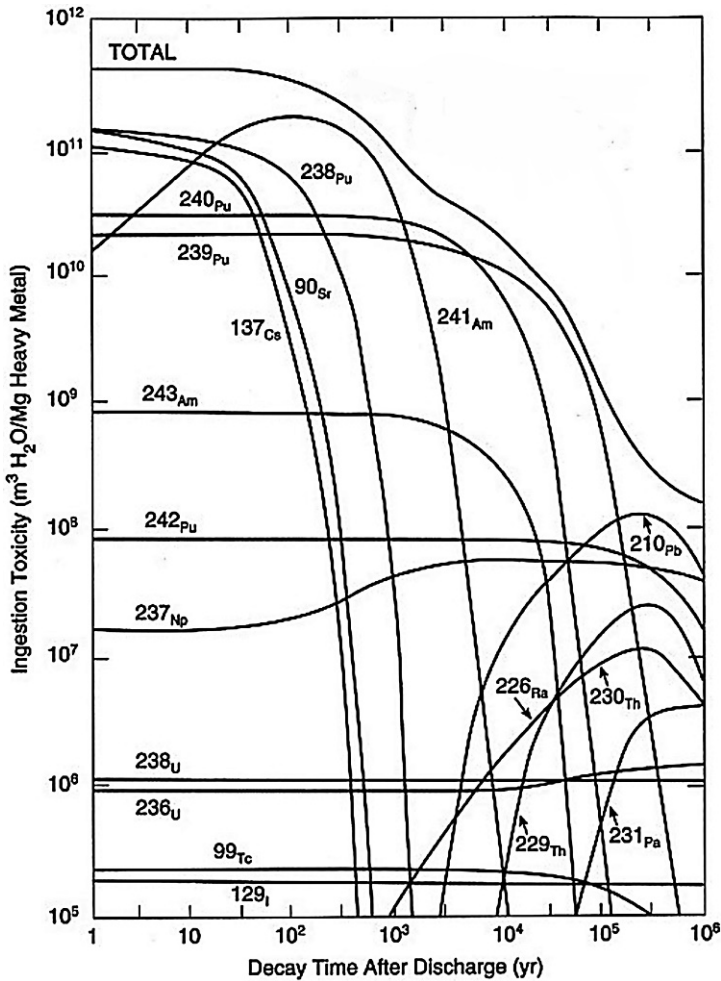
Fig. 32.33 *Radiotoxicity of fission products and actinides in spent nuclear fuel. The short-lived fission products determine the heat load and radiotoxicity of spent nuclear fuel during the first* 100 *years after irradiation; after about* 100,000 *years the long-lived actinides become the major contributors* (ORNL1995; NRC, 1996). *The calculations are conducted for PWR spent fuel with* 3.2% *initial enrichment and* 33 *MWd*(th) (*Mg Heavy Metal*)$^{-1}$.

32.4.3 Radioactive waste management

The worldwide enhancement of nuclear energy is threatened by the challenges of safely managing the residual nuclear waste. Clearly, early waste management approaches of dilution and dispersion were inadequate, depicted by the irresponsible injection of massive volumes of radioactive waste effluents into ground

Fig. 32.34 *Radiotoxicity of various spent nuclear fuels as a function of time (Loiseaux et al., 2002). FP are the fission products without transmutation; PWR represents the conventional uranium-based spent fuel from a pressurized water reactor excluding depleted uranium (a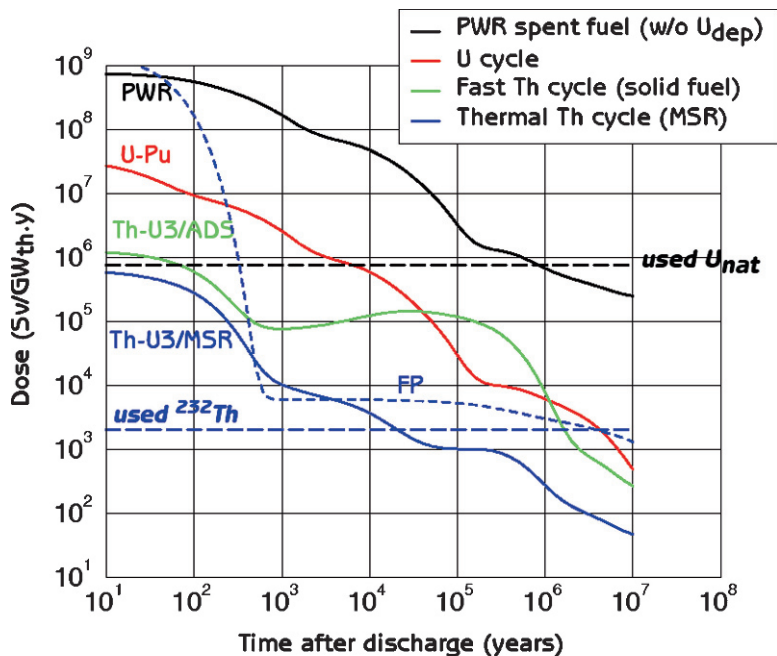fter about one million years the radiotoxicity of spent fuel from PWR reaches that of the natural uranium used); U-Pu represents spent fuel from the fast neutron uranium-based cycle; and Th-U3/ADS and Th-U3/MSR are the thorium-based fast neutron and slow neutron cycles, respectively. Reproduced by permission of Elsevier.*

and water. During the last decades, advanced technologies and increasingly strict regulations have been developed to assure the protection of the environment and mankind from continued exposure to radionuclides in waste. The International Atomic Energy Agency (IAEA) (1995) has developed nine principles of radioactive waste management to provide an international framework for the safe management of nuclear wastes. Today, the safe disposal of radioactive waste has attracted significant public interest and has become a global political issue. Central to the safe management of radioactive waste is the demand to protect the environment and human health now and in the future. This objective is achieved by concentrating, containing and isolating radioactive wastes from human exposure. There are multiple aspects to radioactive waste management, from the nature of waste streams, the difficulties in handling and treating radioactive wastes, the development of radiation-resistant waste forms, to the problem of finding acceptable storage and disposal sites. For more

detailed discussions of aspects related to radioactive waste management we refer the reader to dedicated books and book chapters by Choppin *et al.* (2002) and Cooper *et al.* (2003). An evaluation of nuclear waste forms, including non-crystalline waste forms (silicate, lead-iron glasses), crystalline waste forms (Synroc, ceramics, monazite, concrete), and novel waste forms is provided by Lutze and Ewing (1988).

Processes associated with the use of uranium and plutonium in nuclear fuel and nuclear weapons, from fuel manufacturing to Spent Nuclear Fuel (SNF) processing, generate liquid and solid radioactive wastes of different categories. High-Level Waste (HLW) is defined as spent nuclear fuel or wastes created during SNF processing. It generally contains large fractions of the fission products, including small residues of the actinides, thus carrying the majority of the heat load. Transuranic (TRU) waste contains the actinides beyond uranium from reactor fuel manufacturing, processing, nuclear weapons mainte-nance and disposition, industrial applications or research. Although the heat load in TRU waste is small compared to HLW, it is of great concern for the public and authorities due to the longevity of the actinide elements (Fig. 32.34). Both TRU waste and HLW are candidates for disposal in underground geological forma-tions. The activity of TRU is greater than 100 mCi kg^{-1} of waste material. Low-Level Waste (LLW) is defined as all other radioactive wastes other than HLW or TRU, but it practically contains no TRU. Mixed waste contains both radioactive LLW and hazardous components, such as toxic agents and metals, corrosive, flammable and explosives, or pesticides.

In the absence of nuclear testing, today's accumulation of actinides is occur-ring upon the irradiation of uranium-based fuels in nuclear reactors. Spent nuclear fuel contains about 95%, still slightly enriched (0.7%) uranium, about 1.2% plutonium, 0.14% light actinides, neptunium, americium and curium, and about 5% fission products (data refer to a burn-up of 40 gigawatt day per metric ton for a 4.2% enriched fuel). Most of the spent fuel retrieved from the reactor is stored in large storage pools for 10–20 years. After that, the radiation and decay heat levels are low enough enabling further storage of fuel assemblies in above-ground storage casks. About 10,500 metric tons heavy metals (tHM) spent nuclear fuel accumulates every year from nuclear reactors worldwide, which is expected to increase to about 11,500 tHM per year by 2010 (IAEA, 2008). The total cumulative amount of spent nuclear fuel by beginning of 2004 was nearly 268,000 tHM, which is expected to increase to over 400,000 tHM by 2020. At the end of 2002 over 200 metric tons of plutonium separated from spent nuclear fuel were held in countries worldwide. The annual production of americium and curium is estimated to about 5 kg/year for a 1,000 MW light-water reactor (Choppin *et al.*, 2002). By the end of 2006, about 94,000 tHM spent nuclear fuel had been processed at reprocessing facilities worldwide, with the majority processed in France and the United Kingdom (Table 32.6). France continues to reprocess about 800–850 metric tons of its own spent fuel per year. By 2007, the IAEA estimated the worldwide accumulation of 360,371 m^3 of unprocessed

Table 32.6 *Cumulative amounts (in metric tons heavy metals, tHM) of civil reprocessed spent nuclear fuel by the end of* 2006 (IAEA, 2008).

Country	Site	Fuel type				Total
		GCR	LWR	FBR	MOX	
Belgium	Mol[a]	19[b]	86			105
France	Marcoule, LaHague	18,000[c]	22,450	100	150	40,700
Germany	Karlsruhe[a]		180			180
Japan	Tokai-mura		1,000		18[d]	1,018
Russia	Chelyabinsk		3,550	450		4,000
UK	Sellafield, Dounreay	42,000[e]	5,800[f]			47,800
USA	West Valley[a]		194			194
Total		60,019	33,260	564	168	94,011

[a] Closed facility
[b] CANDU (CANada Deuterium Uranium), GCR (gas-cooled reactor) and other
[c] UNGG (Uranium Naturel Graphite Gaz)
[d] Spent fuel from Fugen reactor
[e] Magnox
[f] LWR/AGR (light-water reactor/advanced gas-cooled reactor).

and 5,033 m^3 processed actinide-containing HLW in storage (compared to 10 m^3 processed and disposed HLW) (NEWMDB, 2008).

It is common practice to dispose of LLW (and intermediate-level wastes, ILW) in shallow trenches below the surface (Fig. 32.35). After about 30 years, the radioactivity in LLW will have decayed to acceptable low levels. Continuous technology development offers several concepts, including burial in deeper trenches, concrete bunkers and integrated vault technologies. Over the last decades various options have been discussed for the disposal of solid HLW, including the chemical reprocessing and partitioning, nuclear transmutation and the disposal strategies in space, ice, deep seabed or deep geologic media. Figure 32.36 illustrates media considered for short- and long-term disposition of radioactive waste. There is no current effort to pursue the option of disposal in space because of the inherent risks involved and also because the cost of transportation would make this option uneconomical. Disposal in ice sheets is unacceptable because of the exposure of the waste canister to water, large transportation costs and extreme weather conditions limiting access to the sites. Strict limitations on the kind and amounts of HLW that can be disposed of in the sea make such HLW disposal inefficient. Today, the most promising technologies for managing HLW are partitioning spent nuclear fuel with subsequent transmutation (Westlén, 2007) and the disposal of significantly reduced volumes of HLW deep underground.

Modern nuclear waste programs around the world have adopted the so-called multi-barrier concept to safely isolate and encapsulate highly-radioactive wastes for hundreds of thousands of years. This concept requires the integration of

Fig. 32.35 *Near-surface disposal of low-level radioactive waste in an active trench* (*DHEC*, 2007). *The vaults are immediately backfilled to fill void spaces and reduce radiation exposure. Reproduced by permission of South Carolina Department of Health and Environmental Control.*
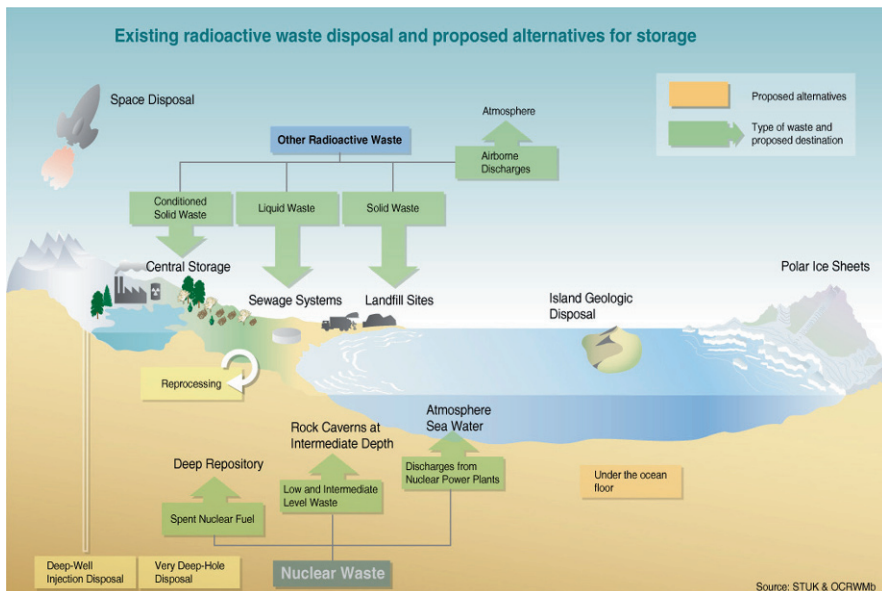

Fig. 32.36 *Existing and proposed short- and long-term disposition of actinides* (*Rekacewicz*, 2004).

several barrier systems (e.g. geologic media, cave buffer or backfill, canister, waste form) increasing safety with a certain redundancy if one or more of the barriers fail. It is to note that science and engineering provides the technological and scientific basis, while the final decision and repository acceptance depend on the political and social environments.

To date, not a single permanent disposal facility for HLW exists and HLW is stored at temporary locations at over 400 nuclear power plants in 30 countries around the world (Hasan, 2007). A consensus has been reached among the countries that developed a plan for nuclear waste disposal to encapsulate and store the HLW and TRU wastes in radiation-resistant matrices that are placed deep underground in geologic formations (Inman, 2005; Alexander and McKinley, 2007). For several decades, research has been performed in underground laboratories in several countries, such as the United States, Germany, Sweden, Switzerland, Belgium, Finland, and France. A review of concepts of underground disposal of radioactive wastes and repository programs around the world is given Zhu and Chan (1989), Witherspoon and Bodvarsson (2001), Alexander and McKinley (2007), Hasan (2007), and Rempe (2008).

Three different types of geologic formations, granite, tuff, and salt have been selected as suitable for nuclear waste disposal. Sweden and Finland are pursuing disposal options in granitic bedrock. The United States is developing a repository for HLW in tuff, and already disposing of TRU in salt. Germany is also studying waste disposition in salt formations. Salt exhibits geophysical characteristics that entrap the waste. Salt is plastic and flows into cracks, sealing the repository, and is also heat and radiation resistant. In general, salt formations have a low water content and impermeability that reduces the potential groundwater actinide migration. Below is a very brief overview of major repository programs worldwide.

Finland. Two underground repositories for nuclear waste at Olkiluoto and Loviisa have been assessed. The repository at Olkiluoto was commissioned in 1992 and consists of two storage rooms for low- and medium-level radioactive waste in a depth up to 100 m. The rock type is micaceous gneiss intercalated with fractured tonalite (Vira, 2006; Äikäs and Anttila, 2008). In 2001, the Finnish Parliament authorized the characterization of a repository for spent nuclear fuel within the granitic bedrock at Olkiluoto at the western coast of Finland. Construction of the repository is planned to begin in 2010 and waste emplacement planned for 2020 (Hasan, 2007). Construction of the underground rock characterization facility ONKALO began in 2004. The repository will be at 420 m deep, but excavations are planned to continue down to 520 m. The repository at Loviisa was commissioned in 1998 and is located about 110 m underground in granitic bedrock. The repository consists of two tunnels for solid LLW and a cavern for waste immobilized in cement.

France. Since 1969 LLW and ILW have been disposed of in Centre de la Manche near La Hague and at Centre de l'Aube. In 2006 the French government evaluated its HLW management policy for a reversible geologic disposal

in 2015–2020 and chose a sedimentary formation at Bure as target host rock (Dupuis, 2007). Shaft sinking in consolidated clay at Bure is in progress while one underground lab is operating.

Germany. Since the 1960s the German repository program has investigated the feasibility of underground disposal of nuclear waste in some of their many geologic salt formations (Warnecke *et al.*, 1994; Kim *et al.*, 1996). In 1967, the Asse salt mine was turned into a temporary storage and research facility for the trial emplacement of LLW. From 1972, intermediate-level radioactive waste disposal was tested. The emplacement license expired end of 1978. Between 1967 and 1978 125,000 barrels with LLW and about 1,300 drums with ILW were disposed in the mine. A total volume of about 47,000 m^3 radioactive waste has been emplaced in the Asse mine. The mine is now being prepared for final closure. The former salt mine at Morsleben was licensed for the emplacement of ILW and LLW. By 1998, a total volume of 36,753 m^3 of radioactive waste had been disposed of, when operations were stopped. In 2001, the German government decided to terminate operations and a concept for the final closure of the Morsleben repository is being prepared. In 1977, the salt dome at Gorleben in Germany was selected as a potential repository for the German nuclear waste and has been under investigation since 1979 (Warnecke *et al.*, 1994; Kim *et al.*, 1996; Kaul and Röthemeyer, 1997). Exploratory shaft drillings down to 600 m depth were carried out by 1995. Starting in October 1996, the cut-through between two shafts 840 m deep took place and the infrastructure area was drifted. With the decision to phase-out of nuclear energy in 2000 the German Government suspended all the exploratory work at the Gorleben salt dome, declaring a moratorium for up to 10 years. Meanwhile, remaining concerns had been addressed and the viability of a salt repository 800 m underground at Gorleben had been proven beyond all reasonable doubt. The moratorium has remained in place for allegedly political reasons.

Russia. The development of the Russian nuclear industry has led to the accumulation of large quantities of radioactive wastes and SNF. Spent fuel is stored at Mayak and the Mountain Chemical Plant in the Krasnoyarsk region, which is the site for a second reprocessing plant starting up in 2015. Russia is developing the capacity to chemically process all of its SNF (with the possible exception of SNF from RBMK reactors) to recover and reuse uranium and plutonium in reactors, while immobilizing and disposing the residual HLW in geologic repositories at the processing sites. Several geologic repository sites are under evaluation including disposal in granite, basalt, clay or salt. For details on the Russian approach to HLW management the authors refer to Bradley (1997) and NATO (1998).

Sweden. Since 1988, intermediate-level, medical and industrial radioactive wastes have been disposed in the underground granitic repository near Forsmark 50 m below the Baltic Sea (WNA, 2008a). It has a capacity of 63,000 m^3 and receives about 1,000 m^3 radioactive waste per year. By the end of 2007, about 4,500 metric tons of SNF were placed to cool for about 50 years in

underground rock caverns of the interim repository at Oskarshamn. Future plans are to place the SNF within bentonite clay in a 500 m deep repository in granite. The selection process of a final underground repository for HLW in Sweden is ongoing (Hasan, 2007). Two granitic sites, Oskarshamn and Osthammer, are candidates undergoing intensive site characterization. Following the site selection, the Swedish Nuclear Fuel and Waste Management Co. (SKB) is expected to apply soon for a permit to build the final repository for HLW.

United Kingdom. The programs in the U.K. for HLW disposal have been inactive for many years and the disposal policy of the country is under consideration. Recommendations are made for geological disposal with interim storage as integral part of robust long-term waste management strategy.

United States. Waste Isolation Pilot Plant (*WIPP*). The WIPP was authorized by the United States Congress in 1979 as a research and development facility to demonstrate the safe disposal of TRU waste. Since 1999, WIPP is a licensed underground repository for TRU waste generated from research and production of nuclear weapons. The WIPP is expected to operate until 2070 with active monitoring for a further 100 years. By 2006, the facility had processed 5,000 shipments of waste. The repository, with a capacity of about 175,600 m^3, is located 655 m deep in the lower part of a 1,000 m thick salt formation (Salado) in southeastern New Mexico (Fig. 32.37). This geologic formation has been stable for hundreds of million years. The salt formation consists of bedded halite (NaCl) and interbeds of anhydrite ($CaSO_4$) and clay (eroded silicates). The Salado formation is sitting on a zone (castile) of alternating layers of anhydrite and calcite. The upper part of the Salado formation consists of a
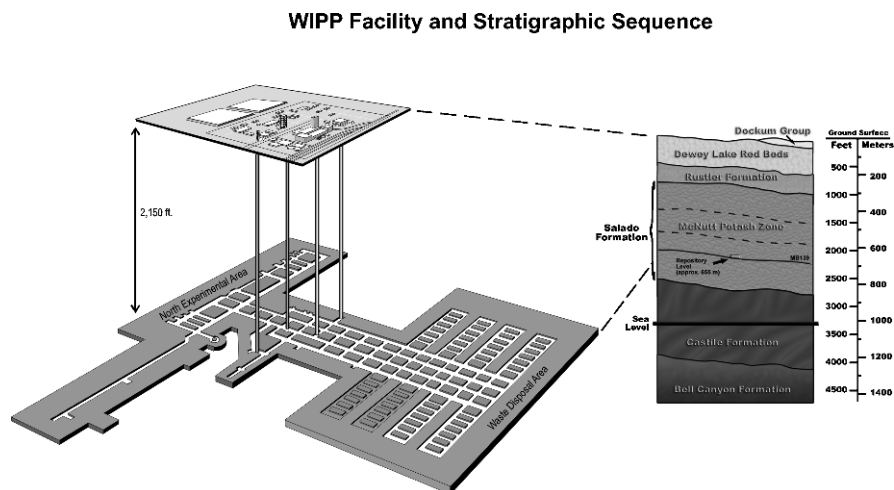
WIPP Facility and Stratigraphic Sequence

Fig. 32.37 *Illustration of the underground WIPP repository. Courtesy of the United States Department of Energy Carlsbad Field Office.*

122 m thick zone rich in potash minerals. Two 8.6 m thick water-bearing zones of fractured dolomite are within the 95 m thick Rustler formation that overlies the Salado. These aquifers are about 435 m above the repository and are considered more permeable and thus a potential pathway for the migration of radionuclides. Performance assessment calculations rely on scientific studies performed over the last 25 years. Calculation predicted that the most dominant release scenario is an inadvertent human drilling intrusion into the disposal areas (Silva *et al.*, 1999). In such an event, water from the overlying dolomite aquifer (Culebra) enters the disposal rooms providing a pathway into the environment. Water conditions are characterized by saturated chloride concentrations with other inorganic (hydroxide, carbonate) and organic ligands from inside the waste packages (EDTA, NTA, citrate). While pockets of high actinide activity may radiolytically create oxidizing conditions that can stabilize actinides in their more soluble, higher oxidation states, the presence of large quantities of iron, microbial activity, presence of organic compounds and the atmosphere-impermeability of the waste packages are expected to maintain a reducing environment.

United States. Yucca Mountain Repository. The remote and arid region of Yucca Mountain in southern Nevada is the potential repository site for HLW in the United States (Canepa *et al.*, 1994; Eckhart, 2000). In 2002, Yucca Mountain was recommended to hold 77,000 metric tons of HLW. In June of 2008, the United States Department of Energy submitted a license application to the Nuclear Regulatory Commission to construct and to operate the Yucca Mountain repository. The location of the repository units is about 300 m below the surface of the mountain and 150–300 m above the static groundwater level. The repository is sited within the unsaturated zone in densely-welded devitrified tuff, which creates oxidizing conditions. Performance assessment calculations are challenged by extremely low groundwater flux at the site. The site-specific geochemical conditions are oxidizing, with near-neutral waters (pH 6.5–8.9) that are low in ionic strength. Many chemistry and transport studies used waters from two wells in the Yucca Mountain region. Well J-13 accesses the water table several miles east of Yucca Mountain, and water from well UE-25p is drawn from the deep paleocarbonates underlying the tuff of Yucca Mountain.

32.5 CONCLUDING REMARKS

Since the discovery of the enormous energy released in nuclear fission we have come far in understanding the behavior of actinides in the environment. During the wartime development of weapons, when the impact of environmental radioactivity was neither known nor of primary concern, relatively large inventories of actinides were injected into soils, rivers, ponds and holding tanks. This changed in the 1970s and 1980s when mining, materials processing and waste management began to be designed to produce much less waste and to isolate the

actinides from human exposure. Still, many sites worldwide have yet to address the legacy of early weapons development and the dramatic expansion of nuclear arsenals.

Electricity generation from uranium-based light water reactors has had a much different environmental "footprint". Mining ore for fuel produced large tailings, but overall byproducts are generally much simpler to treat or remediate. In addition, the actinides involved in the nuclear power cycle are certainly more localized than the global fallout from early above-ground weapons testing. Like the weapons legacy, actinides in the environment from power production have been cleaned up at a few, but by far not all of the major sites worldwide.

With the growth of nuclear energy, particularly dramatic in Asia, there is the potential for greater environmental exposure to actinides. Somewhat counteracting this build-up is increased uranium recycle, development of transmutation, use of thorium-based fuel, and greater use of mixed oxide fuels. Even with these advances, the primary issue of byproducts and consequences remains at the end of the cycle, i.e. the disposition of actinides that are not useful for energy production (neptunium, americium and curium). Repositories are designed to be extremely conservative through siting, strict requirements on contents, waste packaging, and the implementation of multiple barriers between actinides and water, flora, fauna and people. In the future, burner reactors may be developed to reduce the amount of the longest-lived actinides (neptunium, americium and curium), further reducing both the latent radiotoxicity of actinides produced per unit electricity and the potential for illicit use.

Increased understanding of the behavior of actinides in natural systems can enable the maturation of nuclear energy. While several decades ago the focus of environmental actinide measurements was on determining the yield of particular weapons, current and future research is aimed at science-based prediction of actinide retention rates under specific conditions. This effort has advanced from phenomenological observations to the stepwise advance of experimentation, modeling and simulation of increasingly complex mechanisms and systems. It is now established which actinide oxidation states, binary molecular complexes and extended solids are stable under the bounding conditions of water, atmospheric or elevated carbonate, and common concentrations of simple salts and organics. The maximum solubility of individual actinides in aqueous solutions is known from laboratory solubility experiments and the fraction of actinides retained by a single mineral is also known for the most important phases. Recent work has refined our understanding of intrinsic polymeric and colloidal actinide (oxy)hydroxides and carbonates, and has defined new, lower actinide concentrations at which these species form. Models that combine all of these quantitative information from laboratory studies with site conditions are increasingly sophisticated and are building a foundation towards accurate predictive simulations. Most importantly, analyses of environmental samples indicate that predictions are conservative.

We must also recognize that much work is still in front of us. We can accurately predict the speciation and solubility of actinides when only one actinide and up to three of the most common ligands are present, but not when the complexity is increased to that of a natural system. In most cases, the predicted transport rate and soluble actinide concentration are both much higher than the actual rate and concentration measured at contaminated sites; in addition, there are some examples where the rate and concentration are under-predicted. Laboratory studies are needed to include combinations of more components, solutions that cover the limiting relevant ionic compositions and a range of oxygen and temperature. Many experimental research projects are aimed at examining details that are important for actinide chemistry, but do not contribute to the critical needs for understanding actinide environmental chemistry or nuclear waste isolation. For example, the detailed formation mechanisms and structures of intrinsic actinide colloids synthesized under highly acidic conditions are scientifically interesting, but are much less important than either studies of actinide colloids at near-neutral pH or studies of actinides adsorbed onto colloid-sized particulates of major natural minerals or organics. Arguably the largest lack in laboratory studies is quantitative adsorption data for actinides interacting with the complex assemblages of inorganic and biotic particulate matter that have a broad and irregular distribution of sizes, surface areas, and functional groups. Only recently have spectroscopic, imaging, and modeling tools been available that enable researchers to distinguish between sorption mechanisms on a molecular scale within complex mixtures. In addition, data from actinide adsorption studies are only recently being critically reviewed and down-selected in the same way that solubility and complex formation constants have been evaluated by the OECD/NEA.

The greatest needs in environmental actinide studies are robust sampling and analysis methods, meter-scale demonstration projects, and field-scale studies. It is possible that higher-than-expected actinide concentrations in environmental samples are in fact artifacts of samples being contaminated in the field or during analysis. The difficulty of collecting unbiased samples and sufficient numbers of samples required for statistically sound results is underestimated. It is fair to conclude that enough sites have been sampled, and analyzed well enough to provide accurate results. Compared to the number of laboratory experiments and environmental samples that have been analyzed, the number of field-scale actinide experiments is astonishingly small.

There is also a significant difference in our understanding of the various actinide elements. Because we have natural analogues to learn from and because they have relatively low radioactivity, there is much more research done for thorium and uranium and their chemistries and environmental behaviors are relatively well understood. Neptunium and plutonium are much more difficult to study given the coexistence of multiple redox states (specifically for neptunium and plutonium) and higher reactivity and radioactivity. Americium has a simpler redox behavior, but higher radioactivity, and is relatively little studied

in comparison. The need to study these transuranium actinides grows as the future use of higher burn-up, mixed-actinide fuels, and reprocessed fuel increases. Spent uranium-based fuels have been studied, including very important leaching and aging experiments where alteration phases have been characterized. It is not known how the incorporation of neptunium, plutonium and americium changes the physical and chemical behavior of these alteration phases.

Much has been written about the risks of actinides, especially related to nuclear power. In this context, it is important to remember that the energy released per mass unit from nuclear fission is a million times greater than the energy released in the combustion of fossil fuels. The same energy per mass difference applies when nuclear energy is compared to other chemical- or photon-based energy sources. That fact underlines the likelihood that positive, peaceful uses of nuclear fission will expand and greatly reinforces the need to understand the fate of the actinides in the environment.

LIST OF ABBREVIATIONS

Bq	Becquerel
Ci	Curie
DBP	dibutylphosphate
DFB	desferrioxamine B
DFE	desferrioxamine E
DMRB	dissimilatory metal reducing bacteria
DOC	dissolved organic carbon
DOE	Department of Energy
EBq	exabecquerel (1 EBq $= 10^{18}$ Bq)
EDTA	ethylendiaminetetraacetic acid
EXAFS	extended X-ray absorption fine structure
HEU	highly enriched uranium
HLW	high-level (radioactive) waste
IAEA	International Atomic Energy Agency
IDA	iminodiacetic acid
ILW	intermediate-level waste
IRSN	Institut de Radioprotection et de Sûreté Nucléaire
LET	linear energy transfer
LLW	low-level waste
MOX	mixed oxide
NTA	nitrilotriacetic acid
NTS	Nevada Test Site
OECD	Organization for Economic Co-operation and Development
PBq	petabecquerel (1 PBq $= 10^{15}$ Bq)

PUREX	plutonium uranium recovery by extraction
RBMK	Reactor Bolshoy Moshchnosty Kanalny (high-power channel reactor)
RFETS	Rocky Flats Environmental Technology Site
SCC	Siberian Chemical Combine
SIT	specific ion-interaction theory
SKB	Swedish Nuclear Fuel and Waste Management Co.
SNF	spent nuclear fuel
TBq	terabecquerel (1 TBq = 10^{12} Bq)
TBP	tri(n-butyl) phosphate
tHM	metric tons heavy metals
TRU	transuranium elements
TRUEX	transuranic extraction
U.K.	United Kingdom
UNSCEAR	United Nations Scientific Committee on the Effects of Atomic Radiation
UREX	uranium recovery by extraction
U.S.	United States
WIPP	Waste Isolation Pilot Plant
WNA	World Nuclear Association
XANES	X-ray absorption near-edge spectroscopy

REFERENCES

Adams, C. E., Farlow, N. H., and Schell, W. R. (1960) *Geochim. Cosmochim. Acta*, **18**, 42–56.

Agnew, S. F. (1995) Hanford Defined Wastes: Chemical and Radionuclide Compositions, Report LAUR 94-2657 Rev. 2, Los Alamos National Laboratory, Los Alamos, NM, pp. 143.

Äikäs, T. and Anttila, P. (2008) *Rev. Eng. Geol.*, **XIX**, 67–71.

Al Mahamid, I. and Becraft, K. A. (1995) *Radiochim. Acta*, **68**, 63–68.

Albright, D. (2004) Separated Civil Plutonium Inventories: Current Status and Future Directions. Institute for Science and International Security. http://www.isis-online.org/global_stocks/separated_civil_pu.html.

Albright, D., Berkhout, F., and Walker, W. (1997) *Plutonium and Highly Enriched Uranium 1996: World Inventories*, *Capabilities and Policies*, Oxford University Press, Oxford, pp. 534.

Alexander, W. R. and McKinley, L. E. (2007) *Deep Geological Disposal of Radioactive Waste*. Elsevier, Amsterdam, The Netherlands, pp. 273.

Al-Hashimi, A., Evans, G. J., and Cox, B. (1996) *Water*, *Air Soil Poll.*, **88**, 83–92.

Allard, B., Kipatsi, H., and Liljenzin, J. O. (1980) *J. Inorg. Nucl. Chem.*, **42**, 1015–1027.

Allen, P. G., Bucher, J. J., Clark, D. L., Edelstein, N. M., Ekberg, S. A., Gohdes, J. W., Hudson, E. A., Kaltsoyannis, N., Lukens, W. W., Neu, M. P., Palmer, P. D., Reich, T., Shuh, D. K., Tait, C. D., and Zwick, B. D. (1995) *Inorg. Chem.*, **34**, 4797–4807.

Allen, P. G., Bucher, J. J., Shuh, D. K., Edelstein, N. M., and Reich, T. (1997) *Inorg. Chem.*, **36**, 4676–4683.

Altmaier, M., Neck, V., and Fanghänel, T. (2004) *Radiochim. Acta*, **92**, 537–543.

Alvarez, R. (2005) *Sci. Global Sec.*, **13**, 43–86.

Anderson, R. T., Vrionis, H. A., Ortiz-Bernad, I., Resch, C. T., Long, P. E., Dayvault, R., Karp, K., Marutzky, S., Metzler, D. R., Peacock, A., White, D. C., Lowe, M., and Lovley, D. R. (2003) *Appl. Environ. Microbiol.*, **69**, 5884–5891.

André, C. and Choppin, G. R. (2000) *Radiochim. Acta*, **88**, 613–616.

Andreychuck, N. N., Frolov, A. A., Rotmanov, K. V., and Vasiliev, V. Y. (1990) *J. Radioanal. Nucl. Chem. Art.*, **143**, 427–432.

Aragon, A., Espinosa, A., De La Cruz, B., and Fernandez, J. A. (2008) *J. Environ. Radioact.*, **99**, 1061–1067.

Arai, Y., Marcus, N., Tamura, J. A., Davis, J. A., and Zachara, J. M. (2007) *Environ. Sci. Technol.*, **41**, 4633–4639.

AREVA (2007) Liquid Releases Annually Report 2007. AREVA, France. http://www.areva-nc.fr/scripts/areva-nc/publigen/content/templates/show.asp?P=67&L=EN&SYNC=Y.

AREVA (2008) Tricastin: AREVA to invest extra €20 million to improve environment around facilities. AREVA, France. http://www.areva-nc.com/scripts/areva-nc/publigen/content/templates/Show.asp?P=7936&L=EN.

Arnold, L. (1995) *Windscale 1957. Anatomy of a Nuclear Accident*, Macmillan Press Ltd., London, pp. 264.

Artinger, R., Buckau, G., Zeh, P., Geraedts, K., Vancluysen, J., Maes, A., and Kim, J. I. (2003) *Radiochim. Acta*, **91**, 743–750.

Assinder, D. J. (1999) *J. Environ. Radioact.*, **44**, 335–347.

Atlas, R. M. and Bartha, R. (1993) *Microbial Ecology: Fundamentals and Applications*, Benjamin/Cummings Publishing Company, Redwood City, CA, pp. 576.

Baade, W., Burbridge, G. R., Hoyle, F., Burbridge, E. M., Christy, R. F., and Fowler, W. A. (1956) *Publ. Astron. Soc. Pacific*, **68**, 296–300.

Baas-Becking, L. G. M., Kaplan, I. R., and Moore, D. (1960) *J. Geol.*, **68**, 243–284.

Bailey, R. A., Clark, H. M., Ferris, J. P., Krause, S., and Strong, R. L. (2002) *Chemistry of the Environment*, Academic, San Diego, CA, pp. 835.

Banaszak, J. E., Rittmann, B. E., and Reed, D. T. (1999) *J. Radioanal. Nucl. Chem.*, **241**, 385–435.

Baston, G. M. N., Berry, J. A., Brownsword, M., Heath, T. G., Ilett, D. J., Tweed, C. J., and Yui, M. (1997) The Effect of Temperature on the Sorption of Technetium, Uranium, Neptunium, and Curium on Bentonite, Tuff, and Granodiorite. In *Scientific Basis for Nuclear Waste Management XX* (Pittsburgh, PA) (eds. W. J. Gray and I. R. Triay), Materials Research Society, pp. 805–812.

Bea, F. (1999) Uranium: Element and Geochemistry, pp. 630–635. In *Encyclopedia of Geochemistry* (eds. R. W. Fairbridge and M. R. Rampino), Kluwer, Dordrecht, The Netherlands, pp. 645–654.

Bearden, D. M. and Andrews, A. (2007) Radioactive Tank Waste from the Past Production of Nuclear Weapons: Background and Issues for Congress, Report RS21988, Congressional Research Service, The Library of Congress, Washington D.C., pp. 6.

Beasley, T. M. and Ball, L. A. (1980) *Nature*, **287**, 624–625.

Beasley, T. M., Cooper, L. W., Grebmeier, J. M., Aagard, K., Kelley, J. M., and Kilius, L. R. (1998a) *J. Environ. Radioact.*, **39**, 255–277.

Beasley, T. M., Kelley, J. M., Maiti, T. C., and Bond, L. A. (1998b) *J. Environ. Radioact.*, **38**, 133–146.

Begg, B. D., Vance, E. R., and Conradson, S. D. (1998) *J. Alloys Compd.*, **271–273**, 221–226.

Berkey, E. and Zachry, T. E. (2005) *Subsurface Contamination and Remediation. Accomplishments of the Environmental Management Science Program.* American Chemical Society, United States, pp. 408.

Bernhard, G., Geipel, G., Brendler, V., and Nitsche, H. (1998) *J. Alloys Compd.*, **271–273**, 201–205.

Bernkopf, M. F. and Kim, J. I. (1984) Hydrolysereaktion und Karbonatkomplexierung von dreiwertigem Americium in natürlichen aquatischen Systemen, RCM02284, Report, Technische Universität München, München, pp. 200.

Berry, J. A., Yui, M., and Kitamura, A. (2007) Sorption Studies of Radioelements on Geological Materials, Report JAEA-Research – 2007-074, Japan Atomic Energy Agency, Tokai, Ibaraki, pp. 104.

Berzero, A. and D'Alessandro, M. (1990) The Oklo Phenomenon as an Analog of Radioactive Waste Disposal. A Review, Report EUR 12941, Comm. Eur. Communities Eur., pp. 86.

Betti, M. (2003) *J. Environ. Radioact.*, **64**, 113–119.

Blyth, A., Frape, S., Ruskeeniemi, T., and Blomqvist, R. (2004) *Appl. Geochem.*, **19**, 675–686.

Bodu, R., Bouzigues, H., Morin, N., and Pfiffelmann, J. P. (1972) *C. R. Acad. Sci. Paris*, **275D**, 1731–1734.

Bogatov, S. S. (1998) Remediation of the Chernobyl Accident Site. In *Actinides in the Environment* (eds. P. A. Sterne, A. Gonis, and A. A. Borovoi), Kluwer, Dordrecht/Boston/London, pp. 391–422.

Bouby, M., Billard, I., and Maccordick, H. J. (1999) *Czech. J. Phys.*, **49**, 147–150.

Boukhalfa, H., Reilly, S. D., Smith, W. H., and Neu, M. P. (2004) *Inorg. Chem.*, **43**, 5816–5823.

Boukhalfa, H., Reilly, S. D., and Neu, M. P. (2007) *Inorg. Chem.*, **46**, 1018–1026.

Boulyga, S. F. and Becker, J. S. (2002) *J. Anal. Atomic Spectrosc.*, **17**, 1143–1147.

Bradley, D. J. (1997) *Behind the Nuclear Curtain: Radioactive Waste Management in the Former Soviet Union*, Battelle Press, Columbus, OH, pp. 716.

Brainard, J. R., Strietelmeier, B. A., Smith, P. H., Unkefer, P. J., Barr, M. E., and Ryan, R. R. (1992) *Radiochim. Acta*, **58/59**, 357–363.

Brissot, R., Heuer, D., Le Brun, C., Loiseaux, J.-M., Nifenecker, H., and Nuttin, A. (2001) Nuclear Energy With (Almost) No Radioactive Waste? Laboratoire de Physique Subatomique et de Cosmologie, Grenoble, France. http://lpsc.in2p3.fr/gpr/english/NEWNRW/NEWNRW.html.

Bros, R., Turpin, L., Gauthier-Lafaye, F., Holliger, P., and Stille, P. (1993) *Geochim. Cosmochim. Acta*, **57**, 1351–1356.

Bros, R., Hidaka, H., Kamel, G., and Ohnuki, T. (2003) *Appl. Geochem.*, **18**, 1807–1824.

Bruno, J., Duro, L., and Grive, M. (2002) *Chem. Geol.*, **190**, 371–393.

Buddemeier, R. W. and Hunt, J. R. (1989) *Appl. Geochem.*, **3**, 535–548.

Buesseler, K. O. (1997) *J. Environ. Radioact.*, **36**, 69–83.

Buesseler, K. O. and Sholkowitz, E. R. (1987) *Geochim. Cosmochim. Acta*, **51**, 2623–2637.

Bunzl, K. and Kracke, W. (1994) *J. Alloys Compd.*, **213/214**, 212–218.

Büppelmann, K., Kim, J. I., and Lierse, C. (1988) *Radiochim. Acta*, **44/45**, 65–70.

Burbridge, G. R., Hoyle, F., Burbridge, E. M., Christy, R. F., and Fowler, W. A. (1956) *Phys. Rev.*, **103**, 1145–1149.

Burkart, W. (1991) Uranium, Thorium, and Decay Products. II.33. In *Metals and Their Compounds in the Environment* (ed. E. Merian), VCH Verlagsgesellschaft, Weinheim, Germany, pp. 1275–1287.

Burns, P. C. (1999) *Rev. Mineral.*, **38**, 23–90.

Burns, P. C. and Finch, R., (eds.) (1999) *URANIUM: Mineralogy*, *Geochemistry and the Environment*. Mineralogical Society of America, Washington, D.C., pp. 679.

Burns, C. J., Neu, M. P., Boukhalfa, H., Gutowski, K. E., Bridges, N. J., and Rogers, R. D. (2004a) The Actinides. In *Comprehensive Coordination Chemistry II* (eds. J. A. McCleverty and T. J. Meyer), Elsevier Pergamon, Amsterdam, The Netherlands, pp. 189–346.

Burns, P. C., Deely, K. M., and Skanthakumar, S. (2004b) *Radiochim. Acta*, **92**, 151–160.

Canepa, J. A., Triay, I. R., Rogers, P. S. Z., Hawley, M. E., and Zyvoloski, G. A. (1994) in *The Yucca Mountain Site Characterization Project: Site-Specific Research and Development on the Chemistry and Migration of Actinides*. Chemistry and Migration Behaviour of Actinides and Fission Products in the Geosphere, *Proceedings of the Fourth International Conference*, Charleston, SC, 1993, Oldenbourg Verlag, Munich, pp. 813–820.

Carson, J. (1993) *Sci. Global Sec.*, **4**, 111–128.

Carvalho, F. P., Madruga, M. J., Reis, M. C., Alves, J. G., Oliveira, J. M., Gouveia, J., and Silva, L. (2007) *J. Environ. Radioact.*, **96**, 39–46.

Chisholm-Brause, C., Conradson, S. D., Buscher, C. T., and Eller, P. G. (1994) *Geochim. Cosmochim. Acta*, **58**, 3625–3631.

Choppin, G. R. (1983) *Radiochim. Acta*, **32**, 43–53.

Choppin, G. R. (1988) *Radiochim. Acta*, **43**, 82–83.

Choppin, G. R. (1992) *Radiochim. Acta*, **58/59**, 113–120.

Choppin, G. R., and Du, M. (1992) *Radiochim. Acta*, **58/59**, 101–104.

Choppin, G. R. and Wong, P. J. (1998) *Aquatic Geochem.*, **4**, 77–101.

Choppin, G. R., Liljenzin, J.-O., and Rydberg, J. (2002) *Radiochemistry and Nuclear Chemistry*, Butterworth-Heinemann, Woburn, MA, pp. 709.

Christensen, G. C., Romanov, G. N., Strand, P., Salbu, B., Malyshev, S. V., Bergan, T. D., Oughton, D., Drozhko, E. G., Glagolenko, Y. V., Amundsen, I., Rudjord, A. L., Bjerk, T. O., and Lind, B. (1997) *Sci. Total Environ.*, **202**, 237–248.

Christensen, J. N., Dresel, P. E., Conrad, M. E., Maher, K., and DePaolo, D. J. (2004) *Environ. Sci. Technol.*, **38**, 3330–3337.

Christensen, J. N., Conrad, M. E., DePaolo, D. J., and Dresel, P. E. (2007) *Vadose Zone J.*, **6**, 1018–1030.

Chung, K. H., Klenze, R., Park, K. K., Paviet-Hartmann, P., and Kim, J. I. (1998) *Radiochim. Acta*, **82**, 215–219.

Ciavatta, L. (1980) *Ann. Chim.* (*Rome*), **70**, 551–567.

Clark, D. L., Janecky, D. R., and Lane, L. J. (2006) *Phys. Today*, **59**, 34–40.

Clark, D. L., Neu, M. P., Runde, W., and Keogh, D. W. (2007) Thorium and Thorium Compounds. In *Kirk-Othmer Encyclopedia of Chemical Technology*, Wiley Interscience, New York, pp. 753–782.

Cleveland, J. M. and Rees, T. F. (1981) *Science*, **212**, 1506–1509.

Cleveland, J. M. and Rees, T. F. (1982) *Environ. Sci. Technol.*, **16**, 347–439.

Conradson, S. D. (1998) *Appl. Spectrosc.*, **52**, 252A–279A.

Cooper, J. R., Randle, K., and Sokhi, R. S. (2003) *Radioactive Releases in the Environment: Impact and Assessment*, Wiley, West Sussex, pp. 473.

Cowan, G. A. (1976) *Sci. Am.*, **235/236**, 36–47.

CRWMS (2000a) Commercial Spent Nuclear Fuel Degradation in Unsaturated Drip Tests, Report ACC: MOL.20000107.0209, Civilian Radioactive Waste Management. System Management and Operating Contractor, Las Vegas, NV.

CRWMS (2000b) Total System Performance Assessment for the Site Recommendation, Report TDF-WIS-PA-00001, Civilian Radioactive Waste Management. System Management and Operating Contractor, Las Vegas, NV.

Curtis, D. B., Fabryka-Martin, J., Aguilar, R., Attrep, M., and Roensch, F. (1992) 3rd Annual International Conference Proceedings (Am. Nucl. Soc.), **1**, p. 338–394

Dai, M., Kelley, J. M., and Buesseler, K. O. (2002) *Environ. Sci. Technol.*, **36**, 3690–3699.

De Geer, L.-E. (1977) *Science*, **198**, 925–927.

Deditius, A. P., Utsunomiya, S., and Ewing, R. C. (2007) *J. Alloys Compd.*, **444/445**, 584–589.

Deditius, A. P., Utsunomiya, S., and Ewing, R. C. (2008) *Chem. Geol.*, **251**, 33–49.

Degueldre, C., Triay, I., Kim, J. I., Vilks, P., Laaksoharju, M., and Miekeley, N. (2000) *Appl. Geochem.*, **15**, 1043–1051.

Dekoussar, V., Dyck, G. R., Galperin, A., Ganguly, C., Todosow, M., and Yamawaki, M. T. (2005) Thorium Fuel Cycle – Potential Benefits and Challenges, Report IAEA-TECHDOC-1450, Report, International Atomic Energy Agency, Vienna, Austria, pp. 105.

deMarcillac, P., Coron, N., Dambier, G., Leblanc, J., and Moalic, J. P. (2003) *Nature*, **422**, 876–878

Demirbas, A. (2005) *Energy Sour.*, **27**, 597–603.

Dhami, P. S., Gopalakrishnan, V., Kannan, R., Ramanujam, A., Salvi, N., and Udupa, S. R. (1998) *Biotech. Lett.*, **20**, 225–228.

DHEC (2007) Commercial Low-Level Radioactive Waste Disposal In South Carolina, Report CR-000907, South Carolina Department of Health and Environmental Control, Columbia, South Carolina, pp. 20.

Ditz, R., Sarbas, B., Schubert, P., and Töpper, W. (1990) *Thorium. Suppl. Vol. A1a. Natural Occurrence. Minerals* (*Excluding Silicates*), Springer, Berlin.

DOE (1999) Groundwater/Vadose Zone Integration Project Summary Description, Report DOE/RL-98-48, Vol. I, Rev.0, U.S. Department of Energy.

Donaldson, L. R., Seymour, A. H., and Nevissi, A. E. (1997) *Health Physics* **73**, 214-222.

Dozol, M. and Hagemann, R. (1993) *Pure Appl. Chem.*, **65**, 1081–1102.

Duff, M. C. and Amrheim, C. (1996) *Soil Sci. Soc. Am. J.*, **60**, 1393–1400.

Duff, M. C., Hunter, D. B., Triay, I. R., Bertsch, P. M., Reed, D. T., Sutton, S. R., SheaMccarthy, G., Kitten, J., Eng, P., Chipera, S. J., and Vaniman, D. T. (1999) *Environ. Sci. Technol.*, **33**, 2163–2169.

Duffa, C. and Renaud, P. (2005) *Sci. Total Environ.*, **348**, 164–172.

Dupuis, M.-C. (2007) International Conference on Radioactive Waste Disposal, Bern, Switzerland, p. 6.

Eckhart, R. (2000) Yucca Mountain–Looking Ten Thousand Years into the Future. In *Los Alamos Science* (ed. N. G. Cooper), Los Alamos National Laboratory, Los Alamos, NM, pp. 464–489.

Efurd, D. W., Rokop, D. J., and Perrin, R. E. (1993) Characterization of the Radioactivity in Surface-Waters and Sediments Collected at the Rocky Flats Facility, Report LA-UR-93-4373, Los Alamos National Laboratory, Los Alamos, NM, pp. 53.

Efurd, D. W., Runde, W., Banar, J. C., Janecky, D. R., Kaszuba, J. P., Palmer, P. D., Roensch, F. R., and Tait, C. D. (1998) *Environ. Sci. Technol.*, **32**, 3893–3900.

Espinosa, A., Aragon, A., Martinez, J., and Gutierrez, J. (1999) Experience with Environmental Behaviour of Pu at Palomares, Spain, Report IAEA-TECDOC-1148, International Atomic Energy Agency, Vienna, pp. 173–186.

Essien, I. O. (1991) *J. Radioanal. Nucl. Chem.*, **147**, 269–275.

Eyrolle, F., Claval, D., Gontier, G., and Antonelli, C. (2008) *J. Environ. Monit.*, **10**, 800–811.

Fanghänel, T., Könnecke, T., Weger, H., Paviet-Hartmann, P., Neck, V., and Kim, J. I. (1999) *J. Solut. Chem.*, **4**, 447–462.

Farr, J. D., Schulze, R. K., and Honeyman, B. D. (2000) *Radiochim. Acta*, **88**, 675–679.

Farr, J. D., Neu, M. P., Schulze, R. K., and Honeyman, B. D. (2007) *J. Alloys Compd.*, **444/445**, 533–539.

Felmy, A. R., Rai, D., and Fulton, R. W. (1990) *Radiochim. Acta*, **50**, 193–204.

Fernandes, H. M., Franklin, M. R., Veiga, L. H. S., Freitas, P., and Gomiero, L. A. (1996) *J. Environ. Radioact.*, **30**, 69–95.

Finch, R. and Ewing, R. (1990) Uraninite alteration in an oxidizing environment and its relevance to the disposal of spent nuclear fuel. Svensk Kärnbränslehantering AB, Report SKB TR 91-15, University of New Mexico, Albuquerque, New Mexico, pp. 132.

Finn, P. A., Buck, E. C., Gong, M., Hoh, J. C., Emery, J. W., Hafenrichter, L. D., and Bates, J. K. (1994) *Radiochim. Acta*, **66/67**, 189–195.

Fish, W. (1993) Sub-Surface Redox Chemistry: A Comparison of Equilibrium and Reactor-Based Approaches. 3, In *Metals in Groundwater* (eds. H. E. Allen, E. M. Perdue, and D. S. Brown), Lewis Publishers, Chelsea, MI, pp. 73–102.

Fletcher, M. and Murphy, E. (2001) Transport of microorganisms in the subsurface: The role of attachment and colonization of particle surfaces. In *Subsurface Microbiology Biogeochemistry* (eds. J. K. Fredrickson and M. Fletcher), Wiley, New York, NY, pp. 39–68.

Fowle, D. A., Fein, J. B., and Martin, A. M. (2000) *Environ. Sci. Technol.*, **34**, 3737–3741.

Froidevaux, P., Geering, J.-J., Valley, J.-F., and Volkle, H. (1999) *Strahlenschutz Praxis*, **5**, 31–33.

Frondel, C. (1955) *Intern. Conf. Peaceful Uses of Atomic Energy*, Geneva, United Nations, **6**, pp. 568–577.

Gadd, G. M. (2004) *Geoderma*, **122**, 109–119.

Galperin, A., Reichert, P., and Radkowsky, A. (1997) *Sci. Global Sec.*, **6**, 265–290.

Garland, J. A. and Wakeford, R. (2007) *Atmos. Environ.*, **41**, 3904–3920.

Gauthier-Lafaye, F., Pourcelot, L., Eikenberg, J., Beer, H., Le Roux, G., Rhikvanov, L. P., Stille, P., Renaud, P., and Mezhibor, A. (2008) *J. Environ. Radioact.*, **99**, 680–693.

Geckeis, H. and Rabung, T. (2008) *J. Contam. Hydrol.*, **102**, 187–195.

Ghiorso, A., Thompson, S. G., Higgins, G. H., Seaborg, G. T., Studier, M. H., Fields, P. R., Fried, S. M., Diamond, H., Mech, J. F., Pyle, G. L., Huizenga, J. R., Hirsch, A., Manning, W. M., Browne, C. I., Smith, H. L., and Spence, R. W. (1955) *Phys. Rev.*, **99**, 1048–1049.

Gillow, J. B., Dunn, M., Francis, A. J., Lucero, D. A., and Papenguth, H. W. (2000) *Radiochim. Acta*, **88**, 769–774.

Gmelin (1972) *Uranium. Main Volume* (*With an Appendix Covering the Transuranium Elements*), Springer, Berlin, Germany, pp. 279.

Gmelin (1978) *Thorium. Main Volume*, Springer, Berlin, Germany, pp. 406.

Gmelin (1979) *Uranium. Deposits*. Suppl. A1, Springer, Berlin, Germany, pp. 280.

Gmelin (1981) *Uranium. Technology*, *Use*. Suppl. A3, Springer, Berlin, Germany, pp. 297.

Gmelin (1988) *Thorium. Technology*, *Uses*, *Irradiated Fuel*, *Reprocessing*. Suppl. A3, Springer, Berlin, Germany, pp. 215.

Gmelin (1990) *Thorium. Natural Occurrence*, *Minerals* (*excluding Silicates*). Suppl. A1a, Springer, Berlin, Germany, pp. 391.

Gmelin (1991) *Thorium. Minerals* (*Silicates*), *Deposits*, *Mineral Index*. Suppl. A 1b, Springer, Berlin, Germany, pp. 440.

Goff, G. S., Brodnax, L. F., Cisneros, M. R., Peper, S. M., Field, S. E., Scott, B. L., and Runde, W. (2008) *Inorg. Chem.*, **47**, 1984–1990.

Gorby, Y. A. and Lovley, D. R. (1992) *Environ. Sci. Technol.*, **26**, 205–207.

Grambow, B., Loida, A., Dressler, P., Geckeis, H., Gago, J., Casas, I., DePablo, J., Gimenez, J., and Torrerro, M. E. (1997) Chemical Reaction of Fabricated and High-Burnup Spent UO_2 Fuel with Saline Brine, Report EUR-17111EN, and Wissenschaftliche Berichte, Forschungszentrum Karlsruhe, Germany, Report FZK-5702 (1996), European Commission, Brussels, pp. 181.

Gray, J., Jones, S. R., and Smith, A. D. (1995) *J. Radiol. Protect.*, **15**, 99–131.

Grenthe, I. and Puigdomenech, I. (1997) *Modelling in Aquatic Chemistry*, OECD/NEA, Paris, France, pp. 724.

Grenthe, I., Fuger, J., Konings, R. J. M., Lemire, R. J., Muller, A. B., Nguyen-Trung, C., and Wanner, H. (1992) *Chemical Thermodynamics of Uranium*. North-Holland Elsevier Science Publishers b.V., Amsterdam, The Netherlands, pp. 716.

Grown, G. E. J. and Sturchio, N. C. (2002) *Rev. Miner. Geochem.*, **49**, 1–115.

Haas, J. R., Dichristina, T. J., and Wade, R. (2001) *Chem. Geol.*, **180**, 33–54.

Hakem, N. L., Allen, P. G., and Sylwester, E. R. (2001) *J. Radioanal. Nucl. Chem.*, **250**, 47–53.

Hamilton, D. L. (1963) *Bull. At. Sci.*, **19**, 36–40.

Hamilton, T. F. (2004) Linking legacies of Cold War to arrival of anthropogenic radionuclides in the oceans through the 20th century. In *Marine Radioactivity* (ed. H. D. Livingston), Elsevier, Amsterdam, The Netherlands, pp. 23–78.

Hanson, B., McNamara, B., Buck, E., Friese, J., Jenson, E., Krupka, K., and Arey, B. (2005) *Radiochim. Acta*, **93**, 159–168.

Hardy, E. P., Krey, P. W., and Volchek, H. L. (1973) *Nature*, **241**, 444–445.

Harper, R. M., Kantar, C., and Honeyman, B. D. (2008) *Radiochim. Acta*, **96**, 753–762.

Hart, E. J. (1954) *Radiat. Res.*, **1**, 53–61.

Hartmann, E., Geckeis, H., Rabung, T., Lützenkirchen, K., and Fanghänel, T. (2008) *Radiochim. Acta*, **96**, 699–707.

Harvie, C. E., Möller, N., and Weare, J. H. (1984) *Geochim. Cosmochim. Acta*, **48**, 723–751.

Hasan, S. E. (2007) International practice in high-level nuclear waste management. 4. In *Development in Environmental Science* (eds. D. Sarkar, R. Datta, and R. Hannigan), Elsevier Ltd., Kansas City, MO, pp. 57–78.

Haveman, S. A. and Pedersen, K. (2002) *J. Contamin. Hydrol.*, **55**, 161–174.

He, L. M., Neu, M. P., and Vanderberg, L. A. (2000) *Environ. Sci. Technol.*, **34**, 1694–1701.

Hedrick, J. B. (2004) Thorium. In: *Minerals Yearbook Volume I. – Metals and Minerals*, U.S. Geological Survey, Washington, D.C., pp. 76.1–76.3.

Heylin, M. (1990) *Chem. Eng. News*, **68**, 7–11.

Hidaka, H. (2007) *J. Nucl. Radiochem. Sci.*, **8**, 99–103.

Hill, F. C. (1999) *Rev. Mineral.*, **38**, 635–679.

Hirose, K., Aoyama, M., Kim, C. S., Kim, C. K., and Povinec, P. P. (2006) *Radioact. Environ.*, **8**, 67–82.

Hirose, K., Igarashi, Y., and Aoyama, M. (2008) *Appl. Rad. Isot.*, **66**, 1675–1678.

Hisamatsu, S., and Sakanoue, M. (1978) *Health Phys.*, **35**, 301–307.

Ho, C. H. and Miller, N. H. (1985) *J. Coll. Interface Sci.* **106**, 281–288.

Hoffman, D. C., Lawrence, F. O., Mewherter, J. L., and Rourke, F. M. (1971) *Nature*, **234**, 132–134.

Holleman, J. W., Quiggins, P. A., Chilton, B. D., Uziel, M. S., Pfuderer, H. A., and Longmire, J. A. (1987) Worldwide Fallout of Plutonium from Nuclear Weapons Tests, Report ORNL-6315, Oak Ridge National Laboratory, Oak Ridge, TN, pp. 295.

Holm, E. (1995) *Appl. Radiat. Isot.*, **46**, 1225–1229.

Holm, E. and Persson, B. R. R. (1978) *Nature*, **273**, 289–290.

Hrkal, Z., Gadalia, A., and Rigaudiere, P. (2006) *Environ. Geol.*, **50**, 717–723.

Hummel, W., Anderegg, G., Rao, L., Puigdomenech, I., and Tochiyama, O. (2005) *Chemical Thermodynamics of Compounds and Complexes of U, Np, Pu, Am, Tc, Se, Ni and Zr with Selected Organic Ligands*, Elsevier Science B.V., Amsterdam, The Netherlands, pp. 1088.

Hvinden, T. (1978) *Sivilt Beredskap*, **21**, 2–4.

IAEA (1995) The Principles of Radioactive Waste Management, Report Safety Series 111-F, International Atomic Energy Agency, Vienna, Austria, pp. 25.

IAEA (1998) The Radiological Accident in the Reprocessing Plant at Tomsk, ISBN 92-0-103798-8, Report, International Atomic Energy Agency, Vienna, Austria, pp. 77.

IAEA (2008) Spent Fuel Reprocessing Options, IAEA-TECDOC-1587, Report ISBN 978-92-0-103808-1, International Atomic Energy Agency, Vienna, Austria, pp. 151.

Ibrahim, S. A. and Morris, R. C. (1997) *J. Radioanal. Nucl. Chem.*, **226**, 217–220.

Inman, M. (2005) *Science*, **309**, 1179.

IRSN (2008a) Accidental uranium release at the SOCATRI plant : Water restrictions lifted and new, extended monitoring plan implemented. Institut de Radioprotection et de Sûreté Nucléaire, France. http://www.areva-nc.com/scripts/areva-nc/publigen/content/templates/Show.asp?P=7936&L=EN.

IRSN (2008b) Incident at the SOCATRI plant on the Tricastin site on July 7, 2008. Institut de Radioprotection et de Sûreté Nucléaire, France. http://www.irsn.eu/en/index.php?position=socatri_tricastin_en.

Izrael, Y. A., Stukin, E. D., and Tsaturov, Y. S. (1994) *Meteor. Gidrol.*, **11**, 5–14.

Janeczek, J. and Ewing, R. C. (1992) *J. Nucl. Mater.*, **190**, 157–193.

Jarvis, N. V. and Hancock, R. D. (1991) *Inorg. Chim. Acta*, **182**, 229–232.

Jenne, E. A. (1998) *Adsorption of Metals by Geomedia. Variables*, *Mechanisms*, *and Model Applications*, Academic, San Diego, CA, pp. 583.

Jernström, J., Eriksson, M., Simon, R., Tamborini, G., Bildstein, O., Carlos Marquez, R., Kelhl, S. R., Hamilton, T. F., Ranebo, Y., and Betti, M. (2006) *Spectrochim. Acta Part B*, **61**, 971–979.

John, S., Ruggiero, C. E., Hersman, L., Tung, C., and Neu, M. P. (2001) *Environ. Sci. Technol.*, **35**, 2942–2948.

Johnson, C. A., Kitchen, K. P., and Nelson, N. (2007) *Atm. Environ.* **41**, 3921–3937.

Johnsson, A., Arlinger, J., Pederson, K., Odegaard-Jensen, A., and Albinsson, Y. (2006) *Geomicrobiol. J.*, **23**, 621–630.

Jones, S. (2008) *J. Environ. Radioact.*, **99**, 1–6.

Jones, S. R. and McDonald, P. (1994) The Inventory of Long Lived Artificial Radionuclides in the Irish Sea and Their Radiological Significance, Report XI-5027/94, European Commission, pp. 153–206.

Jones, S. R., Williams, S. M., Smith, A. D., Cawse, P. A., and Baker, S. J. (1996) *Sci. Total Environ.*, **183**, 213–229.

Kalmykov, S. N., Kriventsov, V. V., Teterin, Y. A., and Novikov, A. P. (2007) *C.R. Chim.*, **10**, 1060–1066.

Kalmykov, S. N., Schäfer, T., Claret, F., Perminova, I. V., Petrova (Khasanova), A. B., Shcherbina, N.S., and Teterin, Y. A. (2008) *Radiochim. Acta*, **96**, 685–690.

Kaplan, D. I., Bertsch, P. M., Adriano, D. C., and Orlandini, K. A. (1994) *Radiochim. Acta*, **66/67**, 181–187.

Kaszuba, J. P. and Runde, W. (1999) *Environ. Sci. Technol.*, **33**, 4427–4433.

Kaul, A. and Röthemeyer, H. (1997) *Nucl. Eng. Des.*, **176**, 83–88.

Keeney-Kennicutt, W. L., and Morse, J. W. (1985) *Geochim. Cosmochim. Acta*, **49**, 2577–2588.

Keiling, C. and Marx, G. (1991) *Radiochim. Acta*, 287–290.

Keiling, C., Esser, V., and Marx, G. (1988) *Radiochim. Acta*, **44/45**, 277–281.

Kelley, J. M., Bond, L. A., and Beasley, T. M. (1999) *Sci. Total Environ.*, **237/238**, 483–500.

Kelm, M., Pashalidis, I., and Kim, J. I. (1999) *Appl. Radiat. Isot.*, **51**, 637–642.

Kersting, A. B., Efurd, D. W., Finnegan, D. L., Rokop, D. J., Smith, D. K., and Thompson, J. L. (1999) *Nature*, **397**, 56–59.

Kessler, J. (1999) Colloid Transport and Deposition in Water-Saturated and Unsaturated Sand and Yucca Mountain Tuff. Center, E. D., Report TR-110546, Pacific Northwestern Laboratory and Washington State University, Tri Cities, pp. 64.

Khalturin, V. I., Rautian, T. G., Richards, P. G., and Leith, W. S. (2005) *Sci. Global Sec.*, **13**, 1–42.

Kikuchi, M., Hidaka, H., and Horie, K. (2008) *Phys. Chem. Earth*, **33**, 978–982.

Kim, J. I. (1991) *Radiochim. Acta*, **52/53**, 71–81.

Kim, J.-I. (1993) The chemical behavior of transuranium elements and barrier functions in natural aquifer systems. In *Scientific Basis for Nuclear Waste Management* (Pittsburgh, PA), *Materials Research Society Symposium Proceedings*, Materials Research Society, pp. 3–21.

Kim, J. I., Buckau, G., Li, G. H., Duschner, H., and Psarros, N. (1990) *Fresenius J. Anal. Chem.*, **338**, 245–252.

Kim, J. I., Zeh, P., and Delakowitz, B. (1992) *Radiochim. Acta*, **58/59**, 147–154.

Kim, J. I., Klenze, R., Wimmer, H., Runde, W., and Hauser, W. (1994) *J. Alloys Compd.*, **213/214**, 333–340.

Kim, J. I., Gompper, K., Closs, K. D., Kessler, G., and Faude, D. (1996) *J. Nucl. Mater.*, **238**, 1–10.

Knopp, R., Neck, V., and Kim, J. I. (1999) *Radiochim. Acta*, **86**, 101–108.

Koide, M., Bertine, K. K., Chow, T. J., and Goldberg, E. D. (1985) *Earth Planet. Sci. Lett.*, **72**, 1–8.

Komarov, E. V. (1959) *Zh. Neorg. Khim.*, **4**, 1313–1323.

Komura, K., Sakanoue, M., and Yamamoto, M. (1984) *Health Phys.*, **46**, 1213–1219.

Kraus, K. A. and Nelson, F. (1950) *J. Am. Chem. Soc.*, **72**, 3901–3906.

Krey, P. W., Hardy, E. P., Pachucky, C., Rourke, F., Coluzza, J., and Benson, W. K. (1976) Mass isotopic composition of global fall-out plutonium in soil. In *Transuranium Nuclides in the Environment*, International Atomic Energy Agency, Vienna, Austria, pp. 671-678.

Krey, P. W., Leifer, R., Benson, W. K., Dietz, L. A., Hendrikson, H. C., and Coluzza, J. L. (1979) *Science*, **205**, 583–585.

Krishnaswami, S. (1999) Thorium. In *Encyclopedia of Geochemistry* (eds. C. P. Marshall and R. W. Fairbridge), Kluwer, Dordrecht, The Netherlands, pp. 630–635.

Kubatko, K.-A. H., Helean, K. B., Navrotsky, A., and Burns, P. C. (2003) *Science*, **302**, 1191–1193.

Kuroda, P. K. (1982) *The Origin of the Chemical Elements and the Oklo Phenomenon*, Springer, Berlin/Heidelberg/New York.

Kuroda, P. K. (1996) *J. Radioanal. Nucl. Chem.*, **203**, 591–599.

Kuroda, P. K., and Myers, W. A. (1994) *Radiochim. Acta* **64**, 167–174.

Lagus, T. (2005) *J. Eng. Public Policy* **9.** http://www.wise-intern.org.

Landa, E. R. (2004) *J. Environ. Radioact.*, **77**, 1–27.

Langmuir, D. (1997) *Aqueous Environmental Chemistry*, Prentice Hall, Upper Saddle River, NJ, pp. 600.

Lansard, B., Charmasson, S., Gasco, C., Anton, M. P., Grenz, C., and Arnaud, M. (2007) *Sci. Total Environ.*, **376**, 215–227.

Lee, M. H. and Clark, S. B. (2005) *Environ. Sci. Technol.*, **39**, 5512–5516.

Lee, M. H. and Lee, C. W. (1999) *J. Radioanal. Nucl. Chem.*, **239**, 471–476.

Lemire, R. J. and Garisto, F. (1989) The solubility of U, Np, Pu, Th, and Tc in a geological disposal vault for used nuclear fuel, Report AECL-10009, Pinawa, Atomic Energy of Canada, Ltd., Manitoba, pp. 131.

Lemire, R. J., Fuger, J., Nitsche, H., Potter, P., Rand, M. H., Rydberg, J., Spahiu, K., Sullivan, J. C., Ullman, W. J., Vitorge, R., and Wanner, H. (2001) *Chemical Thermodynamics of Neptunium and Plutonium*, Elsevier Science B.V., Amsterdam, The Netherlands, pp. 845.

Lgotin, V. and Makushin, Y. (1998) Groundwater monitoring to assess the influence of injection of liquid radioactive waste on the Tomsk public groundwater supply, Western Siberia, Russia. In *Groundwater Contaminants and Their Migration* (eds. J. Mather, D. Banks, S. Dumpleton, and M. Fermor), Geological Society, London, pp. 255–264.

Lieser, K. H. and Mohlenweg, U. (1988) *Radiochim. Acta*, **43**, 27–35.

Leslie, B. W., Pickett, D. A., and Pearcy, E. C. (1999) *Materials Research Society Symposium Proceedings*, **556**, p. 833–842.

Lin, A. (1997) *Sci. Total Environ.*, **198**, 13–31.

Lind, O. C., Salbu, B., Janssens, K., Proost, K., and Dahlgaard, H. (2005) *J. Environ. Radioact.*, **81**, 21–32.

Lindahl, P., Roos, P., Holm, E., and Dahlgaard, H. (2005) *J. Environ. Radioact.*, **82**, 285–301.

Livens, F. R. and Singleton, D. L. (1991) *J. Environ. Radioact.*, **13**, 323–329.

Livens, F. R. Morris, K., Parkman, R., and Moyes, L. (1996) *Nucl. Energy* (*British Nuclear Energy Society*), **35**, 331–337.

Livingston, H. D. (ed.) (2004) *Marine Radioactivity*, Elsevier, Oxford, UK, pp. 310.

Lloyd, J. R. (2003) *FEMS Microbiol. Rev.*, **27**, 411–425.

Lloyd, J. R., Yong, P., and Macaskie, L. E. (2000) *Environ. Sci. Technol.*, **34**, 1297–1301.

Loiseaux, J.-M., David, S., Heuer, D., and Nuttin, A. (2002) *C R Phy.*, **3**, 1023–1034.

LoPresti, V., Conradson, S. D., and Clark, D. L. (2007) *J. Alloys Compd.*, **444/445**, 540–543.

Loss, R. (2005) Oklo Fossil Reactors. Curtin University of Technology, Australia. http://www.oklo.curtin.edu.au/Where/index.cfm

Lovley, D. R., Phillips, E. J. P., Gorby, Y. A., and Landa, E. R. (1991) *Nature* (*London*), **350**, 413–416.

Lu, N., Reimus, P. W., Parker, G. R., Conca, J. L., and Triay, I. R. (2003) *Radiochim. Acta*, **91**, 713–720.

Lujaniene, G., Motiejunas, S., and Sapolaite, J. (2007) *J. Radioanal. Nucl. Chem.*, **274**, 345–353.

Lutze, W. and Ewing, R. C. (1988) *Radioactive Waste Forms for the Future*, North-Holland, Amsterdam, The Netherlands, pp. 778.

Macaskie, L. E., Jeong, B. C., and Tolley, M. R. (1994) *FEMS Microbiol. Rev.*, **14**, 351–368.

MacKenzie, A. B., Stewart, A., cook, G. T., Mitchell, L., Ellet, D. J., and Griffiths, C. R. (2006) *Sci. Total Environ.*, **369**, 256–272.

Maes, N., Wang, L., Hicks, T., Bennett, D., Warwick, P., Hall, T., Walker, G., and Dierckx, A. (2006) *Phys. Chem. Earth*, **31**, 541–547.

Magirius, S., Carnall, W. T., and Kim, J. I. (1985) *Radiochim. Acta*, **38**, 29–32.

Markham, O. D., Puphal, W., and Filer, T. D. (1978) *J. Environ. Qual.*, **7**, 421–428.

Mathieu, R., Zetterstrom, L., Cuney, M., Gauthier-Lafaye, F., and Hidaka, H. (2001) *Chem. Geol.*, **171**, 147–171.

Matonic, J. H., Scott, B. L., and Neu, M. P. (2001) *Inorg. Chem.*, **40**, 2638–2639.

Matsunaga, T., Nagao, S., Ueno, T., Takeda, S., Amano, H., and Tkachenko, Y. (2004) *Appl. Geochem.*, **19**, 1581–1599.

Mboulou, M. O., Hurtgen, C., Hofkens, K., and Vandecasteele, C. (1998) *J. Environ. Radioact.*, **39**, 231–237.

McCarthy, J. and Zachara, J. (1989) *Environ. Sci. Technol.*, **23**, 496–502.

McCubbin, D. and Leonard, K. S. (1995) *Radiochim. Acta*, **69**, 97–102.

McDonald, P., Cook, G. T., Baxter, M. S., and Thompson, J. C. (2001) *J. Environ. Radioact.*, **267**, 109–123.

McKinley, I. G. and Alexander, W. R. (1993) *J. Contam. Hydrol.*, **13**, 249–259.

McKinley, J. P., Zachara, J. M., Wan, J., McCready, D. E., and Heald, S. M. (2007) *Vadose Zone J*., **6**, 1004–1017.

McMahon, C. A., Vintro, L. L., Mitchell, P. I., and Dahlgaard, H. (2000) *Appl. Radiat. Isot*., **52**, 697–703.

Meece, D. and Benninger, L. K. (1993) *Geochim. Cosmochim. Acta*, **57**, 1447–1458.

Meinrath, G. and Kim, J. I. (1991) *Radiochim. Acta*, **52/53**, 29–34.

Meinrath, A., Schneider, P., and Meinrath, G. (2003) *J. Environ. Radioact*., **64**, 175–193.

Min, M. Z., Zhai, J. P., and Fang, C. Q. (1998) *Chem. Geol*., **144**, 313–328.

Mitchell, P. I., Vintro, L., Dahlgaard, H., Gasco, C., and Sanchez-Cabeza, J. A. (1997) *Sci. Total Environ*., **202**, 147–153.

Morgenstern, M., Klenze, R., and Kim, J. I. (2000) *Radiochim. Acta*, **88**, 7–16.

Moulin, V. and Moulin, C. (2001) *Radiochim. Acta*, **89**, 773–778.

Moulin, V. and Ouzounian, G. (1992) *Appl. Geochem.* Suppl. **1**, 179–186.

Moulin, V., Robouch, P., Vitorge, P., and Allard, B. (1988) *Radiochim. Acta*, **44/45**, 33–37.

Moulin, V., Tits, J., Moulin, C., Decambox, P., Mauchien, P., and Deruty, O. (1992a) *Radiochimica Acta*, **58-9**, 121–128.

Moulin, V., Tits, J., and Ouzounian, G. (1992b) *Radiochim. Acta*, **58/59**, 179–190.

Moulin, V. M., Moulin, C. M., and Dran, J.-C. (1996) *ACS Symp. Ser*., **651**, 259–271.

Müller, K., Brendler, V., and Foerstendorf, H. (2008) *Inorg. Chem*., **47**, 10127–10134.

Muramatsu, Y., Rühm, W., Yoshida, S., Tagami, K., Uchida, S., and Wirth, E. (2000) *Environ. Sci. Technol*., **34**, 2913–2917.

Muramatsu, Y., Hamilton, T., Uchida, S., Tagami, K., Yoshida, S., and Robison, W. L. (2001) *Sci. Total Environ*., **278**, 151–159.

Murphy, W. M. and Grambow, B. (2008) *Radiochim. Acta*, **96**, 563–567.

Myasoedov, B. F. and Drozhko, E. G. (1998) *J. Alloys Compd*., **271/273**, 216–220.

Myers, D. (1991) *Surfaces, Interfaces, and Colloids. Principles and Applications*, VCH Publishers, New York, pp. 433.

Nagasaki, S., Tanaka, S., and Suzuki, A. (1997) *J. Nucl. Mater*., **248**, 323–327.

Nagasaki, S., Tanaka, S., Todoriki, M., and Suzuki, A. (1998) *J. Alloys Compd*., **271–273**, 252–256.

Nash, K. L., Cleveland, J. M., Sullivan, J. C., and Woods, M. (1986) *Inorg. Chem*., **25**, 1169–1173.

NATO (1998) *Defense Nuclear Waste Disposal in Russia: International Perspective*, Springer, Dordrecht, The Netherlands, pp. 364.

NATO (2005) *Use of Humic Substances to Remediate Polluted Environments*, Springer, Dordrecht, The Netherlands, pp. 506.

Naudet, R. (1975) *IAEA Bull*., **17**, 22–32.

Neck, V., Fanghänel, T., Rudolph, G., and Kim, J. I. (1995a) *Radiochim. Acta*, **69**, 39–67.

Neck, V., Runde, W., and Kim, J. I. (1995b) *J. Alloys Compd*., **225**, 295–302.

Neck, V., Kim, J. I., Seidel, B. S., Marquardt, C. M., Dardenne, K., Jensen, M. P., and Hauser, W. (2001) *Radiochim. Acta*, **89**, 439–446.

Neck, V., Altmaier, M., Müller, R., Bauer, A., Fanghänel, T., and Kim, J. I. (2003) *Radiochim. Acta*, **91**, 253–262.

Neck, V., Altmaier, M., and Fanghänel, T. (2007a) *C R Chimie*, **10**, 959–977.

Neck, V., Altmaier, M., Seibert, A., Yun, J. I., Marquardt, C. M., and Fanghänel, T. (2007b) *Radiochim. Acta*, **95**, 193–207.

Neilands, J. B. (1981) *Ann. Rev. Biochem*., **50**, 715–731.

Neu, M. P., Schulze, R. K., Conradson, S. D., Farr, J. D., and Haire, R. G. (1997) Polymeric Plutonium(IV) Hydroxide: Formation, Prevalence, and Structural and Physical Characteristics. In: *Plutonium Future-The Science*. Los Alamos National Laboratory, Los Alamos, NM, pp. 89–90

Neu, M. P., Matonic, J. H., Ruggiero, C. E., Christy, E., and Scott, B. L. (2000) *Angew. Chem., Internat. Ed.*, **39**, 1442–1444.

Neu, M. P., Ruggiero, C. E., and Francis, A. J. (2002) Bioinorganic Chemistry of Plutonium and Interactions of Plutonium with Microorganisms and Plants. In *Advances in Plutonium Chemistry 1967–2000* (ed. D. Hoffman), American Nuclear Society, Lagrange Park, IL, pp. 169–211.

Neu, M. P., Icopini, G. A., and Boukhalfa, H. (2005) *Radiochim. Acta*, **93**, 705–714.

NEWMDB (2008) The IAEA Radioactive Waste Management Database. International Atomic Energy Agency. http://newmdb.iaea.org/datacentre.aspx.

Newton, T. W. (2002) Redox Reactions of Plutonium Ions in Aqueous Solutions. In *Advances in Plutonium Chemistry 1967–2000* (ed. D. Hoffman), American Nuclear Society, La Grange Park, IL, pp. 24–57.

Nitsche, H., Gatti, R. C., Standifer, E. M., Lee, S. C., Muller, A., Prussin, T., Deinhammer, R. S., Maurer, H., Becraft, K., Leung, S., and Carpenter, S. A. (1993) Measured solubilities and speciations of neptunium, plutonium, and americium in a typical groundwater (J-13) from the Yucca Mountain Region, Report LA-12562-MS, Los Alamos National Laboratory, Los Alamos, NM, pp. 127.

Norris, S. and Kristensen, H. M. (2006) *Bull. At. Sci.*, **July/August**, 64–66.

Novikov, A. P., Kalmykov, S. N., Utsunomiya, S., Ewing, R. C., Horreard, F., Merkulov, A., Clark, S. B., Tkachev, V. V., and Myasoedov, B. F. (2006) *Science*, **314**, 638–641.

NRC (1996) *Nuclear Wastes: Technologies for Separation and Transmutation*. National Research Council (U.S.), Committee on Separations Technology and Transmutation Systems, National Academies Press, pp. 571.

NRC (2007) Fact Sheet on the Three Mile Island Accident. United States Nuclear Regulatory Commission. http://www.nrc.gov/reading-rm/doc-collections/fact-sheets/3mile-isle.html.

O'Boyle, N., Nicholson, G., Piper, T., Taylor, D., Williams, D., and Williams, G. (1997) *Appl. Radiat. Isot.*, **48**, 183–200.

Oberti, R., Ottolini, L., Camara, F., and DellaVentura, G. (1999) *Am. Mineral.*, **84**, 913–921.

Odintsov, A. A., Khan, V. E., Krasnov, V. A., and Pazukhin, E. M. (2007) *Radiochem.*, **49**, 534–540.

OECD/NEA (2003) *Uranium 2003: Resources, Production and Demand*, Organisation for Economic Co-operation and Development, Nuclear Energy Agency, Paris, France, pp. 292.

OECD/NEA (2005) *Uranium 2005. Resources, Production and Demand*, Organisation for Economic Co-operation and Development, Nuclear Energy Agency and the International Atomic Energy Agency, pp. 392.

OECD/NEA (2008) *Uranium 2007: Resources, Production and Demand* (*Red Book*), Organisation for Economic Co-operation and Development, Nuclear Energy Agency and the International Atomic Energy Agency, pp. 422.

ORNL (1995) Technical Drawing, ORNL-DWG-95A-534, Oak Ridge National Labo-
  ratory.

Östhols, E., Bruno, J., and Grenthe, I. (1994) *Geochim. Cosmochim. Acta*, **58**, 613–623.

OTA (1991) Long-Lived Legacy: Managing High-Level and Transuranic Waste at the
  DOE Nuclear Weapons Complex. Office, U. S. G. P., Report OTA-BP-O-83, U.S.
  Congress, Office of Technology Assessment, Washington, D.C., pp. 99.

Oviedo, C. and Rodriguez, J. (2003) *Quím. Nova*, **26**, 901–905.

Pabalan, R. T., Turner, D. R., Bertetti, F. P., and Prikryl, J. D. (1998) Uranium(VI)
  Sorption onto Selected Mineral Surfaces: Key Geochemical Parameters. In *Adsorption
  of Metals by Geomedia* (ed. E. A. Jenne), Academic, San Diego, CA, pp. 100–130.

Panak, P., Klenze, R., and Kim, J. I. (1996) *Radiochim. Acta*, **74**, 141–146.

Panak, P. J., Booth, C. H., Caulder, D. L., Bucher, J. J., Shuh, D. K., and Nitsche, H.
  (2002) *Radiochim. Acta*, **90**, 315–321.

Parrish, R. R. and Noble, S. R. (2003) Zircon U-Th-Pb Geochronology by Isotope
  Dilution – Thermal Ionization Mass Spectrometry (ID-TIMS). In *Zircon. Reviews in
  Mineralogy and Geochemistry*, *Mineralogical Society of America* (eds. J. Hanchar and
  P. Hoskin), Mineralogical Society of America, Washington, D.C., pp. 183–213.

Pashalidis, I., and Kim, J. I. (1992) Chemisches Verhalten des Sechswertigen Plutoniums
  in Konzentrierten NaCl-Lösungen unter dem Einfluss der Eigenen Alpha-Strahlung,
  Report RCM01092, Institut für Radiochemie, TU München, Germany, pp. 187.

Pashalidis, I., Kim, J. I., Lierse, C., and Sullivan, J. C. (1993) *Radiochim. Acta*, **60**,
  99–101.

Pathak, P. N. and Choppin, G. R. (2007) *J. Radioanal. Nucl. Chem.*, **274**, 517–523.

Payne, T. E., Edis, R., and Seo, T. (1992) *Materials Research Society Symposium
  Proceedings*, **257**, pp. 481–488.

Payne, T. E., Davis, J. A., and Waite, T. D. (1996) *Radiochim. Acta*, **74**, 239–243.

Pearcy, E. C., Prikryl, J. D., Murphy, W. M., and Leslie, B. W. (1994) *Appl. Geochem.*, **9**,
  713–732.

Peiper, J. C. and Pitzer, K. S. (1982) *J. Chem. Thermodyn.*, **14**, 613.

Perez del Villar, L., De la Cruz, B., Pardillo, J., Pelayo, M., Rivcas, P., and Astudillo, J.
  (1993) *Est. Geol.* (*Madrid*), **49**, 187–198.

Perkins, R. W. and Thomas, C. W. (1980) Worldwilde Fallout. In: *Transuranic Elements
  in the Environment Worldwide Fallout* (ed. W. C. Hanson), Technical Information
  Center, Department of Energy, Springfield, MO, pp. 53–82.

Perna, L., Jernström, J., Aldave de las Heras, L., Hrnecek, E., de Pablo, J., and Betti, M.
  (2005) *J. Radioanal. Nucl. Chem.*, **263**, 367–373.

Pitzer, K. S. (1991) *Activity Coefficients in Electrolyte Solutions*, CRC Press, Boca Raton,
  FL, pp. 560.

Pompe, S., Schmeide, K., Bubner, M., Geipel, G., Heise, K. H., Bernhard, G., and
  Nitsche, H. (2000) *Radiochim. Acta*, **88**, 553–558.

Powell, B. A., Duff, M. C., Kaplan, D. I., Fjeld, R. A., Newville, M., Hunter, D. B.,
  Bertsch, P. M., Coates, J. T., Eng, P., Rivers, M. L., Serkiz, S. M., Sutton, S. R., Triay,
  I. R., and Vaniman, D. T. (2006) *Environ. Sci. Technol.*, **40**, 3508–3514.

Rabideau, S. W., Bradley, M. J., and Cowen, H. D. (1958) Alpha-Particle Oxidation and
  Reduction in Aqueous Plutonium Solutions, LAMS-2236, Report, Los Alamos Scien-
  tific Laboratory, Los Alamos, NM, pp. 28.

Rai, D. (1984) *Radiochim. Acta*, **35**, 97–106.

Rai, D., Serne, R. J., and Swanson, J. L. (1980) *J. Environ. Qual.* **9**, 417-420.

Rai, D., Strickert, R. G., Moore, D. A., and Serne, R. J. (1981) *Geochim. Cosmochim. Acta*, **45**, 2257–2265.

Rai, D., Hess, N. J., Felmy, A. R., Moore, D. A., Yui, M., and Vitorge, P. (1999) *Radiochim. Acta*, **86**, 89–99.

Rai, D., Moore, D. A., Felmy, A. R., Choppin, G. R., and Moore, R. C. (2001) *Radiochim. Acta*, **89**, 491–498.

Rai, D., Gorby, Y., Fredrickson, J., Moore, D., and Yui, M. (2002) *J. Soln. Chem.*, **31**, 433–453.

Rao, L. F., Rai, D., Felmy, A. R., Fulton, R. W., and Novak, C. F. (1996) *Radiochim. Acta*, **75**, 141–147.

Rao, L., Zhang, Z., PierLuigi Zanonato, P., Plinio Di Bernardo, P., Bismondo, A., and Clark, S. B. (2004) *J. Chem. Soc. Dalton Trans.*, **18**, 2867–2872.

Ratledge, C. and Dover, L. G. (2000) *Ann. Rev. Microbiol.*, **54**, 881–941.

Reeder, R. J., Nugent, M., Lamble, G. M., Tait, C. D., and Morris, D. E. (2000) *Environ. Sci. Technol.*, **34**, 638–644.

Reilly, S. D., Myers, W. K., Stout, S. A., Smith, D. M., Ginder-Vogel, M. A., and Neu, M. P. (2003) Plutonium Futures - The Science: Third Topical Conference on Plutonium and Actinides, *AIP Conference Proceedings*, **673**, p. 375–376.

Reiller, P. (2005) *Radiochim. Acta*, **93**, 43–55.

Reiller, P., Moulin, V., Casanova, F., and Dautel, C. (2002) *Appl. Geochem.*, **17**, 1551–1562.

Reilly, S. D. and Neu, M. P. (2006) *Inorg. Chem.*, **45**, 1839–1846.

Rekacewicz, P. (2004) Existing radioactive waste disposal and proposal alternatives for storage. UNEP/GRID-Arendal Maps and Graphics Library, Arendal, Norway, http://maps.grida.no/go/graphic/existing-radioactive-waste-disposal-and-proposal-alternatives-for-storage.

Rempe, N. T. (2008) *Deep Geologic Repositories*. Geological Society of America, Boulder, CO, pp. 119.

Rey, A., Giménez, J., Casas, I., Clarens, F., and de Pablo, J. (2008) *Appl. Geochem.*, **23**, 2249–2255.

Righetto, L., Bidoglio, G., Marcandalli, B., and Bellobono, I. R. (1988) *Radiochim. Acta*, **44/45**, 73–75

Robison, W. L. and Noshkin, V. E. (1999) *Sci. Total Environ.*, **237/238**, 311–327.

Royer, R. A., Burgos, W. D., Fisher, A. S., Unz, R. F., and Dempsey, B. A. (2002) *Environ. Sci. Technol.*, **36**, 1939–1946.

Ruggiero, C. E., Matonic, J. H., Reilly, S. D., and Neu, M. P. (2002) *Inorg. Chem.*, **41**, 3593–3595.

Runde, W. (2000) The Chemical Interactions of Actinides in the Environment. In *Los Alamos Science* (ed. N. G. Cooper), Los Alamos National Laboratory, Los Alamos, NM, pp. 392–415.

Runde, W., Neu, M. P., and Clark, D. L. (1996) *Geochim. Cosmochim. Acta*, **60**, 2065–2073.

Runde, W., Conradson, S. D., Efurd, D. W., Lu, N., VanPelt, C. E., and Tait, C. D. (2002a) *Appl. Geochem.*, **17**, 837–853.

Runde, W., Neu, M. P., Conradson, S. D., Li, D., Lin, M., Smith, D. M., Van Pelt, C. E., and Xu, Y. (2002b) *Geochem. Soil Radionucl.*, **59**, 21–44.

Runde, W., Brodnax, L. F., Goff, G. S., Peper, S. M., Taw, F. L., and Scott, B. L. (2007) *Chem. Commun.*, 1728–1729.

Rusin, P. A., Quintana, L., Brainard, J. R., Strietelmeier, B. A., Tait, C. D., Ekberg, S. A., Palmer, P. D., Newton, T. W., and Clark, D. L. (1994) *Environ. Sci. Technol.*, **28**, 1686–1690.

Sanchez, A. L., Murray, J. W., and Sibley, T. H. (1985) *Geochim. Cosmochim. Acta*, **49**, 2297–2307.

Sandino, A. and Bruno, J. (1992) *Geochim. Cosmochim. Acta*, **56**, 4135–4145.

Sandino, M. C. A. and Grambow, B. (1994) *Radiochim. Acta*, **66/67**, 37–43.

Schäfer, T., Artinger, R., Dardenne, K., Bauer, A., Schuessler, W., and Kim, J. I. (2003) *Environ. Sci. Technol.*, **37**, 1528–1534.

Schild, D. and Marquardt, C. M. (2000) *Radiochim. Acta*, **88**, 587–591.

Schneider, M. and Froggatt, A. (2008) The World Nuclear Industry Status Report 2007, Report, Greens-EFA Group in the European Parliament, Brussels, Belgium, pp. 37.

Schneider, D. L., and Livingston, H. D. (1984) *Nucl. Instrum. Methods Phys. Res., Sect. A*, **233**, 510–516.

Silva, R. J. and Nitsche, H. (2002) Environmental Chemistry. Chapter 6. In *Advances in Plutonium Chemistry 1967–2000* (ed. D. C. Hoffman), American Nuclear Society, La Grange Park, IL, pp. 89–117.

Silva, R. J., Bidoglio, G., Rand, M. H., Robouch, P. B., Wanner, H., and Puigdomenech, I. (1995) *Chemical Thermodynamics of Americium*, North-Holland Elsevier Science B.V., Amsterdam, The Netherlands, pp. 374.

Silva, M. K., Rucker, D. F., and Chaturvedi, L. (1999) *Risk Anal.*, **19**, 1003–1016.

SKB (2002) Analogier, Report, Svensk Kärnbränslehantering AB, Stockholm, Sweden, pp. 7.

Smellie, J. (1995) *Radwaste Magazine*, pp. 18–27.

Smith, J. N., Ellis, K. M., Aarkrog, A., Dahlgaard, H., and Holm, E. (1994) *J. Environ. Radioact.*, **25**, 135–159.

Smith, A. D., Jones, S. R., Gray, J., and Mitchell, K. A. (2007) *J. Radiol. Prot.*, **27**, 115–145.

SNL (1964) SNAP-9A Incident Summary, Sc-TM-64-947, Report, Sandia National Laboratory, Albuquerque, NM, pp. 84.

Spinks, J. W. T. and Woods, R. J. (1990) *An Introduction to Radiation Chemistry*, Wiley, New York, pp. 592.

Stammose, D. and Dolo, J. M. (1990) *Radiochim. Acta*, **51**, 189–193.

Sterne, P. A., Gonis, A., and Borovoi, A. A. (1998) *Actinides in the Environment*, Kluwer, Dordrecht, The Netherlands, pp. 500.

Stout, S. A., Reilly, S. D., Smith, D. M., Myers, W. K., Ginder-Vogel, M. A., Skanthakumar, S., Soderholm, L., and Neu, M. P. (2003) Plutonium Futures - The Science: Third Topical Conference on Plutonium and Actinides, *AIP Conference Proceedings*, **673**, pp. 381–383.

Stumm, W. (1992) *Chemistry of the Solid–Water Interface. Processes at the Mineral–Water and Particle–Water Interface in Natural Systems*, Wiley, New York, NY, pp. 428.

Stumm, W. and Morgan, J. J. (1995) *Aquatic Chemistry: Chemical Equilibria and Rates in Natural Waters*, Wiley, New York, NY, pp. 1040.

Stumpf, S., Stumpf, T., Dardenne, K., Hennig, C., Foerstendorf, H., Klenze, R., and Fanghänel, T. (2006) *Environ. Sci. Technol.*, **40**, 3522–3528.

Sturchio, N. C., Antonio, M. R., Soderholm, L., Sutton, S. R., and Brannon, J. C. (1998) *Science*, **281**, 971–973.

Suzuki, Y., Kelly, S. D., Kemner, K. A., and Banfield, J. F. (2003) *Appl. Environ. Microbiol.*, **69**, 1337–1346.

Sylwester, E. R., Hudson, E. A., and Allen, P. G. (2000) *Geochim. Cosmochim. Acta*, **64**, 2431–2438.

Tao, Z. Y., Li, W. J., Zhang, F. M., and Han, J. (2006) *J. Radioanal. Nucl. Chem.*, **268**, 563–569.

Tavcar, P., Jakopic, R., and Benedik, L. (2005) *Acta Chim. Slov.*, **52**, 60–66.

Tcherkezian, V., Galushkin, B., Goryachenkova, T., Kasharov, L., Liul, A., Roshina, I., and Ruminantsev, O. (1995) *J. Environ. Radioact.*, **27**, 133–139.

Techer, I., Khoury, H. N., Salameh, E., Rassineux, F., Claude, C., Clauer, N., Pagel, M., Lancelot, J., Hamelin, B., and Jacquot, E. (2006) *J. Geochem. Explor.*, **90**, 53–67.

Thomas, P. A. (1999) *Health Phys.*, **78**, 614–624.

Thompson, H. A., Parks, G. A., and Brown, G. E. (1998) Structure and Composition of Uranium[VI] Sorption Complexes at the Kaolinite-Water Interface. 2. In *Adsorption of Metals by Geomedia* (ed. E. A. Jenne), Academic, San Diego, CA, pp. 349–370.

Todosow, M., Galperin, A., Herring, S., Kazimi, M., Downar, T., and Morozov, A. (2005) *Nucl. Technol.* **151**, 168–176.

Triay, I. R., Meijer, A., Conca, J. L., Kung, K. S., Rundberg, R. S., Strietelmeier, B. A., Tait, C. D., Clark, D. L., Neu, M. P., and Hobart, D. E. (1997) Summary and Synthesis Report on Radionuclide Retardation for the Yucca Mountain Site Characterization Project, Report LA-13262-MS, Los Alamos National Laboratory, Los Alamos, NM, pp. 279.

Turner, D. R. (1995) A uniform approach to surface complexation modeling of radionuclide sorption, Report CN-WRA 95-001, Center for Nuclear Waste Regulatory Analyses, San Antonio, TX, pp. 116. www.lsnnet.gov.

UNSCEAR (2000a) Exposures to the Public from Man-made Sources of Radiation. In Sources and Effects of Ionizing Radiation, United Nations Scientific Committee on the Effects of Atomic Radiation, New York, pp. 158–291.

UNSCEAR (2000b) Exposures and Effects of the Chernobyl Accident. In Sources and Effects of Ionizing Radiation, United Nations Scientific Committee on the Effects of Atomic Radiation, New York, pp. 453–566.

Utsunomiya, S., Ewing, R. C., and Wang, L. M. (2005) *Earth Planet. Sci. Lett.*, **240**, 521–528.

Villani, S. (1979) *Uranium Enrichment*, Springer, New York, pp. 322.

Vintro, L., Mitchell, P. I., Condren, O. M., Moran, M., Vives i Batlle, J., and Sanchez-Cabeza, J. A. (1996) *Nucl. Instr. Meth. Phys. Res. A*, **369**, 597–602.

Vintro, L., Mitchell, P. I., Condren, O. M., Downes, A. B., Papucci, C., and Delfanti, R. (1999) *Sci. Total Environ.*, **237/238**, 77–91.

Vintro, L., Mitchell, P. I., Smith, K. J., Kershaw, P. J., and Livingston, H. D. (2004) Transuranium Nuclides in the World's Oceans. In *Marine Radioactivity* (ed. H. D. Livingston), Elsevier, Amsterdam, The Netherlands, pp. 79–108.

Vira, J. (2006) *Mat. Res. Soc. Symp. Proc.*, **932**, 3–12.

Vitorge, P. (1992) *Radiochim. Acta*, **58/59**, 105–107.

Vorobiova, M. I., Degteva, M. O., Burmistrov, D. S., Safronova, N. G., Kozheurov, V. P., Anspaugh, L. R., and Napier, B. A. (1999) *Health Phys.*, **76**, 605–618.

Waber, N., Schorscher, H. D., and Peters, T. (1991) Mineralogy, petrology, and geo-chemistry of the Pocos de Caldas analogue study sites, Minas Gerais, Brazil. I. Osamu Utsumi uranium mine, Report SKB 90-11, Mineral.-Petrogr. Institute, Bern, Switzerland, pp. 514.

Waite, T. D., Davis, J. A., Payne, T. E., Waychunas, G. A., and Xu, N. (1994) *Geochim. Cosmochim. Acta*, **58**, 5465–5478.

Wanty, R. B. (1999) Eh–pH Relations. In *Encyclopedia of Geochemistry* (eds. R. W. Fairbridge and M. R. Rampino), Kluwer, Dordrecht, The Netherlands, pp. 183–186.

Warnecke, E., Hollmann, A., Tittel, G., and Brennecke, P. (1994) Gorleben Radionu-clide Migration Experiments: More Than 10 Years of Experience. In *Proceedings of the Fourth International Conference on the Chemistry and Migration Behaviour of Actinides and Fission Products in the Geosphere*, Charleston, SC, 1993, Oldenbourg Verlag, Munich, pp. 821–827.

Warwick, P. E., Croudace, I. W., and Carpenter, R. (1996) *Appl. Radiat. Isot.*, **47**, 627.

Waters, R. D., Compton, K. L., Novikov, V., and Parker, F. L. (1999) Releases of Radionuclides to Surface Waters at Krasnoyarsk-26 and Tomsk-7, Report RR-99-3, International Institute for Applied Systems Analysis, Laxenberg, Austria, pp. 118.

Weinbauer, M. G., Beckmann, C., and Hofle, M. G. (1998) *Appl. Environ. Microbiol.*, **64**, 5000–5003.

Wellmann, D. M., Pierce, E. M., Richards, E. L., Fruchter, J. S., and Vermeul, V. R. (2008) WM2008, Phoenix, AZ, Conference Proceedings, pp. 1–15.

Westlén, D. (2007) *Progr. Nucl. Energy*, **49**, 597–605.

White, D. L., Durbin, P. W., Jeung, N., and Raymond, K. N. (1988) *J. Med. Chem.*, **31**, 8–11.

Wilhelm, R. G. (2004) Understanding Variation in Partition Coefficient, K_d Values. Volume III: Review of Geochemistry and Available K_d Values for Americium, Arse-nic, Curium, Iodine, Neptunium, Radium and Technetium, Report EPA 402-R-04-002188 United States Environmental Protection Agency, Office of Air and Radiation, Washington, D.C., pp. 188.

Witherspoon, P. A., and Bodvarsson, G. S. (2001) *Geological Challenges in Radioactive Waste Isolation. Third Worldwide Review*, Lawrence Berkeley National Laboratory, Berkeley, CA, pp. 335.

WNA (2008a) Nuclear Power in Sweden. World Nuclear Association. http://www.world-nuclear.org/info/inf42.html.

WNA (2008b) World Uranium Mining. World Nuclear Association. http://www.world-nuclear.org/info/inf23.html, http://www.world-nuclear.org/info/inf23.html.

WNA (2009) World Nuclear Power Reactors 2007-08 and Uranium Requirements. World Nuclear Association. http://www.world-nuclear.org/info/reactors.html, http://www.world-nuclear.org/info/reactors.html.

Wronkiewicz, D. J., and Buck, E. C. (1999) Uranium Mineralogy and the Geologic Disposal of Spent Nuclear Fuel. In *Uranium: Mineralogy, Geochemistry, and the Environment* (ed. P. H. Ribbe), Mineralogical Society of America, Washington, D. C., pp. 475–494.

Wronkiewicz, D. J., Bates, J. K., Gerding, T. J., Veleckis, E., and Tani, B. S. (1992) *J. Nucl. Mater.*, **190**, 107–127.

Yamaguchi, T., Sakamoto, Y., and Ohnuki, T. (1994) *Radiochim. Acta*, **66/67**, 9–14.

Yamamoto, M., Ishiguro, T., Tazaki, K., Komura, K., and Ueno, K. (1996) *Health Phys.*, **70**, 744–748.

Yanase, N., Sato, T., Iida, Y., and Sekine, K. (1998) *Radiochim. Acta*, **82**, 319–325.

Yong, P., and Macaskie, L. E. (1998) *J. Chem. Technol. Biotechnol.*, **71**, 15–26.

Yui, M., Shibutani, T., Shibutani, S., Rai, D., and Ochs, M. (2001) A plutonium geochemical database for performance analysis of high-level radioactive waste repositories. In *Plutonium in the Environment* (ed. A. Kudo), Elsevier Science, Amsterdam, The Netherlands, pp. 159–174.

Zeh, P., Czerwinski, K. R., and Kim, J. I. (1997) *Radiochim. Acta*, **76**, 37–44.

Zeh, P., Kim, J. I., Marquardt, C. M., and Artinger, R. (1999) *Radiochim. Acta*, **87**, 23–28.

Zetterström, L. (2000) Oklo: A Review and Critical Evaluation of Literature, Technical Report TR-00-17, Report, SKB, Stockholm, Sweden, pp. 37.

Zhao, D. and Ewing, R. C. (2000) *Radiochim. Acta*, **88**, 739–749.

Zhu, J. L., and Chan, C. Y. (1989) *IAEA Bulletin*, **31**, 5–13.